2012

The Neural Circuit for Behavioral Responses to Pheromone and Social Behavior in Caenorhabditis Elegans

Heeun Jang

THE NEURAL CIRCUIT FOR BEHAVIORAL RESPONSES TO PHEROMONE AND SOCIAL BEHAVIOR IN *CAENORHABDITIS ELEGANS*

A Thesis Presented to the Faculty of

The Rockefeller University

in Partial Fulfillment of the Requirements for

the degree of Doctor of Philosophy

by

Heeun Jang

June 2012

THE NEURAL CIRCUIT FOR BEHAVIORAL RESPONSES TO PHEROMONE AND SOCIAL BEHAVIOR IN *CAENORHABDITIS ELEGANS*

Heeun Jang, Ph.D.

The Rockefeller University 2012

Social behavior is a widespread phenomenon across species from microorganisms to humans. Chemical communication using pheromones is particularly interesting for its versatile use in many organisms, and has been studied at both molecular and circuit levels. However, the central issue of how genes and molecular components contribute to neural circuits that eventually lead to complex social behaviors remains unclear.

Using the nematode model organism *Caenorhabditis elegans*, I have examined two behavioral responses to pheromones, pheromone avoidance and pheromone-regulated social aggregation behavior, at genetic and circuit levels.

The known *C. elegans* pheromones are a set of related compounds called ascarosides. Specific ascarosides are known to regulate development and male attraction to potential mates. To characterize hermaphrodite responses to ascarosides, I used a behavioral assay for acute avoidance called the drop test, which measures reversals of a forward-moving worm upon an encounter with a diluted pheromone. I found that wild-type hermaphrodites from the laboratory N2 strain avoid one of the ascarosides, ascr#3/C9. Through i*n vivo* functional imaging using a genetically encoded calcium sensor and behavioral analysis of sensory mutants, I found that the nociceptive ADL

neurons sense ascr#3/C9. Behavioral analysis of synaptically manipulated worms indicated that ADL chemical synapses promotes avoidance behavior.

Animals with null mutation in the neuropeptide receptor *npr-1* have reduced avoidance of ascr#3/C9. I found that this effect is mediated by ADL participation in a gap junction circuit with the "social" hub interneuron RMG. Thus ADL chemical synapses and ADL gap junctions appear to have antagonistic effects on behavior. Avoidance is further suppressed by another modulatory ascaroside cue, ascr#5/C3, sensed by the ASK sensory neurons that are also connected to RMG by gap junctions.

Males do not avoid ascr#3/C9, and they have reduced ADL sensory responses to this ascaroside. Genetic masculinization of ADL does not reduce its sensory responses, suggesting that the sensory change has a non-autonomous component. *npr-1* males appear to be attracted to ascr#3/C9, and in these animals ASK strongly responds to ascr#3/C9 and contributes to the switch in behavioral responses. Together, these results indicate that behavioral avoidance of the pheromone ascr#3/C9 is modulated by neuropeptide signaling and sexual dimorphism that change neuronal properties at the circuit level.

Invertebrate gap junctions are comprised of innexin subunits. I conducted a systematic genetic study to identify innexin genes that affect *npr-1*-dependent aggregation. Several weak suppressors of *npr-1* aggregation behavior were identified, suggesting functional redundancy between innexins. In addition, I found that an allele of *glb-5* present in the wild strain CB4856 suppresses aggregation, probably by modulating sensitivity to oxygen in oxygen-sensing neurons that promote aggregation. My thesis work should help expand our understanding of neural circuits and molecules used for

chemical communication, simple animal social behaviors, and perhaps complex human behaviors.

Acknowledgements

My graduate study at the Rockefeller University would not have been possible without help and support from the many people I was fortunate enough to meet. I thank my thesis committee members, Shai Shaham, Jim Darnell, and Charles Gilbert, and the external examiner Niels Ringstad. The annual committee meeting has always been full of helpful feedback, new insights on the project, and encouraging advice. I especially thank my Chair, Shai Shaham, for valuable discussions and help with programs for data analysis.

My mentor and advisor Cori Bargmann has been one of the biggest blessings in my life. Every encounter with her impacted me with new inspiration and fresh motivation. I learned the essentials of doing science- to approach the problem analytically, work patiently, view the data critically, and think rigorously. She has the wisdom, personality, and professionalism that I would like to model in my career. During my most difficult times, either scientifically or personally, she showed me unfailing support and constant encouragement. I cannot agree more with what I heard when first starting my rotation: "Cori is the best advisor one could have."

I also thank Cori for creating and maintaining such an excellent laboratory environment that I have been always happy to work in. I especially enjoyed working with Manuel Zimmer, who was my mentor for my rotation project on the activity-dependent synaptic development in the oxygen-sensing neurons. I thank Manuel for patiently and efficiently introducing me to the basics of molecular biology, behavioral analysis, and functional imaging in *C. elegans*, and becoming such a good friend and now a wonderful

collaborator. I also thank Navin Pokala and Andy Chang, who tremendously helped me settle in the lab early on with kind heart and valuable guidance. I am grateful to Patrick McGrath for much help with gas flow assays, critical analysis, and timely advice, part of which led to identification of *glb-5* as a social suppressor. I have received motherly care and affection from Manoush Ardzivian and Holly Hunnicutt, for which I am very thankful. I also thank former and present Bargmann lab members that I owe intellectual input, reagents, and numerous amusing moments.

I was particularly fortunate to have wonderful collaborators on the pheromone circuit project. I truly enjoyed my intellectual interactions with Piali Sengupta and Kyuhyung Kim, which led to a very interesting body of work. I also thank Rebecca Butcher for her expertise, and synthesizing all the pheromones we used in the study. In addition, I am grateful to the Kwanjeong Educational Foundation in Korea for financial support, and the Dean's office for constant care.

I deeply thank my husband and the love of my life, Sung-Young, whom I was blessed to meet in New York City, and who has become the best companion in the scientific journey. I also thank our baby Junhee for being my new joy and happiness. My dear parents and beloved sister Seiyun have been a steadfast mental support far away from Korea, for which I am grateful. I thank my grandparents, aunt, and Youngjue Yu for all the sincere prayers. Lastly but most importantly, I deeply thank God for opening the doors and guiding me through the graduate years.

Table of Contents

List of Figures

List of Tables

Chapter 1:

Introduction

Social behavior is a fascinating aspect of neuroscience. It encompasses the functions of neural circuits within an individual brain, interactions between brains within a social group, and interactions of the group with its surroundings. Moreover, social behavior is often innate, and is widely observed across species from microorganisms to humans; it is important not only in primates or social insects that maintain complex hierarchical societies, but also in lower organisms. Deficits in human social interactions are characteristic of early developmental disorders such as autism, as well as later-onset mental disorders including schizophrenia (particularly the negative symptoms), depression (which is associated with social withdrawal), and social anxiety disorder.

Commonly observed social behaviors in animals and humans include aggression, mating, and parental behavior. Aggression can be observed when individuals of the same or different species compete to maintain or obtain territory or social dominance, attempt mating, or initiate or defend against predatory behaviors. It is usually enhanced in stressful conditions such as a shortage of environmental resources and high population density. Previous socialization experiences and seasonal and developmental changes in hormones can also affect aggression. In humans, aggression is generally considered as a non-adaptive behavior, but may contribute to enhance survival and reproduction of individuals in more pressured situations [1].

Mating is a reproductive interaction involving fertilization of the gametes, which is essential for maintenance of the species. A sequence of behaviors constitute mating: sexual advertisement and courtship behavior that refers to interactions aimed to entice a mating partner, followed by sexual bonding, copulation, and post-copulatory behavior [1]. For mating, many organisms have developed elaborate reproductive organs and finely-

tuned genetic sex-determination mechanisms. Based on the number of partners and the stability of pair-bonding, mating systems can be classified into promiscuity, polygamy, and monogamy [2]. In most human societies, mating is monogamous, and involves complex social and cultural processes.

Parental behavior refers to a set of care-providing behaviors to promote and support the physical and social development of young offspring. It is a unilateral investment from the parent(s) to enhance the offspring's survival [1]. In general, animals that have a smaller brood size and longer lifespan mature more slowly, and tend to have more prolonged and sophisticated parental behavior. Parental behavior ranges from simple forms such as egg-guarding or egg-carrying in some insects to more extensive care such as building nests, lactation and/or feeding, and protection in many birds and mammals. Human parental behavior is especially lengthy, providing considerable care to their children through puberty and beyond.

The keys to understanding the social behaviors lie in elucidating the behavioral algorithms employed by individuals, and the mechanisms of information flow between individuals or between groups. Neuroscience research on social behavior, also called social neuroscience, has been performed at largely two separate levels: social psychology that is based on human data grounded in the discipline of psychology, and molecular and cellular approaches that are based on data from animal models grounded in biology and biomedicine [3].

Social psychology focuses on defining social and cognitive functions as well as social interactions, and correlating these with specific activities in brain regions in human subjects. It is mainly empowered by noninvasive imaging such as functional magnetic

resonance imaging (fMRI), positron emission tomography (PET), and electroencephalography (EEG), and assisted by lesion studies in neurological patients, transcranial magnetic stimulation, pharmacological interventions, and computational modeling to simulate a particular behavior.

Neuroanatomy of social behavior

The brain regions implicated in social processing partly overlap with brain areas involved in general cognitive functions. For instance, damage to the left and right frontal lobe in the patient Phineas Gage led to dramatic changes in personality and social capacity, due to defects in rational decision-making and emotional processing [4].

However, the existence of social-specific illnesses such as autism suggest the existence of dedicated circuits for social function. Multiple brain regions have been associated with those socially relevant functions. For example, human social perception is heavily visual, and the fusiform area in the occipital-temporal junction is described as critical for face recognition [5]. The superior temporal sulcus (STS) is linked to the detection of biological motion [6, 7], and the medial prefrontal cortex and midline cortical structures are linked to perspective-taking as well as self-related processing and awareness [8, 9]. The amygdala is important for recognition of social emotions such as guilt and arrogance, perception of fear, and making judgments [8, 10-12], and the temperoparietal junction, along with medial prefrontal cortex and temporal poles, are related to mentalizing, the process by which we make inferences about mental states [8, 10]. Furthermore, the mirror neuron (MN) system seems to be an important part of the social brain [13]. The MN system includes the inferior frontal gyrus and the adjacent

ventral premotor cortex, the primary motor cortex, and the posterior parietal cortex [14-16]. fMRI and EEG studies show that MN system functions to match the external sensory description of an action observed or heard and its corresponding internal motor representation [17-20]. Moreover, it is implicated in anticipating and predicting others' behavior, therefore affecting social interaction [21, 22].

Limitations in social psychology, however, primarily lie in its reliance on non-invasive methodology. For instance, amygdala activation detected by fMRI in human subjects in response to appetitive and aversive stimuli does not mean the same neural circuitry has been activated. Indeed, different cells within the amygdala respond to appetitive versus aversive stimuli when electrophysiological recording is performed in monkeys [3, 23]. Therefore, studies in animal models using more diverse and extensive tools need to be performed in parallel to human studies.

Molecular mechanisms of social behavior

Social behavioral research in animal model systems employs genetic, molecular, cellular, biochemical, and electrophysiological tools. One focus is on identifying molecular components that regulate social behavior and determining their sites of function and the relevant circuits in the nervous system. Identified molecules include intercellular signaling molecules such as hormones, neurotransmitters, and neuropeptides, intracellular signaling molecules, channels, transporters, many other structural molecules required for a functional brain, and their transcriptional and translational regulators.

For example, aggression and dominance behaviors are regulated by the neuropeptide arginine vasotocin (AVT) in many fish species; larger or more

numerous AVT-ir cells or higher production of AVT within the gigantocellular preoptic area (gPOA) exhibits a positive relationship with aggressive behavior, whereas the same features in the parvocellular preoptic area (pPOA) show a negative relationship [24-29]. In lobsters and crayfish, two amine neurotransmitters serotonin and octopamine modulate aggression in an antagonistic fashion. A dominant-looking posture can be produced by serotonin injection into the hemolymph, a fluid equivalent to blood in most invertebrates, whereas a subordinate-looking posture arises from octopamine injection [30].

Male sexual behavior in the fruit fly is largely regulated by the *fruitless* gene, which encodes a set of transcriptional regulators [31-33]. Genetic evidence indicates that expression of male-specific Fru^M isoforms specifies the early male-specific steps of courtship behavior [34-36]. In rodents, male-specific mating behavior is stimulated by secreted androgen steroids, which act on transcription factors in a variety of brain regions [37, 38]. Mouse studies demonstrate competitive interactions between mating and aggression behaviors in the circuit level; the mating-promoting circuit and the aggression-promoting circuit coexist in ventromedial hypothalamus and inhibit the other's activity [39].

Parental behavior in rodents also involves multiple modulators. Elevated levels of the steroid hormone estradiol in late pregnancy and increased estrogen receptor activation in specific brain regions, such as the medial preoptic area (mPOA), contribute to maternal behavior [40-43]. High expression of receptors for the neuropeptide hormone oxytocin in mPOA, ventral tegmental area, and nucleus accumbens is correlated with a strong maternal behavior [44, 45], as is an increased level of the neurotransmitter dopamine in

the nucleus accumbens [46]. Distinct receptor expression patterns determine social attachment between mates. The expression of vasopressin receptor V1a (V1aR) determined by the promoter sequences of the *V1aR* gene is found in distinct brain distributions in monogamous prairie voles compared to non-monogamous vole species [47-49].

Chemical communication in social behavior

To achieve diverse social behaviors, many species use multiple communicational channels that include chemical, auditory, visual, tactile and electrical signaling [1]. Failure of these communications leads to maladaptation to the environment or society that can be potentially life-threatening. In humans, one of the crucial diagnostic domains of social disorders is deficiency in verbal and nonverbal communications [50]. Among many means of communication, chemical communication is particularly diverse and widely used in different species, such that each species develops a unique chemical communication repertoire. Pheromones refer to the chemical substances released by one individual and received by conspecifics, delivering specific information and thereby inducing a reaction such as a stereotyped behavior or endocrinological changes [51, 52].

Bacteria exhibit collective behaviors via a cell-to-cell chemical communication mechanism referred to quorum sensing (QS). The QS system is activated when the cell population reaches a threshold density and regulates virulence, secondary metabolite production, motility and swarming, conjugation, biofilm formation and growth inhibition [53, 54]. *N*-acylhomoserine lactone (AHL) is a well-studied class of QS signaling molecules used by Gram negative bacteria, consisting of homoserine lactone (HSL) ring

and acyl chains that vary in length, saturation level and oxidation state. The species-specific activated complex of AHL and its cognate receptor LuxR activates or represses transcription of multiple target genes, including the AHL signal synthase LuxI that results in a positive autoinduction circuit. Many bacteria possess multiple LuxR/LuxI/AHL modules, which regulate virulence by biofilm formation in the human pathogen *Pseudomonas aeruginosa* [55, 56] and antibiotic production in the insect pathogen *Photorhabdus luminescences* [57]. Another QS signaling molecule, autoinducer-2 (AI-2) refers to a group of diffusible molecules that act through LuxS protein and regulate bioluminescence in *Vibrio* species [58-61], virulence in *Vibrio cholerae* [62], and competence in *Bacillus subtilis* [63]. Autoinducing peptides (AIPs), 5 to 34 amino acids that typically contain unusual chemical structures, impede attachment and development of a biofilm in *Staphylococcus aureus* [64, 65].

Intraspecies communication is observed not only between bacterial species that produce the same AHL but also between bacteria and mammalian cells, plants and algae, as well as other bacteria that secrete molecules that can either activate or inhibit QS, sometimes by chemically modifying QS signaling molecules. For example, active AI-2 produced by *Bacillus subtilis* is able to mediate activation of light production in *Vibrio harveyi* [66, 67]. One of the AHL derivatives 3-oxo-C_{12}-HSL reduces lipopolysaccharide (LPS)-induced production of the pro-inflammatory cytokine IL-12 by monocytes, modulating host inflammatory responses [68, 69]. Salicylic acid, the defense signal molecule in plants, upregulates expression of AHL-degrading enzyme in *Agrobacterium tumefaciens* [70]. Red algae produce brominated furanones that inhibit AHL-dependent

QS, whereas plant root exudates contain compounds that stimulate both AHL and AI-2 biosensors [71, 72].

Moving to chemical signaling in eukaryotes, the *Dictyostelia* social amoebas are unicellular eukaryotes that shift to multicellular life forms via chemical communication that generates collective behavior in the population. Upon starvation, up to a million *Dictyostelium* cells aggregate and develop into fruiting bodies, in which a proportion of cells sacrifice their proliferative capacitie to build the stalk and the remainder differentiates into resilient dormant spores (reviewed in [73]). This process involves highly coordinated cell movement as well as tightly controlled cell differentiation, and is well studied in the model organism *Dictyostelium discoideum*.

During growth, unicellular *D. discoideum* amoebae constantly secret a glycoprotein called pre-starvation factor (PSF). When the ratio of PSF relative to that of bacterial food exceeds a threshold, cells stop proliferation. PSF, together with conditioned medium factor (CMF), a second glycoprotein secreted during starvation, potentiate cyclic adenosine monophosphate (cAMP) signaling by inducing genes involved in cAMP synthesis and detection [74, 75]. A few starving cells start to secret oscillatory pulses of cAMP [76], which are relayed and act as an extracellular chemoattractant leading to rapid aggregation of cells into multicellular mounds. As the pre-spore cells reduce the expression of proteins that are essential for generating and sensing cAMP gradients, the pre-stalk cells selectively move to the oscillating tip [77-79]. A resulting structure called ‘the slug’ migrates towards signals such as light and warmth to the top layer of the soil, and transforms into the fruiting structure [80].

At higher levels of complexity, multicellular animals possess specialized organs and neuronal circuits for pheromone sensation. Whereas general odors can give rise to many experience-dependent behaviors, pheromones in general appear to activate labeled-line pathways in which pheromone input leads to a direct behavioral or physiological output [52].

Insects principally sense pheromones by a class of sensory hair structures called trichoid sensilla that are distributed in the major olfactory organ antenna. Trichoid sensilla are innervated by the olfactory sensory neuron (OSN) that expresses odorant receptors (ORs) (reviewed in [81]). In the silk moth *Bombyx mori*, *BmOR1* and *BmOR3* members of the insect OR gene superfamily are specifically expressed in the male antenna and sense female sex attractant pheromones bombykol and bombykal, respectively [82, 83]. In *Drosophila melanogaster*, the volatile male pheromone *cis*-vaccenyl acetate (cVA) exhibits multiple functions; it elicits male–male aggression [84], suppresses male courtship towards males and mated females [34, 85, 86], attracts females to males [86], and promotes aggregation in both sexes [87, 88]. Two distinct circuits defined by odorant receptors Or67d and Or65a sense cVA [86, 89-91]. The Or67d function requires another membrane protein Or83b, an essential subunit for receptor complex and sensory neuron membrane protein (SNMP), and is facilitated by odorant-binding proteins such as LUSH [88, 92-94]. Action potentials evoked by cVA are transmitted along OSN axons to the antennal lobe, where Or67d-expressing OSNs converge onto the DA1 glomerulus [86, 95, 96].

In addition, non-volatile hydrocarbons on the cuticle sensed by gustatory receptors (GRs) modulate mating behavior in male flies. GR68a is expressed specifically

in male-specific sensilla on the forelegs, and facilitates normal courtship with females, presumably sensing female attractant [97, 98]. GR32a and GR33a are required for suppressing male courtship behavior to males or to mated females, presumably sensing inhibitory male pheromone [98-100].

The insect pheromone receptors are thought to be ionotropic, consisting of a heteromeric complex that serves as the ligand-gated ion channel [101]. The resulting fast responses to the olfactory environment may be advantageous in the evolution of flying insects, such as flies and moths, which need to identify their mates and food sources during flight [52]. In contrast to insects, vertebrates sense pheromones by metabotropic GTP-binding protein (G protein)-coupled receptors (GPCRs), activating a signaling pathway that produces an intracellular messenger such as cAMP, cGMP, or IP3 turnover [102-104].

In mammals, pheromone compounds are often found in the urine. Two separate olfactory organs in the nasal cavity express pheromone receptors and sense structurally diverse pheromone compounds: the main olfactory epithelium (MOE) and the vormeronasal organ (VNO) [98, 105-111]. In the MOE, the canonical olfactory sensory neurons (OSNs) that utilize cAMP-dependent signal transduction are thought to detect pheromones. In addition, a subset of OSNs that express the trace-amine-associated receptors (TAARs) or transient receptor potential channel TRPM5, and another subset of OSNs that are cGMP-dependent are thought to detect pheromones [108, 109, 111, 112]. Detection of the non-volatile major histocompatibility complex (MHC) class 1 peptides in urine by cAMP-sensitive OSNs in the MOE alters social preference of males [106]. The highly volatile (methylthio)methanethiol (MTMT) present in male urine

is detected by TRPM5-expressing OSNs in the MOE and enhances urine attractiveness to females [109, 113].

The VNO is the primary sensor of the accessory olfactory system (AOS) that seemingly specializes in social interactions. The vomeronasal sensory neurons (VSNs) in VNO express two distinct families of vomeronasal receptors (V1R and V2R) [114-116] and formyl peptide receptors (FPRs) [117, 118], and function via the activation of transient receptor potential cation channel C2 (TRPC2). VNO-mediated sensory signals are sent to glomeruli in the accessory olfactory bulb (AOB), which then projects to the basal forebrain to regions important for mating and aggressive behaviors. V1Rs recognize volatile pheromones such as 2-heptanone, a urine component that causes extension of the estrous cycle and promote aggressiveness and sexual behavior [119, 120]. V2Rs sense non-volatile polypeptide ligands including major urinary proteins (MUPs), MHC peptides, and the exocrine gland–secreting peptide (ESP) family [121]. The MUP complex, comprised of specialized lipocalin proteins bound to small organic molecules [122, 123], activates the VNO circuit via V2Rs, leading to male-male aggression [124]. MHC class 1 peptide elicits sensory responses in V2R-expressing VSNs and mediates the formation of a pheromone recognition memory in females [125]. In addition, non-volatile sulphated steroids that are present in mouse urine activate VSNs, presumably informing the physiological status of the donor [126].

The nematode *Caenorhabditis elegans* senses pheromones via ciliated sensory neurons located in the amphid, a pair of laterally located sensilla in the head that are open to the external world. Ascarosides, the identified *C. elegans* pheromone component, are a family of derivatives of the dideoxysugar ascarylose linked to fatty acid-like side chains

of different lengths and occasionally other functional groups [127-132]. The ascarosides have individual or synergistic activities that serve as male attractants at lower concentrations and as population density signals at higher concentrations, regulating entry into the non-feeding and highly persistent dauer larva stage of *C. elegans* development [127, 129, 132, 133]. The chemoreceptors SRBC-64 and SRBC-66 expressed in the bilateral ASK amphid chemosensory neuron pair mediate dauer formation in response to a subset of ascarosides- ascr#5/C3, ascr#2/C6, and ascr#3/C9 [133]. Like vertebrate pheromone receptors, SRBC-64 and SRBC-66 are metabotropic; they are heterotrimeric G protein-coupled receptors (GPCRs) that activate the Gα protein GPA-3-dependent signaling pathway and inhibit DAF-11 guanylate cyclase activity, downregulating cGMP levels in ASK [133]. Members of another chemosensory receptor family, SRG-36 and SRG-37, detect ascr#5/C3 in ASI chemosensory neurons and promote dauer formation [134].

C. elegans as a model system for social behavior

Although the chemical communication systems in each species are being elucidated in more detail, the central issue of how genes and molecular components generate circuits that eventually lead to complex social behaviors remains unclear. Human genetic and genomics studies have identified numerous synaptic molecules associated with autism and schizophrenia, suggesting that there is an important component of social function that arises at the level of the synapse [135]. The nematode *Caenorhabditis elegans* is a good model organism to study social behaviors at genetic and circuit levels. It is a multicellular animal with a short lifespan of three weeks, yet it

has diverse social behaviors including aggregation (social feeding) [136], male-hermaphrodite mating [137, 138] and regulation of entry into dauer, an alternative developmental stage [139, 140]. Genetic analysis in this organism is convenient because strains can be propagated as self-fertilizing hermaphrodites producing about 300 genetically identical progeny from a single animal, and can also be propagated as interbreeding males and hermaphrodites. Circuit analysis is convenient because it has a small nervous system consisting of only 302 neurons in hermaphrodites and 473 neurons in males, whose positions are reproducible between individuals and whose anatomical connectivity has been elucidated by electron microscopy [141].

Aggregation, also called social feeding, is one of the social behaviors observed in *C. elegans*. A group of individuals at one location is referred to as an aggregate, whether consisting of one sex or both sexes. Aggregation of *C. elegans* occurs in all developmental stages, and is naturally regulated by the animal's sex (males have a higher propensity to aggregate) as well as by environmental cues.

Among environmental cues, food is an important regulator of aggregation. Aggregation is commonly observed and studied in the presence of food. Animals clump in aggregates consisting of a few to hundreds of worms, usually along the edge of a bacterial lawn where the bacterial density is high [136]. Aggregation behavior has been best studied in a high-aggregating (social) strain with a strong loss-of-function mutation in the *npr-1* gene, which will be described below. It is also observed in most wild strains and in the standard lab strain N2 background under specific conditions, for example immediately after removal of food.

Oxygen is another important environmental cue that regulates aggregation. Aggregation is strongest at 21% oxygen, and is suppressed at lower levels of oxygen [142]. Worms are naturally found in low-oxygen environments, so oxygen is likely to act as a metabolic stressor at atmospheric levels. Within an aggregate, worms consume oxygen to lower it to their desired levels [143]. A preference for lower oxygen levels also explains why worms prefer the edge of a bacterial lawn, which is denser and therefore has lower oxygen levels [142].

In addition, density is a regulator of aggregation; increased population density accelerates and enhances aggregation [144]. Stressful conditions in general may also stimulate aggregation [144], consistent with observations in other animals and the social amoeba *Dictyostelium discoideum* [1, 73].

Genetic analysis has defined molecules and circuits involved in aggregation. Genes have been identified both by finding mutations that increase aggregation, like the *npr-1(lf)* mutant, and by finding mutations that decrease aggregation in high-aggregating strains. The *npr-1* mutant that causes high aggregation affects a neuropeptide receptor related to neuropeptide Y receptors [136]. It was first identified as a loss of function mutation in the wild-type N2 strain. Most wild-type *C. elegans* strains aggregate more than N2, and this behavior is associated with a polymorphism that affects a coding residue in NPR-1, changing a single amino acid (215) from valine in N2, to phenylalanine in the high-aggregating strains [136]. In genetic assays, the *215F* allele has lower activity than the *215V* allele, but more activity than a null mutation [136, 144, 145]. Although the 215F/V change was initially believed to be a natural polymorphism, it was subsequently recognized that the 215V high-activity allele arose in the laboratory in

association with the domestication of N2, and increases the success of laboratory strains in multiple assays [146].

The *npr-1* polymorphism affects aggregation by modifying responses to several environmental cues. First, *npr-1* or wild strains with the *npr-1(215F)* allele avoid high oxygen levels on food more robustly than the N2 strain with the *npr-1(215V)* allele [142, 143]. This oxygen avoidance on food promotes accumulation at the border and retention in aggregates in *npr-1* strains. All strains show strong avoidance of high oxygen levels in the absence of food, indicating the existence of an *npr-1*-independent sensory response. A second modified response that might be relevant to aggregation is tolerance to carbon dioxide (CO_2) [147, 148]. The wild-type N2 *npr-1(215V)* strain avoids acute CO_2 stimulus as low as 1% and accumulates at concentrations lower than 1% in a linear CO_2 gradient, whereas strains with reduced *npr-1* activity do not avoid CO_2 [147, 148]. As CO_2 levels are higher within an aggregate, it is possible that tolerance of high CO_2 contributes to aggregation, although there is not a direct behavioral evidence supporting this hypothesis. A third response modified by *npr-1* is the response to pheromones. Animals with reduced *npr-1* function exhibit mild attraction or reduced repulsion to certain identified ascarosides [149], while wild-type N2 with the *npr-1(215V)* allele is repelled by higher concentration of ascarosides [132, 149]. Ascarosides should be present at higher levels within an aggregate, but it is unclear whether pheromone production and perception is required for aggregation; this question will be discussed further in the thesis.

As mentioned earlier, both wild-type N2 strains with the *npr-1(215V)* allele and wild strains with the *npr-1(215F)* allele are able to aggregate in some circumstances.

Thus, the *npr-1* mutation does not affect the ability to aggregate, but the probability that aggregation occurs in particular environments.

Another set of mutations that suppress aggregation in the wild-type N2 *npr-1(215V)* strain are a set of genes involved in transforming growth factor beta (TGF-β) signaling – *daf-7* encoding TGF-β, *daf-1* and *daf-4* encoding its receptors, and *daf-8* and *daf-14* encoding downstream signaling components [150]. Animals with mutations in these genes aggregate in a wild-type N2 *npr-1(215V)* background and aggregate more strongly in an *npr-1* mutant background, indicating that this signaling pathway is independent or parallel of the *npr-1* pathway [144]. This TGF-β pathway is best characterized for its role in regulating dauer formation, where it mediates the detection of stressful conditions such as crowding and high density [140]. The behavioral phenotypes of TGF-β stress-sensing mutants, together with the known roles of environmental stressors in promoting aggregation, support the conclusion that aggregation is a stress-induced behavior.

Genetic suppressors of aggregation in *npr-1* mutant strains or wild strains with the *npr-1(215F)* allele have yielded insights into genes that promote aggregation (summarized in Table 3-1 in Chapter 3). Many sensory mutants that affect nociception are defective in aggregation. For example, mutations in the oxygen sensors *gcy-35* and *gcy-36,* a pair of guanylyl cyclase required for oxygen avoidance, suppress aggregation [142, 151]. Mutations in the transient receptor potential vanilloid (TRPV) channels *ocr-2* and *osm-9* also suppress aggregation, due to their action in the ASH and ADL nociceptive neurons [144]. Mutations in the cGMP-gated channel genes *tax-2* and *tax-4*

suppress aggregation both by diminishing oxygen sensation [142, 152], and by reducing the function of pheromone- and food-sensing ASK neurons [149].

Current understanding of the circuit for aggregation behavior is based on characterization of the site of *npr-1* action, and is called "the hub and spoke circuit" (see Figure 2-5d in Chapter 2). In this model, various environmental and social cues discussed above are sensed by multiple sensory neurons – the spokes – whose functions require many identified genetic suppressors of aggregation in *npr-1.* The spokes include ASH and ADL the nociceptive neurons, URX the oxygen-sensing neurons, and ASK the pheromone-sensing neurons. The sensory inputs from these spokes are integrated and coordinated by the RMG interneurons – the hub – through a network of gap junctions predicted by the *C. elegans* wiring diagram [141, 149]. RMG then promotes aggregation by regulating body movement via chemical synaptic output to head muscles, motorneurons and command interneurons [149]. RMG is the site of action for *npr-1* in the regulation of aggregation behavior. In wild-type N2 strain, NPR-1 215V inhibits RMG, thereby uncoupling the sensory inputs and preventing aggregation. In *npr-1* mutants or wild strains with the *npr-1* (215F) allele, elevated RMG activity and active communication between RMG and the spoke neurons promote aggregation and related behaviors [149].

In my thesis, I sought to study social aggregation behavior at genetic and circuit levels. First, I examined the circuit for responses to one pheromone, the ascaroside ascr#3/C9, using genetic and circuit manipulation approaches combined with neuronal imaging. In Chapter 2, I will discuss the neural circuit that mediates behavioral avoidance of ascr#3/C9. The circuit involves ADL neurons, and is modulated by *npr-1*, by sexual

polymorphism of the circuit, and by another pheromone ascr#5/C3. Second, I sought to identify new genes that regulate aggregation in *npr-1* social animals. In Chapter 3, I will describe those genetic and behavioral experiments, including forward and reverse genetic screens.

Chapter 2:

A regulated circuit for behavioral responses to pheromones

This study was carried out in collaboration with Piali Sengupta and Kyuhyung Kim, who measured *in vivo* Ca^{2+} responses in ADL, ASH and ASK neurons by fluorescence imaging using genetically-encoded Ca^{2+} indicators.

Introduction

Animals evoke physiological or behavioral changes in conspecifics or heterospecifics using multiple lines of sensory communication: chemical, auditory, visual, tactile and electrical [1]. Chemical communication is particularly diverse, as the chemical structure, potency, temporal window of synthesis and secretion, and spatial range can vary greatly. Moreover, different combinations of molecules and different proportions of components can increase the variety of signals. For example, the number of chemical signals used in moth species reaches 2931 combinations from 377 unique chemicals of sex pheromone attractants [153]. Due to these features, pheromones used in chemical communication in lower organisms are sometimes described as a chemical language.

In *C. elegans* and other nematodes, chemical pheromone cues are important regulators of development and of male mating [139, 154-156]. Despite their biological significance and a long history of study, the molecular identity of *C. elegans* pheromones started to be elucidated only a few years ago [130]. The identified *C. elegans* pheromones are ascarosides, a family of derivatives of the dideoxysugar ascarylose linked to fatty acid-like side chains of different lengths and occasionally other functional groups [127-132]. The ascarosides have individual or synergistic activities that serve as a population density signal regulating entry into the non-feeding and highly persistent dauer larva stage of *C. elegans* development [127, 129, 133]. In the pheromone literature, this function is defined as a primer effect that triggers a change in developmental events.

The same set of ascarosides can act as releaser pheromones, defined as changing the probability of performing a certain behavior upon perception. Many ascarosides have

male attraction activities, as listed in Table 2-1 [131, 132]. Another releaser effect is observed in hermaphrodites from the standard laboratory strain N2 (henceforth referred to as 'wild-type') background, which are strongly repelled by ascr#2/C6 and ascr#3/C9 [132, 149]. By contrast, these ascarosides are only mildly repulsive to aggregating *npr-1* mutant adult hermaphrodites, and can be mildly attractive in a mixture with ascr#5/C3 [149]. Among the ascarosides, ascr#3/C9 is a highly potent male attractant and dauer pheromone. It is secreted until the young adult stage, and its peak production correlates well with the temporal window for mating [157]. Another pheromone compound ascr#5/C3 has no male attraction activities [131] but it has synergistic activities in ascr#2/C6 and ascr#3/C9 for dauer formation [129]. Its timing of expression is unknown. These two pheromones are examined in more detail in this thesis.

In this Chapter, I will discuss the neural circuit for avoidance responses to identified ascarosides mainly focusing on ascr#3/C9. This avoidance behavior is modulated by presence of ascr#5/C3. In addition, a parallel mechanism generates sexual dimorphism in pheromone responses leading to reduced ascr#3/C9 avoidance in males. I show that the hub-and-spoke circuit regulated by the neuropeptide receptor NPR-1 diminishes ascr#3/C9 avoidance in the *npr-1(lf)* strain. I will also briefly discuss the potential relevance of the pheromone circuit to the aggregation behavior observed in *npr-1* social mutants.

Results

The ADL neurons detect the repulsive *C. elegans* pheromone ascr#3/C9

As an efficient and powerful readout to quantify avoidance behavior, the drop test was used [158]. In this assay, a drop of a repellent dissolved in buffer is presented to an animal moving forward, and the resulting long reversal responses are compared to those to buffer alone [158] (Figure 2-1a, see Materials and Methods). Using this assay, I examined the responses of wild-type hermaphrodites to a series of individual ascarosides that are relatively potent for male attraction and dauer formation (Table 2-1). Wild-type hermaphrodites specifically avoided ascr#3/C9, but not other ascarosides including ascr#5/C6, ascr#9/C5, ascr#2/C6 and ascr#8/C7-PABA. 2M glycerol, a high osmotic strength repellent sensed by ASH neurons [159] elicited strong avoidance in wild-type animals, serving as a positive control that the animals were capable of making long reversals to repellents (Figure 2-1b).

The ADLL/R (ADL) and ASHL/R (ASH) sensory neuron pairs have previously been implicated in mediating avoidance of chemical repellents [158]. These neurons signal through OSM-9 and OCR-2 transient receptor potential channel, vanilloid (TRPV) channels [158, 160-165]. Both *osm-9(ky10)* and *ocr-2(ak47)* mutants exhibited strong defects in ascr#3/C9 avoidance (Figure 2-2a). The ascr#3/C9 avoidance defects of *ocr-2(ak47)* mutants were rescued upon expression of wild-type *ocr-2* genomic sequences in ADL, but in not in other *ocr-2*-expressing neurons (Figure 2-2b) indicating that OCR-2 can act in the ADL neurons to mediate ascr#3/C9 avoidance. *ocr-2* expression in the ASH nociceptive neurons did not rescue the ascr#3/C9 avoidance defects, although the

defects in ASH-mediated avoidance of high osmotic strength solutions were fully rescued [165] (Figure 2-2b). According to the sensory transduction model in ADL, the binding of ascr#3/C9 molecules to the unknown ascr#3/C9 receptor is followed by the G protein-regulated activation of OSM-9/OCR-2 TRPV channels, which allow the influx of Na^+ and Ca^{2+} ions, leading to the depolarization of ADL (Figure 2-2d). Although we found evidence for a TRPV requirement, we do not know the nature of the other elements of this transduction cascade for ascr#3/C9. The known pheromone receptors *srbc-64(tm1946);srbc-66(tm2943)* have no defect in ascr#3/C9 avoidance (Figure 2-2c). This is not surprising since they are not expressed in ADL [133]. We also failed to find a defect in ascr#3/C9 avoidance in *odr-8(ky173),* which is mutant for ciliary localization of some chemoreceptors [166], or in several mutants of G protein subunits with reported ADL expression [167, 168] (Figure 2-2c).

To test the hypothesis that ADL directly senses ascr#3/C9, we used a microfluidic system to deliver ascarosides to the nose of a worm that expressed the genetically encoded calcium (Ca^{2+}) sensor *G-CaMP3.0* [169] in the ADL neurons, and monitored intracellular Ca^{2+} dynamics in ADL [170] (Figure 2-3a, see Materials and Methods). These animals had no behavioral defect in ascr#3/C9 avoidance (Figure 2-3b), indicating that *G-CaMP3.0* molecules did not eliminate intracellular sensory transduction in ADL. A pulse of ascr#3/C9 induced a rapid and transient increase in ADL intracellular Ca^{2+} levels (Figure 2-3c and Figure 2-3d), which was abolished in *ocr-2(ak47)* mutants (Figure 2-3d). Consistent with ascr#3/C9-specific avoidance mediated by ADL, the ASH neurons did not respond to this ascaroside or to other pheromone components with Ca^{2+} transients (Figure 2-3e), and no changes in Ca^{2+} dynamics were observed in the ADL

neurons upon addition of ascr#5/C3 or ascr#2/C6 ascarosides, either singly or in combination (Figure 2-3f).

To determine whether the ADL response was direct or perhaps an indirect signal relayed to ADL from another sensory neuron, we examined *unc-13*, a mutant defective in neurotransmitter release [171]. *unc-13* mutants had a normal Ca^{2+} response to ascr#3/C9 in ADL (data not shown). These results suggest that wild-type hermaphrodites directly sense ascr#3/C9 via OCR-2/OSM-9 TRPV sensory channel function in the ADL sensory neurons (Figure 2-2d). The ADL Ca^{2+} response was not maintained during longer exposure to ascr#3/C9, showing fast adaptation compared to other sensory responses. In addition, the response to a second pulse was highly reduced (Figure 2-3d), although it recovered to baseline after ~60 seconds. The significance of these observations is not known.

The anatomical wiring diagram of *C. elegans* hermaphrodites indicates that the ADL neurons signal via chemical synapses to the AVA and AVD backward command interneurons, as well as several other interneurons that regulate body movement (Figure 2-4a) [141, 172]. In the simplest model, ADL-mediated avoidance behavior could be driven via synaptic output of the ADL neurons and activation of the backward command interneurons. To examine this possibility, we either inhibited ADL synaptic output via cell-specific expression of the tetanus toxin light chain (*TeTx*) [173], or potentiated ADL activity by expressing a constitutively active protein kinase C allele (*pkc-1(gf)*) that stimulates neuropeptide release and possibly neurotransmitter release [174, 175]. Blocking synaptic transmission in ADL significantly suppressed ascr#3/C9 avoidance responses, whereas enhancement of ADL output increased avoidance (Figure 2-4b and 2-

4c). Control experiments demonstrated that the ADL transgenes did not affect the osmotic avoidance behavior mediated by the ASH neurons (Figure 2-4b). Conversely, transgenes that affected ASH synaptic transmission interfered with osmotic avoidance behavior, but not with ascr#3/C9 avoidance. Thus, the ADL neurons promote ascr#3/C9 avoidance via chemical synaptic transmission (Figure 2-4a).

Suppression of ascr#3/C9 avoidance in *npr-1* social mutants

Hermaphrodites with mutated or naturally-occurring low-activity alleles of the *npr-1* neuropeptide receptor gene aggregate in the presence of food (Figure 2-5a) and exhibit a variety of associated sensory changes, including repulsion from high oxygen levels, tolerance to carbon dioxide, altered locomotion on food, and mild attraction to ascaroside mixtures [136, 142, 143, 147, 149]. Consistent with the increased attraction and aggregation behaviors exhibited by *npr-1* mutants [136, 149], the loss of function mutant *npr-1(ad609)* exhibited decreased avoidance of lower ascr#3/C9 concentrations in the drop test (Figure 2-5b and 2-5c). The effective concentration of ascr#3/C9 for avoidance was lower in the presence than in the absence of food, for both wild-type and *npr-1* genotypes (Figure 2-5b and 2-5c).

NPR-1 suppression of aggregation requires the RMG inter/motorneurons, which form the hub of a neuronal circuit that is connected to sensory neuron spokes via gap junctions (Figure 2-5d) [141, 149]. Reduced NPR-1 signaling activates RMG, which in turn increases the pheromone responsiveness of the ASK spoke chemosensory neuron to promote aggregation [149]. Like the ASK neurons, the ADL neurons are spokes of the hub-and-spoke circuit that are connected to RMG via gap junctions (Figure 2-5d) [141].

We therefore investigated whether ADL responses are also regulated by NPR-1 function in RMG. Indeed, the defect in ascr#3/C9 avoidance of *npr-1* mutants was rescued upon expression of wild-type *npr-1* sequences in RMG (Figure 2-5e), indicating that NPR-1 acts in RMG to potentiate ADL-dependeant ascaroside avoidance.

Ca^{2+} imaging of ascr#3/C9-induced Ca^{2+} responses in ADL neurons were qualitatively similar in *npr-1* mutants and in wild-type animals (Figure 2-6a), although there were subtle changes in the dynamics and magnitude of the response (Figure 2-6a and data not shown). ascr#3/C9 avoidance in *npr-1(ad609)* animals was not altered by *G-CaMP3.0* expression (Figure 2-6b), confirming that *G-CaMP3.0* molecules did not disturb the ascr#3/C9 avoidance circuit. These results suggest that NPR-1 activity in RMG has a subtle effect on sensory responses in ADL.

Silencing ADL synaptic output in *npr-1* mutants via cell-specific expression of *TeTx* had no further effect on their weak behavioral responses to ascr#3/C9 (Figure 2-6c). However, potentiation of ADL via cell-specific expression of *pkc-1(gf)* in *npr-1* mutants resulted in robust ascr#3/C9 avoidance behavior (Figure 2-6c). This enhanced avoidance behavior was suppressed upon co-expression of *TeTx* in ADL, suggesting that it requires synaptic output (Figure 2-6c). The ADL::*TeTx* and ADL::*pkc-1(gf)*se transgenes did not affect ASH-mediated avoidance of glycerol (Figure 2-6c). Thus, it appears that the *npr-1*-regulated RMG gap junction circuit (which includes ADL) acts antagonistically to the ADL chemical synapses to regulatein ascr#3/C9 avoidance (Figure 2-8g).

The proposed ligands of NPR-1 are FLP-21 and FLP-18, with stronger genetic and biochemical evidences for a role of FLP-21 [145] . *flp-21* mutants had a defect in ascr#3/C9 avoidance that resembled the defect in *npr-1* mutants on and off food (Figure

2-6d and 2-6e). These preliminary results suggest that FLP-21, encoding GLGPRPLRFamide, could be an NPR-1 ligand that regulates ascr#3/C9 avoidance. As a broader examination of the roles of secreted neuropeptides in ascr#3/C9 avoidance, the neuropeptide synthesis mutants *egl-3(n150ts)* and *egl-21(n611)* were examined. EGL-3/Proprotein convertase 2 cleaves a peptide precursor at dibasic or monobasic sites to generate prepetides, and EGL-21/Carboxypeptidease removes C-terminal basic amino acids from intermediate peptides to generate mature peptides [176-178]. *egl-21(n611)* but not *egl-3(n150ts)* had a defect in ascr#3/C9 avoidance in the wild-type background (Figure 2-6d), consistent with the possibility that EGL-21 processes a ligand for NPR-1.

Suppression of ascr#3/C9 avoidance in males

Unlike wild-type hermaphrodites, males from the wild-type *C. elegans* strain are attracted to very low ascaroside concentrations [132]. Male attraction behavior to ascr#3/C9 requires the ASK neurons and the male-specific CEM sensory neurons [132]. In addition, we found that wild-type males did not avoid high concentrations of ascr#3/C9 in the drop test (Figure 2-7a).

The altered male responses to ascarosides were associated with sexually dimorphic sensory responses in the ADL neurons. ascr#3/C9 induced intracellular Ca^{2+} dynamics in the ADL neurons in males, but these responses were dampened and significantly delayed in wild-type males compared to hermaphrodites (Figure 2-7b). As was observed in *npr-1* mutants, enhancement of ADL synaptic output by expression of *pkc-1(gf)* was sufficient to induce avoidance of high ascr#3/C9 concentrations (Figure 2-7c). These functional and behavioral experiments indicate that male ADL neurons are

deficient in responding to ascr#3/C9 compared to hermaphrodites, but maintain a partial response.

In *C. elegans*, the sexual fate of the majority of somatic cells including neurons is largely determined by a well-described genetic cascade that acts in a cell autonomous manner [179]. Cellular sexual fate can be switched by manipulating the *tra-1* master switch gene or its regulator *fem-3* [180-184]. We examined whether the sexual identity of the ADL neurons confers sex-specific sensory responses by overexpressing the FEM-3 protein in hermaphrodite ADL neurons and examining ascr#3/C9 avoidance behavior and ascr#3/C9-induced Ca^{2+} dynamics. Masculinization of ADL using *sre-1* or *srh-234* promoters partially reduced the C9 avoidance behavior of hermaphrodites (Figure 2-7d). However, masculinized ADL neurons continued to exhibit robust Ca^{2+} responses to ascr#3/C9 (Figure 2-7e). Thus, the intrinsic sexual identity of ADL may have a partial role in avoidance, but it is not sufficient to generate fully male-like behavioral or functional responses to ascr#3/C9. More widespread expression of FEM-3 under a pan-neuronal *rab-3* promoter led to further masculinization of hermaphrodite behavior (Figure 2-7e), but ADL Ca^{2+} responses have not been examined in this strain, so the identity of the neurons that alter ADL calcium signals remains to be determined.

The decreased sensory responses to ascr#3/C9-induced calcium transients in male ADL neurons were reduced, like those in *npr-1* mutant hermaphrodites (compare Figures 2-6a and 2-7b). *npr-1* mutations and male development could represent two distinct ways to modulate ascr#3/C9 responses in ADL, or alternatively, could represent a common pathway, i.e. *npr-1* mutations could activate wild-type male behaviors in hermaphrodites. To distinguish between these two possibilities, we compared ascr#3/C9 responses in *npr-*

1 males and wild-type males. Both behavioral results and Ca^{2+} dynamics in the ADL neurons indicated that *npr-1* mutations and male development had independent, additive effects on ascr#3/C9 responses. First, ascr#3/C9 strongly suppressed spontaneous reversals in *npr-1* males, an effect it did not have oan either wild-type males or *npr-1* hermaphrodites (Figure 2-8a). Second, the majority of ADL neurons in *npr-1* mutant males failed to exhibit any significant change in Ca^{2+} levels upon ascr#3/C9 addition (Figure 2-8b), a stronger effect than was observed in wild-type males or in *npr-1* mutant hermaphrodites. These results indicate that NPR-1 and male sexual identity act via parallel and additive pathways to regulate ascr#3/C9pheromone responses.

Based on the biased random walk model for chemotaxis behaviors in *C. elegans,* the suppression of spontaneous reversals by ascr#3/C9 in *npr-1* males suggests that they are attracted to this pheromone (Figure 2-8a) [185, 186]. We next asked whether NPR-1 acts in the RMG neurons to promote this attraction-related behavior. Expression of wild-type *npr-1* sequences in RMG was sufficient to shift the ascr#3/C9 behavioral responses of *npr-1* males toward those exhibited by wild-type males, with failure to avoid or be attracted to lower ascr#3/C9 concentrations (Figure 2-8c). Moreover, whereas inhibition of RMG synaptic output via expression of *TeTx* had no effect on the behavior of wild-type males (Figure 2-8c), the attraction to ascr#3/C9 in *npr-1* males was abolished (Figure 2-8c). Thus, both in males and in hermaphrodites, NPR-1 acts via RMG to regulate behavioral responses to ascr#3/C9.

Interestingly, enhancing ADL synaptic activity via expression of the *pkc-1(gf)* induced avoidance of ascr#3/C9 in *npr-1* males, suggesting that the chemical synapses regulated by ADL and the RMG gap junction circuit antagonize each other in males as

well as hermaphrodites. The suppression of reversals by ascr#3/C9 in *npr-1* males suggests that additional *npr-1*-regulated neurons may mediate attraction to ascr#3/C9. Strong candidates for this activity are the ASK amphid sensory neurons or male-specific CEM neurons, which promote male attraction to ascr#3/C9 in a different behavioral assay [132]. Indeed, calcium imaging experiments indicated that ASK neurons were highly responsive to ascr#3/C9 in *npr-1* males, with substantially stronger responses than wild-type hermaphrodites or wild-type males (Figure 2-9a). Taken together, these results suggest that avoidance behavior is decreased in males due to diminished ADL ascr#3/C9 sensory responses, and in addition, loss of NPR-1 function in *npr-1* males enhances ASK responses to ascr#3/C9, leading to attraction (Figure 2-9b).

ascr#5/C3 modulates ascr#3/C9 avoidance in *npr-1* mutants

Unlike wild-type hermaphrodites that avoid ascr#3/C9, *npr-1* mutant animals hermaphrodites are weakly attracted to mixtures of ascarosides, including the ascr#3/C3 and ascr#3/C9 cocktail, but not to single compounds alone [149]. Attraction requires the ASK sensory neurons which respond most robustly to ascr#5/C3 [133]. The ADL neurons have been shown to promote aggregation of hermaphrodites in *npr-1* mutants [144]; based on these results and by analogy with the detection of pheromone blends in other animals [187], the synergistic attraction to blends could result from the recruitment of multiple pheromone-sensing neurons. Therefore, we considered the possibility that ascr#3/C9 sensation by ADL and ascr#5/C3 sensation by ASK interact to antagonize repulsion to ascaroside blends (Figure 2-10c). To address this hypothesis, we used the drop test to detect interaction between pheromones. As described above for male

responses to ascarosides, attractive responses are associated with a suppression of basal reversal rates [185, 186]. Therefore, we reasoned that addition of an attractive chemical in the drop test would suppress the reversal responses to buffer or repellents. To assist in tracking this suppression in reversal rates, assays were performed in the presence of bacterial food, where the basal reversal rate to buffer alone was higher than in the absence of food.

In agreement with the observation that ascr#5/C3 is not highly attractive or repulsive on its own [149], ascr#5/C3 did not induce or suppress reversals to buffer in wild-type or *npr-1* animals hermaphrodites (Figure 2-10a). However, ascr#5/C3 did modify the response to ascr#3/C9 in an *npr-1*-dependent manner. This experiment was conducted with concentrations of ascr#3/C9 (100 nM) that reliably induced avoidance in both wild-type and *npr-1* mutants hermaphrodites (Figure 2-5b). Adding 100 nM ascr#5/C3 to an equal concentration of ascr#3/C9 increased reversals in wild type hermaphrodites, suggesting that the combination of pheromones was more repulsive than ascr#3/C9 alone. By contrast, the mixture of ascr#5/C3 and ascr#3/C9 suppressed reversals in *npr-1* mutants hermaphrodites compared to ascr#3/C9 alone (Figure 2-10a). These results indicate that ascr#5/C3, a neutral pheromone component, differentially modulates behavioral responses to ascr#3/C9 depending on the *npr-1* genotype. The interaction appears to be specific to pheromones, because the attractive odor isoamyl alcohol (IAA), which suppresses basal reversals, does not suppress ascr#3/C9-induced reversals (Figure 2-10c).

We next examined the neuronal basis of the behavioral interaction between ascr#5/C3 and ascr#3/C9 in *npr-1* hermaphroditesmutants. The ASK neurons sense

ascr#5/C3 and are required for attraction to pheromone blends [133, 149], so they were a likely source of the interaction. Genetic ablation of the ASK neurons in *npr-1* mutants hermaphrodites abolished the interaction between ascr#5/C3 and ascr#3/C9 without affecting responses to ascr#3/C9 alone (Figure 2-10b). With the limitation that the drop test probably captures only a subset of behaviors relevant to pheromone attraction in vivo [188], these results are consistent with a circuit tuned to pheromone blends, where ascr#5/C3 detected by ASK only suppresses reversals if ascr#3/C9 is also present and detected by ADL.

ASK-mediated attraction to pheromone mixtures requires RMG, the hub of the hub-and-spoke circuit, and partly depends upon RMG synaptic output [149]. Inhibiting the synaptic output of RMG by expressing *TeTx* in the RMG neurons of *npr-1* hermaphroditemutants eliminated the behavioral interaction between ascr#5/C3 and ascr#3/C9 without affecting avoidance of ascr#3/C9 alone (Figure 2-10b). Restoring wild-type *npr-1* function in RMG neurons of *npr-1* mutants hermaphrodites also eliminated the behavioral interaction between ascr#5/C3 and ascr#3/C9 in *npr-1* mutants (Figure 2-10b), indicating that the interaction depends on the hub-and-spoke circuit. Together, these observations suggest that the behavioral interaction between ascr#5/C3 and C9 requires the ASK and ADL sensory neurons to act via the gap junction circuit with RMG. By contrast, avoidance of C9 alone occurs via ADL chemical synapses, and does not require RMG (Figure 2-10c).

Synaptic outputs from ADL and ASH regulate aggregation behavior in *npr-1* social mutants

The ADL and ASH neurons are required for aggregation and bordering behavior, as evidenced indicated by genetic mutants and cell ablations [144]. It is possible that this function is related to the ADL ascr#3/C9 pheromone detection activity described here. To test this hypothesis, we asked whether synaptic output from ADL and/or ASH regulates aggregation. The synaptic activities of ADL and ASH were altered by expressing *TeTx* and *pkc-1(gf)* constructs in ADL alone, ASH alone, or ADL+ASH neurons, in an *npr-1* mutant background, and the resulting animals hermaphrodites were tested for behavior. Simultaneous synaptic inhibition of both ADL and ASH enhanced aggregation (Figure 2-11a), suggesting that chemical synapses from these neurons antagonize the behavior. Conversely, simultaneous activation of synaptic output form ADL and ASH suppressed aggregation (Figure 2-11a). Bordering behavior was unaffected in all genotypes (Figure 2-11b), presumably due to the ceiling effect of the high bordering index in *npr-1* mutant background. These results suggest that the synaptic output of ADL and ASH inhibits aggregation behavior, reinforcing the importance of the gap junction circuit in the aggregation-promoting activities of these neurons.

Discussion

The conclusions of this chapter are summarized in Figure 2-9a and 2-10c. We found that ADL senses ascr#3/C9. In wild-type hermaphrodites, chemical synapses from ADL promote avoidance of ascr#3/C9. In *npr-1* hermaphrodites, the gap junction circuit suppresses ADL-mediated avoidance of ascr#3/C9, and ASK and ascr#5/C3 sensed by ASK can further antagonize ADL-mediated avoidance of ascr#3/C9. In wild-type males, ADL is less responsive to ascr#3/C9 and less able to drive avoidance; this effect is at least partly non cell-autonomous. In *npr-1* males, the ascr#3/C9 response in ADL is even weaker, and the behavioral response to ascr#3/C9 is shifted to attraction. In addition, *npr-1* males have a stronger ASK response to ascr#35/C93, suggesting multiple changes in the gap junction circuit.

ascr#3/C9 elicits Ca^{2+} dynamics in ADL and immediate reversal behavior

In wild-type hermaphrodites, acsr#3/C9 elicits a sharp and immediate rise in Ca^{2+} level in ADL as well as immediate backward movement. In the independent Ca^{2+} imaging experiment performed in our laboratory using 10 second pulses of 1 μM ascr#3/C9, the Ca^{2+} transients can be detected within 0.37 ± 0.24 s on average, and peak at 2.96 ± 0.53 seconds. Backward movement initiates within 1 second upon exposure to ascr#3/C9 and is completed within 3 seconds (Figure 2-1a). Thus, the kinetics of neuronal activity and behavioral responses to ascr#3/C9 are well-correlated.

Loss of NPR-1 function alters ADL Ca^{2+} dynamics. In *npr-1* hermaphrodites, Ca^{2+} transients can be detected within 0.48 ± 0.30 seconds, but they peaked significantly

more slowly than in wild-type at 4.82 ± 2.19 seconds ($P<0.05$, compared to the wild-type value by two-tailed unpaired t-test). The slower and perhaps smaller and more sustained responses in ADL may be consistent with participation in a gap junction circuit, which would dilute the sensory input over the coupled cells.

The parallel behavioral circuit regulated by sex and *npr-1*

Wild-type males and *npr-1* hermaphrodites share some behavioral traits. They aggregate on the border of bacterial food (Figure 2-8e), avoid high oxygen level and accumulate at 7-14% O_2 (see Appendix 2-B), move quickly in the presence of food [149], and exhibit attraction or reduced avoidance of ascaroside pheromones (Figure 2-5b, 2-5c and 2-7a, [149]). However, our observations suggest that neuronal sex and NPR-1 neuropeptide receptor signaling in the hub-and-spoke circuit represent two parallel mechanisms for modulating pheromone responses (Figure 2-9b). In wild-type males and hermaphrodites, avoidance of ascr#3/C9 is potentiated by ADL chemical synapses; in *npr-1* mutant males and hermaphrodites, this function is antagonized by the ADL gap junction circuit with RMG (Figure 2-9b). We speculate that *npr-1* differentially regulate ADL gap junction circuit while sparing its chemical synapses, a model reminiscent of the regulation of flexible outputs from central pattern generators via neuromodulation [189, 190]. The effects of neuronal sex are evident when examining ADL calcium responses to ascr#3/C9: wild-type and *npr-1* males have diminished responses compared to hermaphrodites. These changes are non cell-autonomous to ADL and probably due to other changes to the core nervous system (Figure 2-9b). *npr-1* affects ASKDL calcium signals as well. In particular, hermaphrodites, there are subtle striking sensory changes

between wild-type male and *npr-1* male ADL responses to ascr#3/C9, but these changes are marked when comparing wild-type and *npr-1* males.

The sexually dimorphic behavior to ascr#C3/C9 in *C. elegans* seems to involve multiple lines of dimorphism in the nervous system. ADL senses ascr#3/C9 both in males and in hermaphrodites. However, the non cell-autonomous male differences in ADL calcium signals and behavioral functions suggest that other neurons affect ADL activity. Among the possible explanations are contributions from male-specific neurons, or sexually dimorphic chemical or electrical connections.

Sexual dimorphism in behavioral responses to pheromone is achieved using a variety of strategies in different organisms. In flies, a single pheromone, 11-*cis*-vaccenyl acetate (cVA), can elicit sexually dimorphic behaviors. In males, cVA promotes aggression toward males [84] and suppresses courtship behavior toward males [34, 85, 86]. In females, cVA promotes receptivity to males [86, 191]. These distinct behaviors are conveyed by two distinct classes of sensory neurons that express OR67b or OR65a [84, 86, 89, 91]. OR67b neurons are present both in males and in females, as is their target glomerulus in the antennal lobe. However, the projection neurons that innervate the target glomerulus have an anatomical dimorphism in their synaptic connections in the brain, and the male neurons impinge upon a neuropil that is present only in males [192]. Thus the dimorphism is thought to arise from sex-specific brain circuits that are anatomically defined during development. In mice, on the contrary, both males and females are thought to develop and maintain fully functional behavioral circuits for both sexes [193]. This conclusion is based on the effects of ablating the vomeronasal organ (VNO), a sensory structure in the nasal septum that senses pheromone. Acute functional

ablation of the VNO leads both males and females to show a mixture of male-typical and female-typical behaviors. These results suggest that the VNO functions as a sex-specific reversible switch that regulates the sex specificity of male-male aggression, courtship, and mounting by males, as well as maternal aggression and lactation in females [120, 193-195].

Ascaroside inputs may be integrated by the RMG interneurons

Pheromone blends with varying pheromone components are used to convey distinct messages and elicit sex- and context-specific behaviors in many organisms [187, 196]. *C. elegans* may encode blend-specific information by using a common central circuit to integrate and process information from individual pheromone components of ascr#3/C9 and ascr#5/C3. The coordination of sensory responses by a central hub neuron RMG, combined with a choice between antagonistic synaptic outputs by input sensory neurons such as ADL, provides an elegant mechanism for sensory integration to generate a coherent but flexible behavioral output [197].

Both wild-type and *npr-1* animals aggregate under some conditions, but not others, suggesting that they both have access to the RMG circuit that is regulated by environmental inputs and by genotype. Our findings suggest that the modular use of alternative circuit motifs may allow small circuits to generate adaptive behaviors under changing conditions.

How does the increased activity of RMG by loss of NPR-1 activity enhances sensory responses of ASK while reducing sensory responses of ADL? A plausible explanation can be found in the differences in sensory transduction in ASK and ADL.

Ca^{2+} levels in ASK fall upon addition of ascarosides, whereas Ca^{2+} levels in ADL rise on addition of ascarosides. I speculate that in an *npr-1* mutant background, RMG might be depolarized, also raising the resting membrane potential in ASK and ADL by active communication via gap junctions. This would generate a larger drop in the membrane potential in ASK in response to ascaroside addition, while generating a smaller rise in the membrane potential in ADL in response to ascaroside addition.

A second hub-and-spoke circuit has been reported in the gentle nose-touch circuit in *C. elegans* [198]. In this circuit, primary nociceptive spoke neurons are connected via gap junctions with RIH, the hub interneuron, which integrates sensory information and allows bidirectional communication and indirect facilitation among the sensory neurons. In this model, RIH acts as a coincidence detector to generate nose touch perception [198].

The role of ADL and ASH nociceptive neurons in regulating aggregation

Sensory transduction through the TRPV channel in ADL and ASH neurons is essential for aggregation behavior in *npr-1* mutants [144]. However, the chemical synaptic output from ADL and ASH neurons inhibits aggregation (Figure 2-10a). Therefore, ADL and ASH seem to play a dual role, in which the chemical synapses from ADL and ASH antagonizes the RMG gap junction circuit where ADL and ASH participate to promote aggregation. ADL and ASH function redundantly -- laser ablation of either ADL or ASH is insufficient to alter aggregation in *npr-1,* while ablation of both ADL and ASH significantly suppresses aggregation [144]. In agreement with this observation, synaptic inhibition or potentiation of either ASH or ADL has considerable weaker effects on aggregation than manipulation of both neurons (Figure 2-10a).

What stimuli do ADL and ASH neurons sense? ADL senses ascr#3/C9, and ASH neurons might sense yet unidentified ascarosides. In addition, ADL and ASH neurons could sense other stimuli relevant for aggregation such as food, metabolic conditions, CO_2, or O_2. With respect to the latter, ASH does not respond to changes in O_2 levels with calcium transients, although it affects avoidance of high O_2 in *npr-1* animals [199, 200]. Nonetheless, many nociceptive neurons are polymodal [198, 201-204], including ASH, which acts as a chemosensory and a mechanosensory neuron [159, 160, 205]. Diverse stimulus may cooperatively activate ADL and ASH neurons to regulate aggregation behavior via the gap junction circuit.

The pheromone circuit and aggregation behavior

Pheromones are multifunctional. Aggregation pheromones are often referred to as sex attractants, because they typically result in the arrival of both sexes at a calling site and increase the density of conspecifics surrounding the pheromone source [206]. Aggregation can enhance defense against predators as well as mate selection. The volatile sex pheromone cVA in flies plays a dual role as an aggregation factor in both females and males [87] and also acts as an inhibitor of male-male courtship [34, 85, 86] and an enhancer of male-male aggression [84].

Our study of the ascr#3/C9 circuit and its modulation by ascr#5/C3 in *npr-1* social mutants shows that pheromone circuits overlap with aggregation circuits in the *C. elegans* brain. However, these studies do not establish whether these particular pheromones function as aggregation pheromones in *npr-1* animals, or anti-aggregation pheromones in wild-type animals. The current circuit model for behavioral alteration in response to ascarosides should be viewed as a framework to advance our understanding of the roles of pheromones in aggregation, and our understanding of the ways in which modulatory cues reset circuit properties.

Table 2-1. Summary of ascarosides tested for avoidance behavior

Name	Structure	Dauer Activity	Mating Activity	Reference
ascr#5/ C3	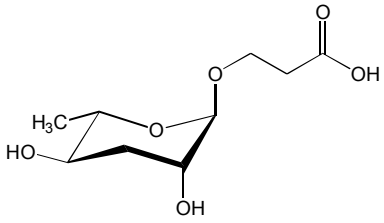	Moderate	Not Tested	[7,8]
ascr#9/ C5	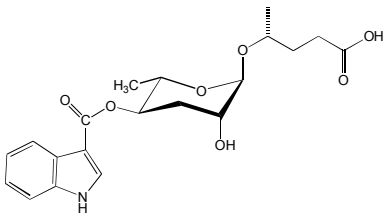	High	None	[6]
ascr#2/ C6	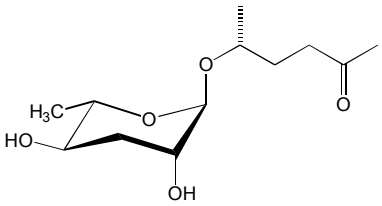	High	Moderate	[5]
ascr#8/ C7-PABA	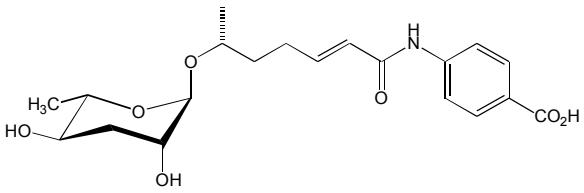	Moderate	High	[8]
ascr#3/ C9	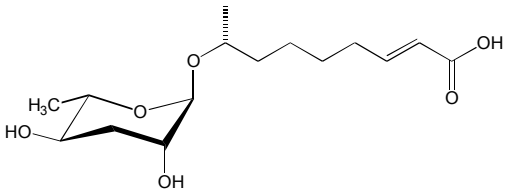	High	High	[5]

Figure 2-1. Wild-type lab strain N2 avoids the pheromone component ascr#3/C9

a. The drop test for avoidance behavior. Upon encountering a repellent delivered by a micro-capillary at 0.0 second, wild-type animals immediately make a long reversal often followed by an omega turn (around 2.4 seconds).

b. Avoidance of various ascarosides in wild-type lab strain N2. From the drop test, the fraction of animals that make long reversals is scored as readout for avoidance behavior. M13 buffer only, ascaroside dissolved in M13 buffer, or 2M glycerol was applied to individual forward moving animal. Assays were performed in the absence of food. *** indicates responses that are different from the responses to buffer alone at $P<0.001$ (chi-square test with Yates' correction for continuity). Error bars indicate standard error of proportion (SEP). n=10-100 animals each.

a

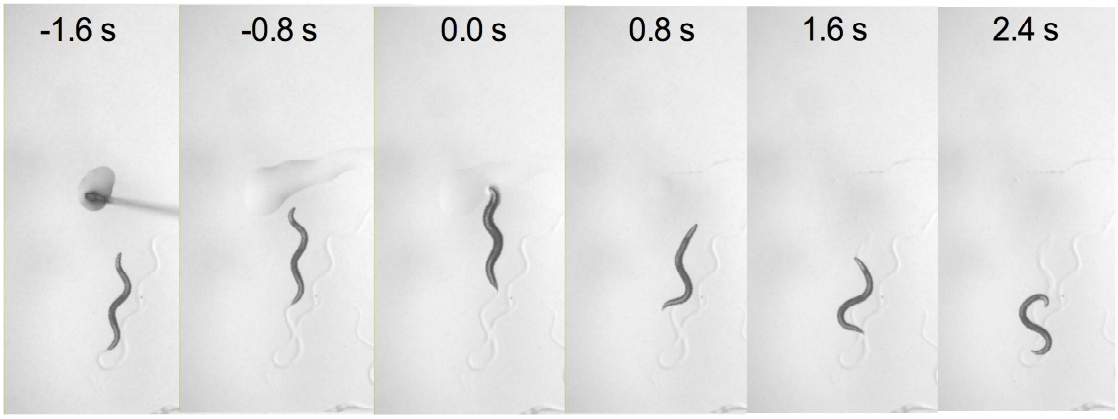
-1.6 s
-0.8 s
0.0 s
0.8 s
1.6 s
2.4 s

b

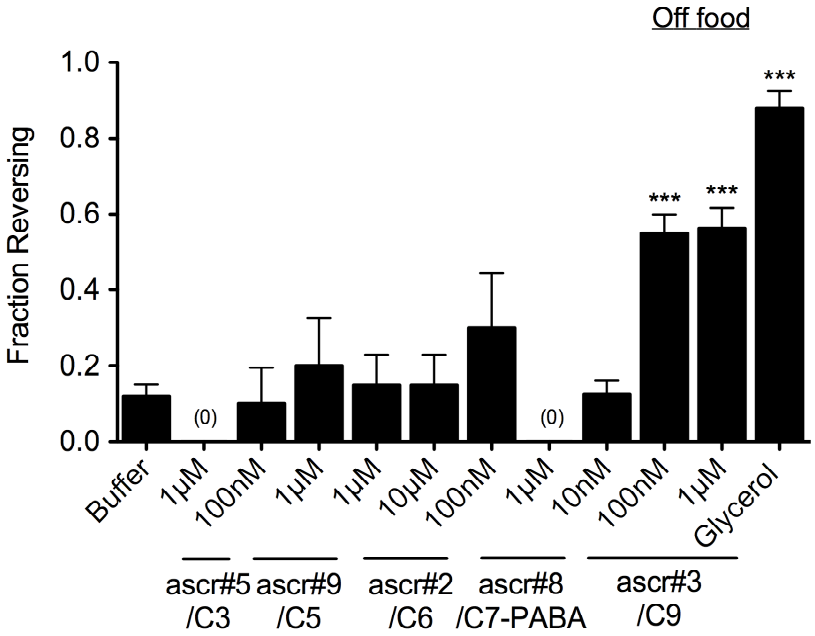
Off food
Fraction Reversing
1.0
0.8
0.6
0.4
0.2
0.0
(0)
(0)
***
***
***
Buffer
1µM
100nM
1µM
1µM
10µM
100nM
1µM
10nM
100nM
1µM
Glycerol
ascr#5 /C3
ascr#9 /C5
ascr#2 /C6
ascr#8 /C7-PABA
ascr#3 /C9

Figure 2-2. The nociceptive ADL neurons mediate ascr#3/C9 avoidance in a TRPV channel-dependent manner

a. TRPV channel mutants *osm-9(ky10)* and *ocr-2(ak47)* fail to avoid ascr#3/C9 in the absence of food. ††† indicates responses that are different from the responses to buffer alone at $P<0.001$. * and *** indicate statistical significances at $P<0.05$ and $P<0.001$ between the values indicated by brackets (chi-square test with Yates' correction for continuity). Error bars are the SEP. n=10-100 animals each. .

b. Expression of *ocr-2* genomic DNA in ADL but not in other *ocr-2* expressing neurons restores ascr#3/C9 avoidance in the absence of food. Promoters used were: *srh-220* for ADL, *sra-6* for ASH, *odr-10* for AWA and *srh-142* for ADF. ** and *** indicate statistical significances at $P<0.01$ and $P<0.001$ between the values indicated by brackets (chi-square test with Yates' correction for continuity). Error bars are the SEP. n=20-100 animals each. .

c. Mutants of ADL-expressed G protein subunits, the chemoreceptor localization mutant *odr-8(ky173)*, or the double mutant of known ascaroside receptors *srbc-64(tm1946);srbc-66(tm2943)* have no defect in ascr#3/C9 avoidance in the absence of food. * and *** indicate responses that are different from the responses to buffer alone for each genotype at $P<0.05$ and 0.001, respectively (chi-square test with Yates' correction for continuity). Error bars are the SEP. n=20-60 animals each. .

d. ADL sensory transduction model. Upon binding of ascr#3/C9 molecules, an unknown ascr#3/C9 G-protein coupled receptor is activated, followed by activation of downstream G-protein signaling, and subsequently the OSM-9/OCR-2 TRPV channel opens to allow the influx of Na^+ and Ca^{2+} ions, leading to the depolarization of ADL.

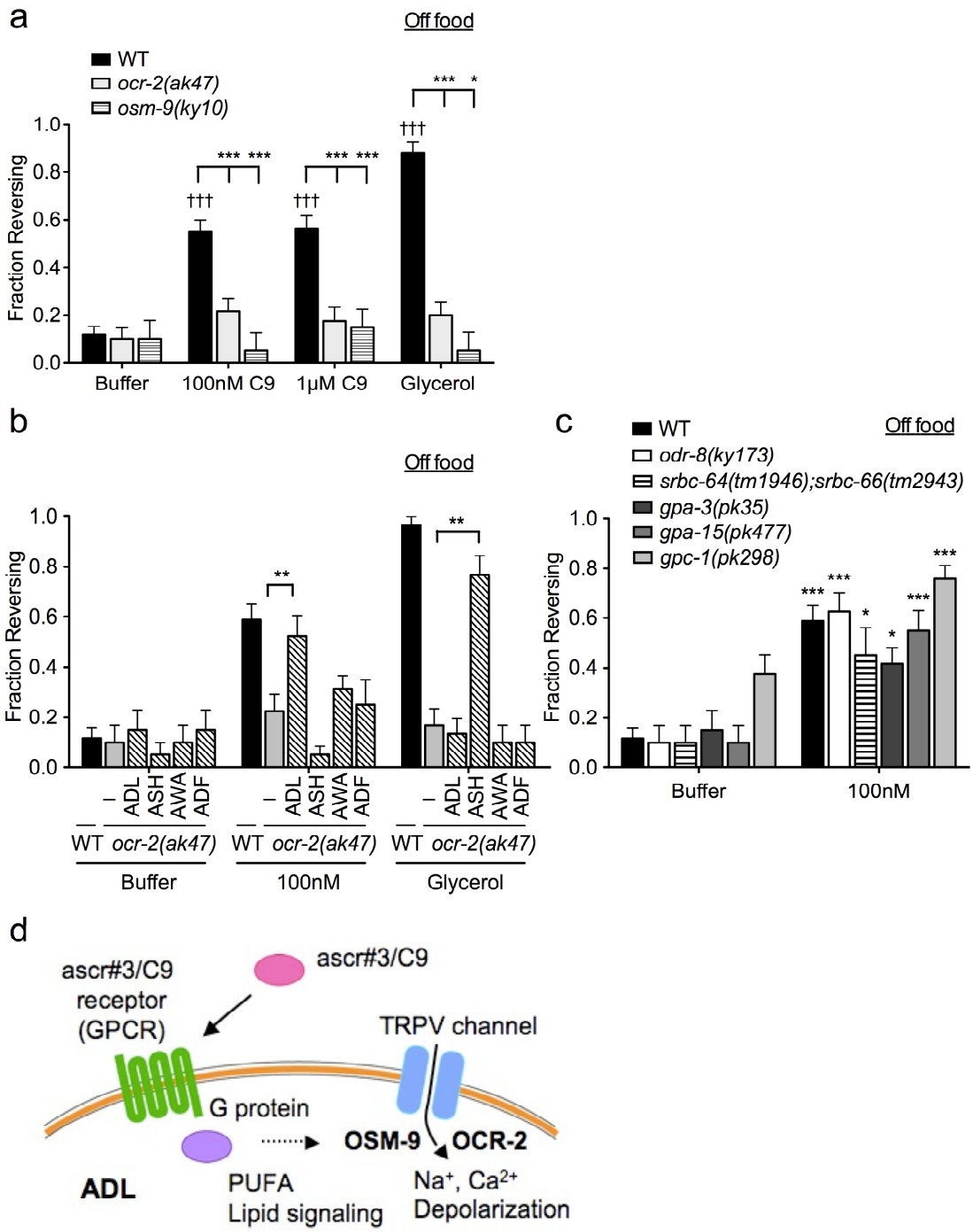
a
Off food
WT
ocr-2(ak47)
osm-9(ky10)
Fraction Reversing
Buffer
100nM C9
1µM C9
Glycerol
b
Off food
Fraction Reversing
ADL
ASH
AWA
ADF
WT
ocr-2(ak47)
Buffer
100nM
Glycerol
c
WT
Off food
odr-8(ky173)
srbc-64(tm1946);srbc-66(tm2943)
gpa-3(pk35)
gpa-15(pk477)
gpc-1(pk298)
Fraction Reversing
Buffer
100nM
d
ascr#3/C9
ascr#3/C9
receptor
(GPCR)
TRPV channel
G protein
OSM-9
OCR-2
ADL
PUFA
Lipid signaling
Na+, Ca2+
Depolarization

Figure 2-3. ADL senses ascr#3/C9

a. The microfluidic chip contains a worm in the green channel. The fluid delivery system consists of two side channels loaded with fluorescent dye (channels 1 and 4), a stimulus channel (channel 2) and a control, or buffer, channel (channel 3). The stimulus and buffer streams are directed by the side flows (gray). In the 'off' state (left), the right dye channel (channel 4) is open and pushes the stimulus stream to exit from the left outlet. In the 'on' state (right), the left dye channel (channel 1) is open, and the nose of the worm is exposed to stimulus (red arrow). Adapted from [170].

b. Wild-type hermaphrodite animals expressing *G-CaMP3.0* construct in ADL have approximately normal ascr#3/C9 avoidance in the absence of food. ** and *** indicates responses that are different from the responses to buffer alone for each genotype at $P<0.01$ and 0.001, respectively (chi-square test with Yates' correction for continuity). Error bars are the SEP. n=20-80 animals each. .

c. Wild-type hermaphrodites exhibit sharp increase in the fluorescence of *G-CaMP3.0* in ADL upon exposure to the ascr#3/C9. 1 μM ascr#3/C9 was applied at 0.0 second. OFF and ON indicates the absence and presence of ascr#3/C9, respectively.

d. (Left) Changes in intracellular Ca^{2+} dynamics in *G-CaMP3.0*-expressing ADL neurons in wild-type and *ocr-2(ak47)* mutant hermaphrodites upon addition of pulses of 100 nM ascr#3/C9 (red horizontal bars). n ≥10 neurons each. Error bars represent the SEM. (Right) Average percentage changes of the peak fluorescence after addition of the first pulse of ascr#3/C9. Error bars are the SEM. Asterisk indicates different from wild-type at $P<0.001$.

e. No Ca^{2+} transients are observed in *G-CaMP3.0*-expressing ASH neurons upon addition of mixtures of ascr#5/C3, ascr#2/C6 and ascr#3/C9 at different concentrations (red horizontal bar). n=7 neurons each. Error bars indicate the SEM.

f. ADL neurons of wild-type (left) or *npr-1* (right) hermaphrodites do not respond to a mixture of ascr#3/C3 and ascr#2/C6 (red horizontal bar). n ≥6 neurons each. Error bars indicate the SEM.

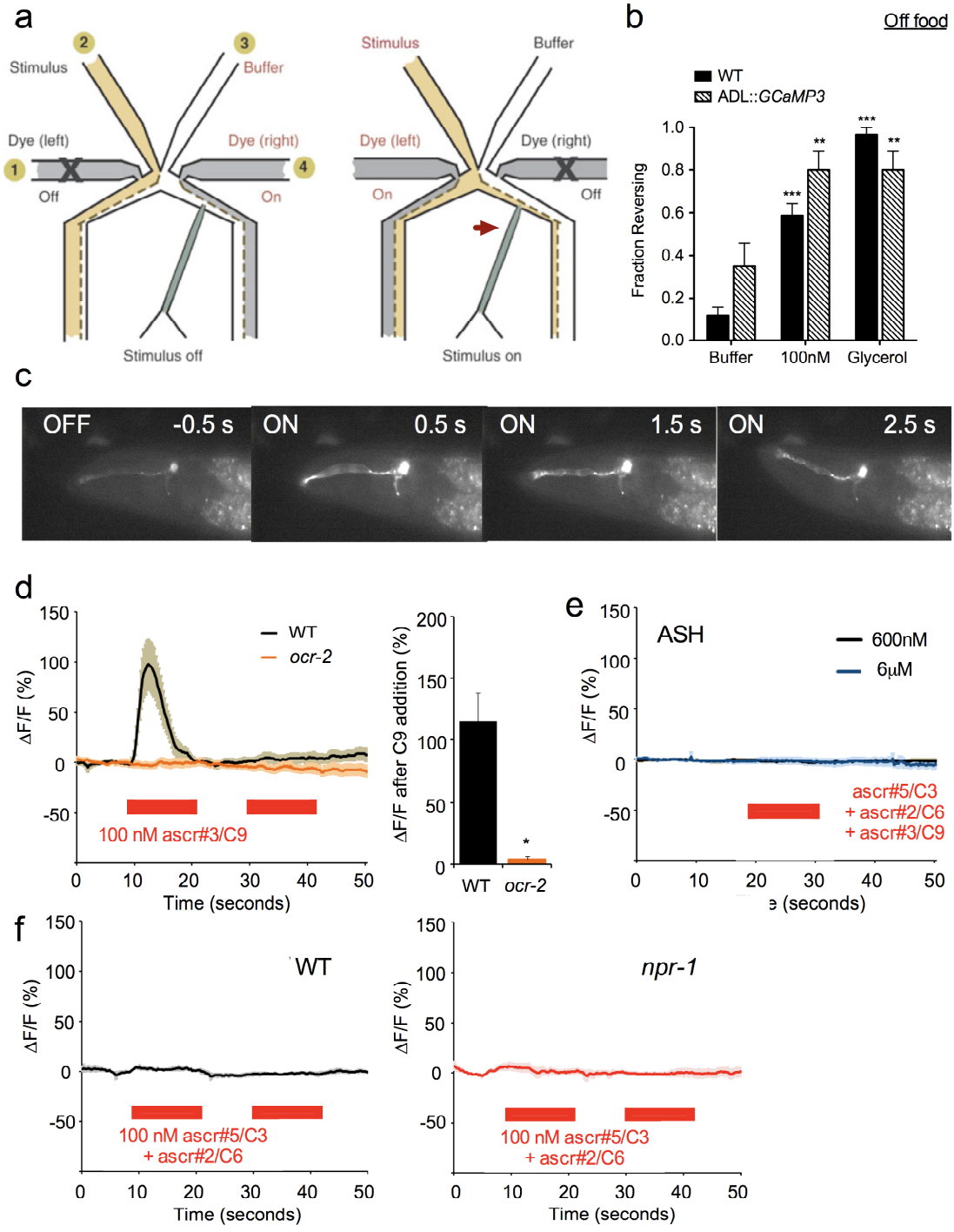
a
Stimulus
Buffer
Dye (left)
Dye (right)
Off
On
Stimulus off
Stimulus on
b
Off food
WT
ADL::GCaMP3
Fraction Reversing
Buffer
100nM
Glycerol
c
OFF -0.5 s
ON 0.5 s
ON 1.5 s
ON 2.5 s
d
WT
ocr-2
ΔF/F (%)
100 nM ascr#3/C9
Time (seconds)
ΔF/F after C9 addition (%)
e
ASH
600nM
6μM
ascr#5/C3
+ ascr#2/C6
+ ascr#3/C9
f
WT
npr-1
100 nM ascr#5/C3
+ ascr#2/C6

Figure 2-4. The synaptic output from ADL promotes avoidance of ascr#3/C9

a. A subset of known postsynaptic partners of ADL (adapted from [141]). Arrows connecting neurons indicate chemical synapses. The objects marked in red are thought to promote behavioral avoidance of ascr#3/C9.

b. Synaptic manipulation of ADL alters ascr#3/C9 avoidance in the absence of food. Synaptic inhibition by expressing tetanus toxin light chain (*TeTx*) decreases ascr#3/C9 avoidance, and neuronal activation by expressing a gain-of-function *pkc-1* mutant cDNA enhances ascr#3/C9 avoidance. The *sre-1* promoter was used to drive specific expression in ADL. Asterisks denote statistical significance (***P*<0.01, ****P*<0.001 by chi-square test with Yates' correction for continuity) compared to wild-type values for each stimulus. Error bars are the SEP. n=20-80 animals each.

c. Synaptic inhibition of ASH suppresses osmotic avoidance but does not suppress ascr#3/C9 avoidance. *sre-1* and *sra-6* promoters were used to drive the expression of *TeTx* in ADL and ASH, respectively. Note that these assays were performed in the presence of food, leading to a higher spontaneous reversal rate to buffer. Asterisks denote statistical significance (**P*<0.05, ***P*<0.01, ****P*<0.001 by chi-square test with Yates' correction for continuity) compared to wild-type values for each stimulus. Error bars are the SEP. n=20-80 animals each.

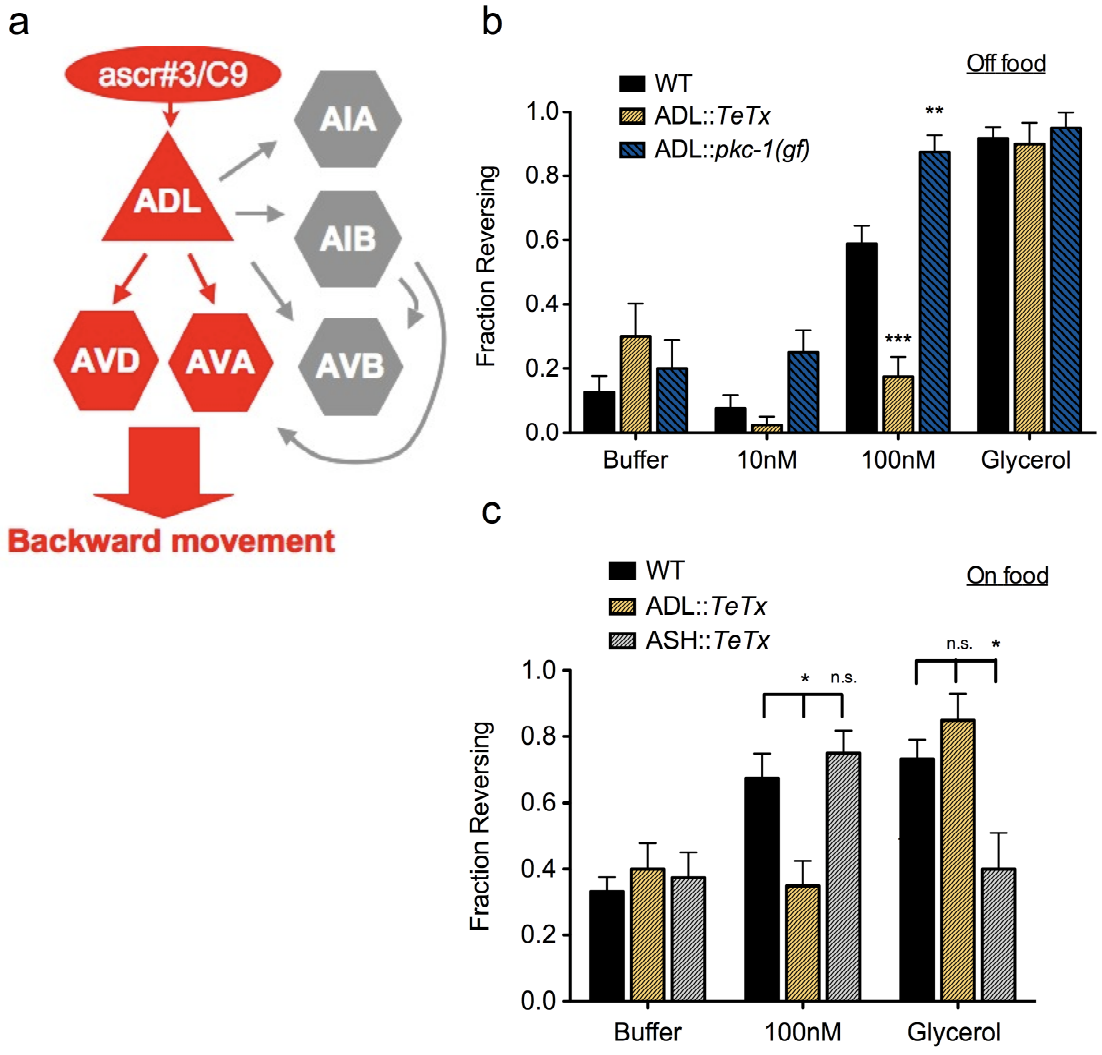
a
ascr#3/C9
ADL
AIA
AIB
AVD
AVA
AVB
Backward movement
b
Off food
WT
ADL::TeTx
ADL::pkc-1(gf)
Fraction Reversing
1.0
0.8
0.6
0.4
0.2
0.0
**
***
Buffer
10nM
100nM
Glycerol
c
On food
WT
ADL::TeTx
ASH::TeTx
Fraction Reversing
1.0
0.8
0.6
0.4
0.2
0.0
*
n.s.
n.s.
*
Buffer
100nM
Glycerol

Figure 2-5. *npr-1(ad609)* social mutants exhibit reduction in avoidancereduced avoidance of to ascr#3/C9

a. Wild-type N2 and *npr-1(ad609)* hermaphrodites. (Left) Wild-type animals disperse on and off food. (Right) *npr-1(ad609)* mutants aggregate in groups on the thick border of the bacterial lawn.

b. *npr-1(ad609)* mutants exhibit reduced ascr#3/C9 avoidance in the absence of food. ** and *** indicate responses that are different from the responses to buffer alone for each genotype at $P<0.01$ and 0.001, respectively. † and ††† indicate values that are different at $P<0.05$ and 0.001 between values indicated by brackets (chi-square test with Yates' correction for continuity). Error bars indicate standard error of proportion (SEP). n=30-80 animals each.

c. *npr-1(ad609)* mutants exhibit reduced ascr#3/C9 avoidance in the presence of food. Note that both wild-type and *npr-1* animals have a higher spontaneous reversal rate on food, and both are more sensitive to ascr#3/C9 as well. *** indicates responses that are different from the responses to buffer alone for each genotype at $P<0.001$. † and ††† indicate values that are different at $P<0.05$ and 0.001 between values indicated by brackets, respectively (chi-square test with Yates' correction for continuity). Error bars indicate standard error of proportion (SEP). n $\geq$20 animals each.

d. The RMG hub-and-spoke circuit. RMG promotes aggregation behavior [149]. (Top) In wild-type animals, NPR-1 expressed in RMG suppresses RMG activity or its communication with sensory neurons via gap junctions, leading to solitary behavior. (Bottom) In *npr-1* mutants, RMG is active and communicates with sensory neurons, promoting social behavior. ADL is one of the gap junction partners of RMG. Capped lines represent gap junctions. Adapted from [141, 149].

e. *npr-1* cDNA expression in RMG restores avoidance of 10 nM ascr#3/C9 to *npr-1(ad609)* mutants in the presence of food. *, ** and *** indicate responses that are different from the responses to buffer alone for each genotype at $P<0.05$, 0.01 and 0.001, respectively (chi-square test with Yates' correction for continuity). Error bars indicate SEP. n=40-100 animals each.

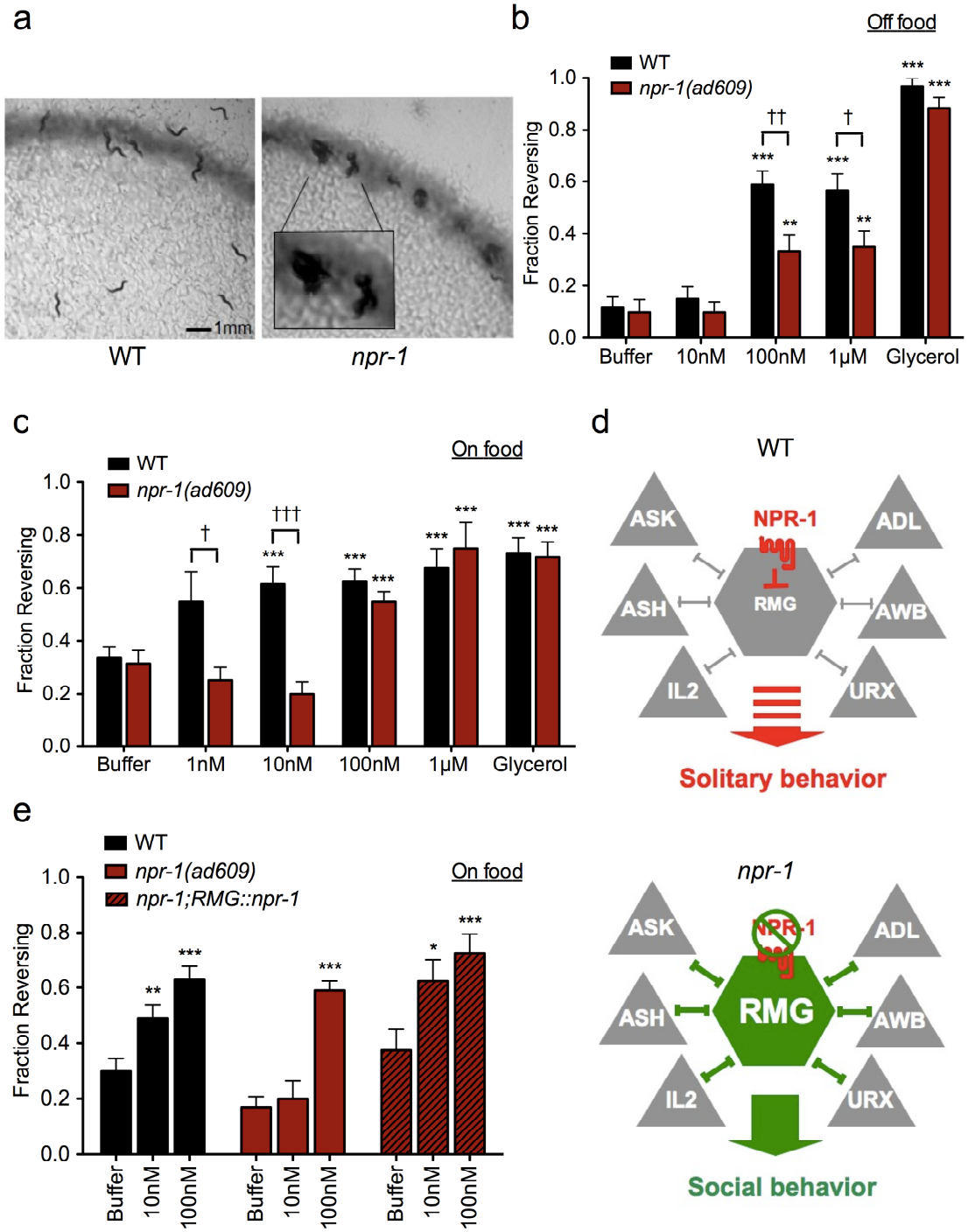
a
1mm
WT
npr-1
b
Off food
WT
npr-1(ad609)
Fraction Reversing
Buffer
10nM
100nM
1µM
Glycerol
c
On food
WT
npr-1(ad609)
Fraction Reversing
Buffer
1nM
10nM
100nM
1µM
Glycerol
d
WT
ASK
NPR-1
ADL
ASH
RMG
AWB
IL2
URX
Solitary behavior
e
WT
npr-1(ad609)
npr-1;RMG::npr-1
On food
Fraction Reversing
Buffer
10nM
100nM
npr-1
ASK
NPR-1
ADL
ASH
RMG
AWB
IL2
URX
Social behavior

Figure 2-6. *npr-1(ad609)* social mutants have subtle alterations in the ADL sensory response to ascr#3/C9.

a. (Left) Changes in *G-CaMP3.0* fluorescence in responses to ascr#3/C9 in ADL neurons of wild-type and *npr-1(ad609)* hermaphrodites. n=12 neurons each. Error bars are the SEM. (Right) Average percentage changes of the peak fluorescence after addition of the first pulse of ascr#3/C9. Error bars are the SEM. Asterisk indicates different from wild-type at $P<0.001$.

b. ascr#3/C9 behavioral avoidance is similar in *npr-1(ad609)* animals expressing *G-CaMP3.0* in ADL and in *npr-1(ad609)* animals. Assays were performed in the absence of food. * and *** indicates responses that are different from the responses to buffer alone for each genotype at $P<0.05$ and 0.001, respectively (chi-square test with Yates' correction for continuity). Error bars are the SEP. n=20-60 animals each.

c. ascr#3/C9 avoidance in *npr-1(ad609)* mutants with synaptic manipulation in ADL. Synaptic inhibition by expressing *TeTx* did not affect avoidance in *npr-1* mutants, but neuronal activation by expressing *pkc-1(gf)* increased ascr#3/C9 avoidance in the presence of food. Asterisks denote statistical significance (*$P<0.05$, ***$P<0.001$ by chi-square test with Yates' correction for continuity) between values indicated by brackets. Error bars are the SEP. n=40-80 animals each. .

d. The neuropeptide biosynthesis mutant *egl-21(n611)* and the ADL-produced neuropeptide mutant *flp-21(ok1601)* are defective in ascr#3/C9 avoidance in the presence of food. † and ††† indicate responses that are different from the responses to buffer alone for each genotype at $P<0.05$ and 0.001, respectively. *, ** and *** indicate values that are different at $P<0.05$, 0.01 and 0.001 between values indicated by brackets (chi-square test with Yates' correction for continuity). n.s. –not significant. Error bars indicate SEP. n=20-60 animals each. .

e. ascr#3/C9 avoidance is reduced in *flp-21(ok889)* mutants in the absence of food. ** and *** indicate responses that are different from the responses to buffer alone for each genotype at $P<0.01$ and 0.001, respectively. † and †† indicate values that are different at $P<0.05$ and 0.001 between values indicated by brackets (chi-square test with Yates' correction for continuity). Error bars indicate SEP. n=20-80 animals each.

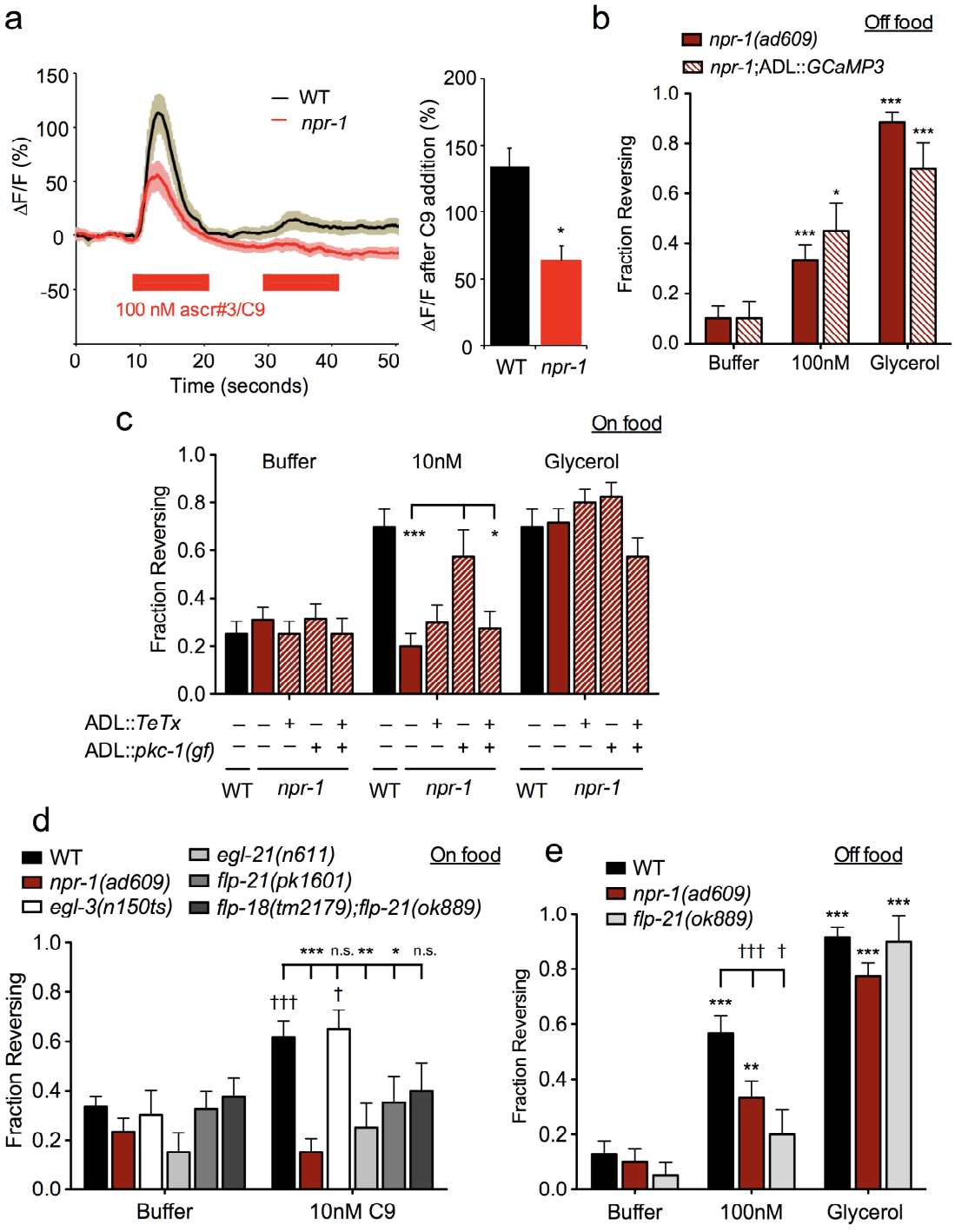
a
WT
npr-1
ΔF/F (%)
100 nM ascr#3/C9
Time (seconds)
ΔF/F after C9 addition (%)
b
Off food
npr-1(ad609)
npr-1;ADL::GCaMP3
Fraction Reversing
Buffer
100nM
Glycerol
c
On food
Buffer
10nM
Glycerol
Fraction Reversing
ADL::TeTx
ADL::pkc-1(gf)
WT
npr-1
d
WT
npr-1(ad609)
egl-3(n150ts)
egl-21(n611)
flp-21(pk1601)
flp-18(tm2179);flp-21(ok889)
On food
n.s.
Buffer
10nM C9
e
Off food
WT
npr-1(ad609)
flp-21(ok889)
Buffer
100nM
Glycerol

Figure 2-7. Wild-type males exhibit reduced avoidance of ascr#3/C9

a. Wild-type males have reduced ascr#3/C9 avoidance compared to wild-type hermaphrodites in the presence of food. *** indicates responses that are different from the responses to buffer alone for each genotype at $P<0.001$. † and ††† indicate values that are different at $P<0.05$ and 0.001 between values indicated by brackets (chi-square test with Yates' correction for continuity). Error bars indicate SEP. n ≥20 animals each. .

b. (Left) Changes in intracellular fluorescence in *G-CaMP3.0*-expressing ADL neurons of wild-type hermaphrodites and males upon addition of 100 nM ascr#3/C9. Both the peak and the initiation of the Ca^{2+} response are delayed. n ≥12 neurons each. Error bars are the SEM. (Right) Average percentage changes of the peak fluorescence after addition of the first pulse of ascr#3/C9. Error bars are the SEM. Asterisk indicates different from wild-type at $P<0.005$.

c. The activation of ADL by expressing *pkc-1(gf)* restores avoidance to ascr#3/C9 at 100 nM but not at 10 nM in wild-type males. ** and *** indicate responses that are different from the responses to buffer alone for each genotype at $P<0.01$ and 0.001, respectively. † indicates values that are different at $P<0.05$ between values indicated by brackets (chi-square test with Yates' correction for continuity). Error bars are SEP. n ≥20 animals each. Assays were performed in the presence of food.

d. Masculinization of ADL partially suppresses ascr#3/C9 avoidance in wild-type hermaphrodites. *fem-3* cDNA was over-expressed to induce somatic masculinization, either in ADL specifically or pan-neuronally. Assays were performed in the presence of food. * and *** indicate responses that are different from the responses to buffer alone for each genotype at $P<0.05$ and 0.001, respectively (chi-square test with Yates' correction for continuity). Error bars are SEP. n ≥20 animals each.

e. (Left) ascr#3/C9 responses in *G-CaMP3.0*-expressing ADL neurons of hermaphrodites expressing sre-1::*fem-3* to masculinize ADL neurons, with wild-type controls. n=8 neurons each. Error bars are the SEM. (Right) Average percentage changes of the peak fluorescence after addition of the first pulse of ascr#3/C9. Error bars are the SEM.

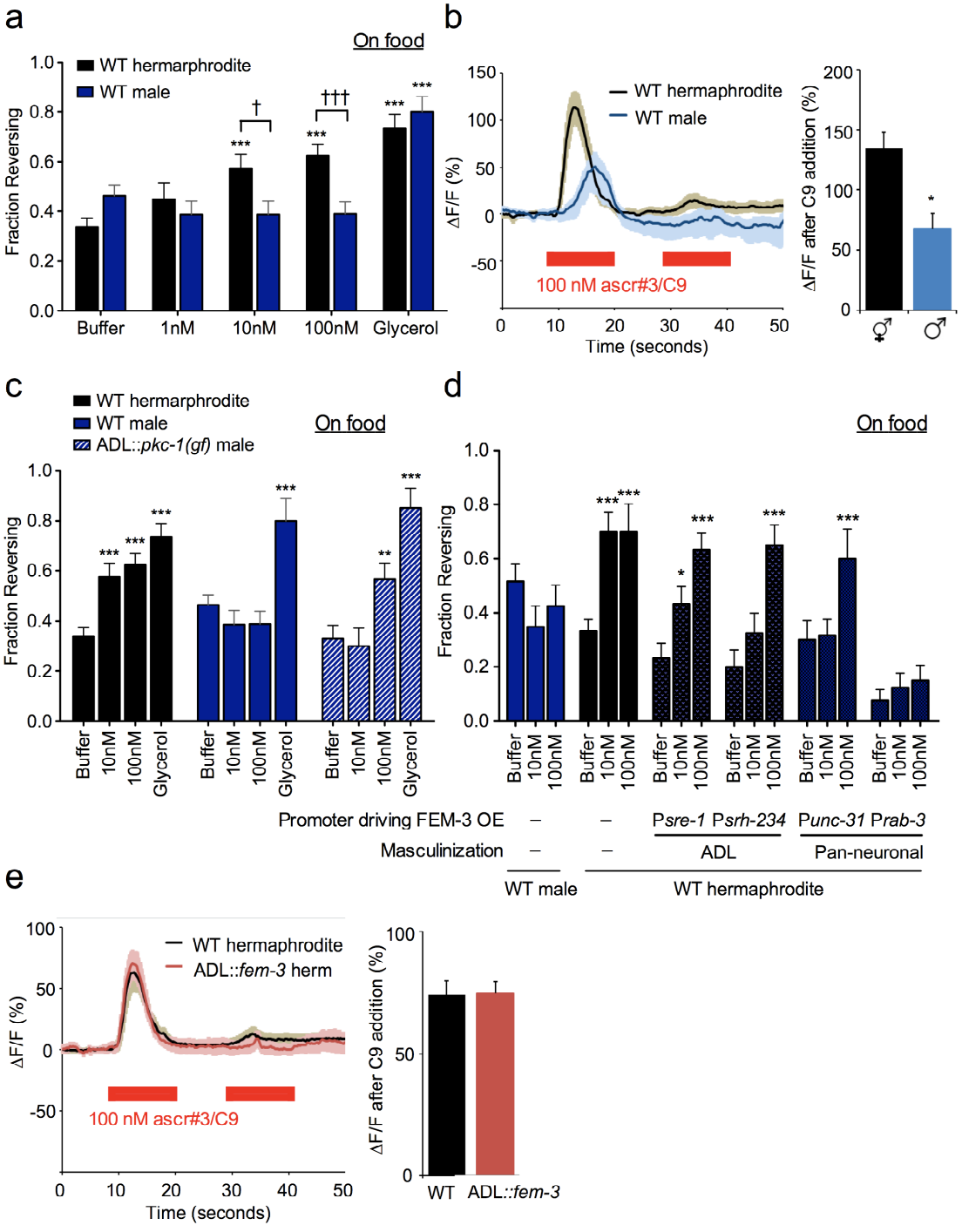
a
On food
WT hermaphrodite
WT male
Fraction Reversing
Buffer
1nM
10nM
100nM
Glycerol
b
WT hermaphrodite
WT male
ΔF/F (%)
100 nM ascr#3/C9
Time (seconds)
ΔF/F after C9 addition (%)
c
WT hermaphrodite
WT male
ADL::pkc-1(gf) male
On food
Fraction Reversing
d
On food
Fraction Reversing
Promoter driving FEM-3 OE
Masculinization
Psre-1 Psrh-234
Punc-31 Prab-3
ADL
Pan-neuronal
WT male
WT hermaphrodite
e
WT hermaphrodite
ADL::fem-3 herm
ΔF/F (%)
100 nM ascr#3/C9
Time (seconds)
ΔF/F after C9 addition (%)
WT
ADL::fem-3

Figure 2-8. The male circuit functions in parallel to the NPR-1 circuit for reduced avoidance of ascr#3/C9

a. *npr-1(ad609)* males have reduced ascr#3/C9 avoidance compared to wild-type males in the presence of food. * and *** indicates responses that are different from the responses to buffer alone for each genotype at $P<0.05$ and 0.001. † and ††† indicate values that are different at $P<0.05$ and 0.001 between values indicated by brackets (chi-square test with Yates' correction for continuity). Error bars indicate SEP. n ≥20 animals each.

b. (Left) Intracellular Ca^{2+} dynamics in *G-CaMP3.0*-expressing ADL neurons of wild-type and *npr-1(ad609)* mutant males in response to 100 nM ascr#3/C9. Only animals with positive responses were included in these averages; n ≥12 neurons for each except for *npr-1* males, where n=4 that exhibited quantifiable changes in fluorescence. Error bars are the SEM. (Right) Scatter plot showing percentage changes in fluorescence in individual ADL neurons of animals of the indicated genotypes in response to a pulse of 100 nM ascr#3/C9. The percentage of ADL neurons that failed to exhibit significant changes in fluorescence were 14% in wild-type hermaphrodites (n=14); 14% in *npr-1* hermaphrodites (n=14); 12% in wild-type males (n=17) and 64% in *npr-1* males (n=11). Bars indicate the median values for each genotype.

c. Synaptic inhibition or *npr-1* rescue of RMG increases ascr#3/C9 avoidance in *npr-1(ad609)* males in the presence of food. Asterisks indicate statistical significance (*$P<0.05$, **$P<0.01$ and ***$P<0.001$ by chi-square test with Yates' correction for continuity) compared to corresponding responses to buffer alone. Error bars are the SEP. n=30-120 animals each. .

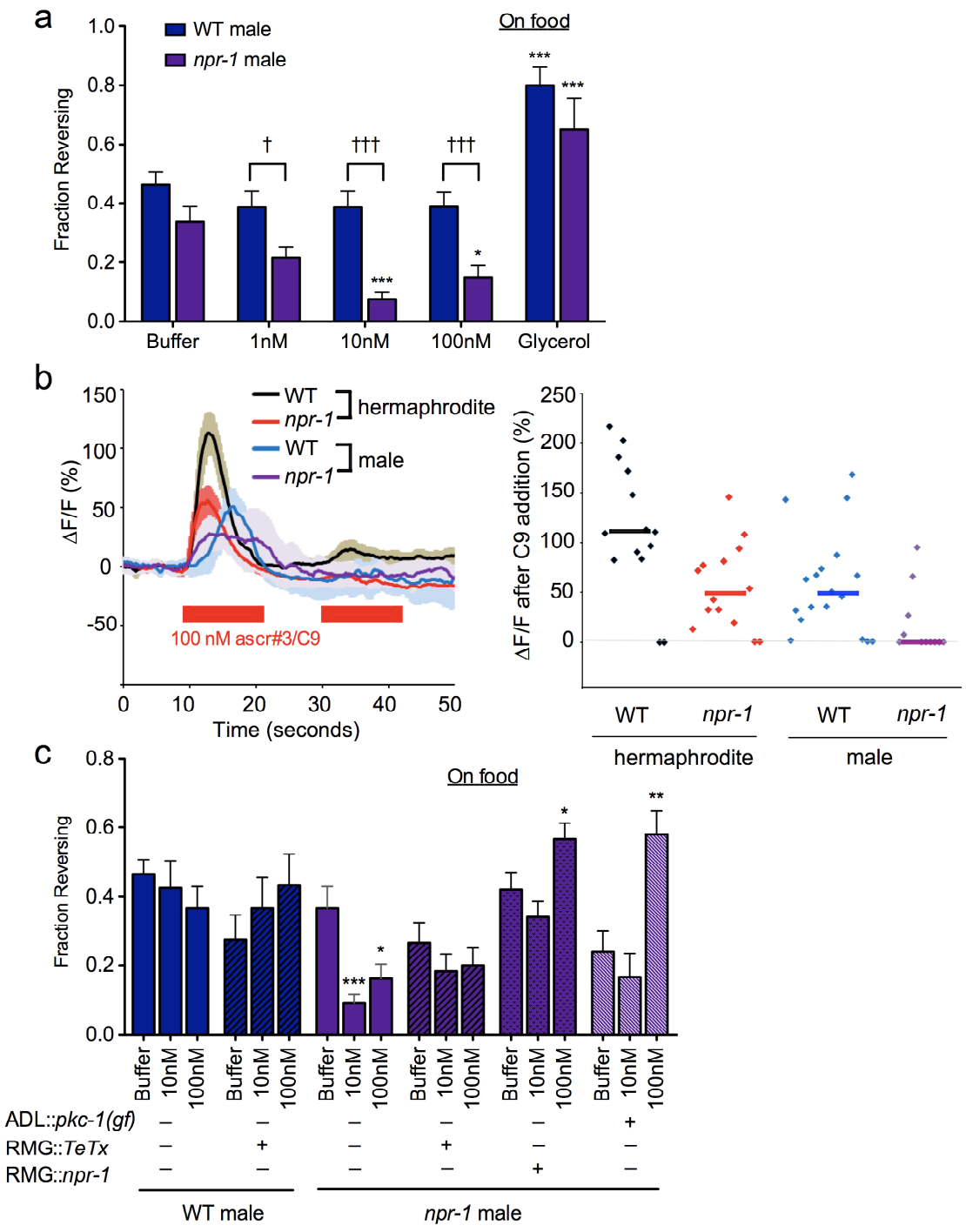
a
On food
WT male
npr-1 male
Fraction Reversing
Buffer
1nM
10nM
100nM
Glycerol
b
WT
npr-1
hermaphrodite
male
ΔF/F (%)
100 nM ascr#3/C9
Time (seconds)
ΔF/F after C9 addition (%)
hermaphrodite
male
c
On food
Fraction Reversing
ADL::pkc-1(gf)
RMG::TeTx
RMG::npr-1
WT male
npr-1 male

Figure 2-9. ASK neurons are altered in *npr-1* males

a. Intracellular Ca^{2+} dynamics in *G-CaMP3.0*-expressing ASK neurons of wild-type hermaphrodites, wild-type males, and *npr-1(ad609)* mutant males and in response to 100 nM ascr#3/C9. Error bars are the SEM.

b. Model of sexually dimorphic and NPR-1 state-dependent responses to ascr#3/C9 generated by the hub-and-spoke circuit. (Top left) In wild-type hermaphrodites, NPR-1 activity in RMG is high, and ADL drives ascr#3/C9 responses and avoidance via ADL chemical synapses. (Bottom left) Avoidance behavior is decreased in males due to diminished ADL ascr#3/C9 sensory responses and synaptic output, which are at least partly non cell-autonomous. (Top right and bottom right) Loss of *npr-1* function activates RMG, which decreases ascr#3/C9 avoidance in both males and hermaphrodites. (Bottom right) In *npr-1* males, changes in ADL, ASK, and possibly other neurons drive the RMG circuit to promote attraction to ascr#3/C9.

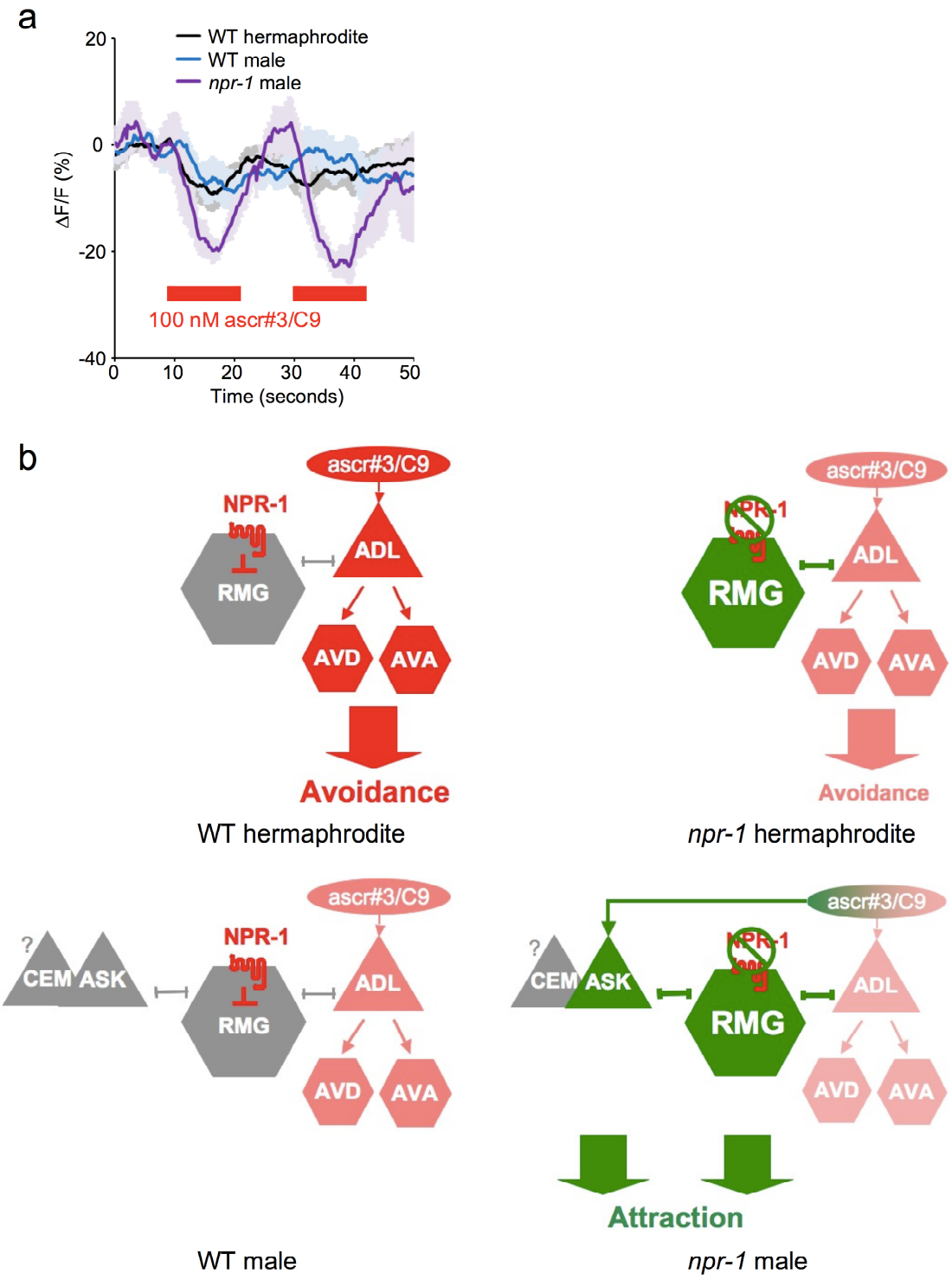
a
WT hermaphrodite
WT male
npr-1 male
20
0
-20
-40
ΔF/F (%)
0
10
20
30
40
50
Time (seconds)
100 nM ascr#3/C9
b
ascr#3/C9
NPR-1
RMG
ADL
AVD
AVA
Avoidance
WT hermaphrodite
npr-1 hermaphrodite
CEM
ASK
?
Attraction
WT male
npr-1 male

Figure 2-10. ascr#5/C3 antagonizes avoidance of ascr#3/C9 in *npr-1(ad609)* mutants hermaphrodites

a. ascr#5/C3 antagonizes avoidance of ascr#3/C9 in *npr-1(ad609)* mutants. ascr#5/C3 and ascr#3/C9 were applied at 100 nM each for both individual and blend stimuli. Isoamyl alcohol (IAA) was 10^{-4} for both individual and blend stimuli. Assays were performed on hermaphrodite animals in the presence of food. *, ** and *** indicate responses that are different from the responses to buffer alone for each genotype at $P<0.05$, 0.01 and 0.001, respectively. † and ††† indicate values that are different at $P<0.05$ and $P<0.001$ between values indicated by brackets (chi-square test with Yates' correction for continuity). n.s. – not significant. Error bars indicate SEP. n ≥40 animals each.

b. The ascr#5/C3 modulation of ascr#3/C9 avoidance is dependent on the activities of ASK and RMG neurons. Ascarosides were used at 100 nM each both individually and in blends. Animals stably expressing integrated sra-9::*mCaspase* were used for ASK specific genetic ablation. Assays were performed on hermaphrodites in the presence of food. Asterisks indicate statistical significance (*$P<0.05$, ***$P<0.001$ by chi-square test with Yates' correction for continuity) compared to values for ascr#3/C9 responses for each genotype. Error bars are the SEP. n=20-80 animals each.

c. Model of NPR-1 state-dependent alternative response behaviors to ascr#5/C3 and ascr#3/C9 generated by the hub-and-spoke circuit. (Left) In wild-type hermaphrodites, high NPR-1 activity suppresses RMG and alters ADL ascr#3/C9 responses and avoidance via ADL chemical synapses. (Right) Loss of *npr-1* function enhances the RMG activity, decreasing ADL ascr#3/C9 responses and synaptic output and increases ASK ascr#5/C3 responses. These paired changes reduce avoidance of pheromone blends in *npr-1* hermaphrodites.

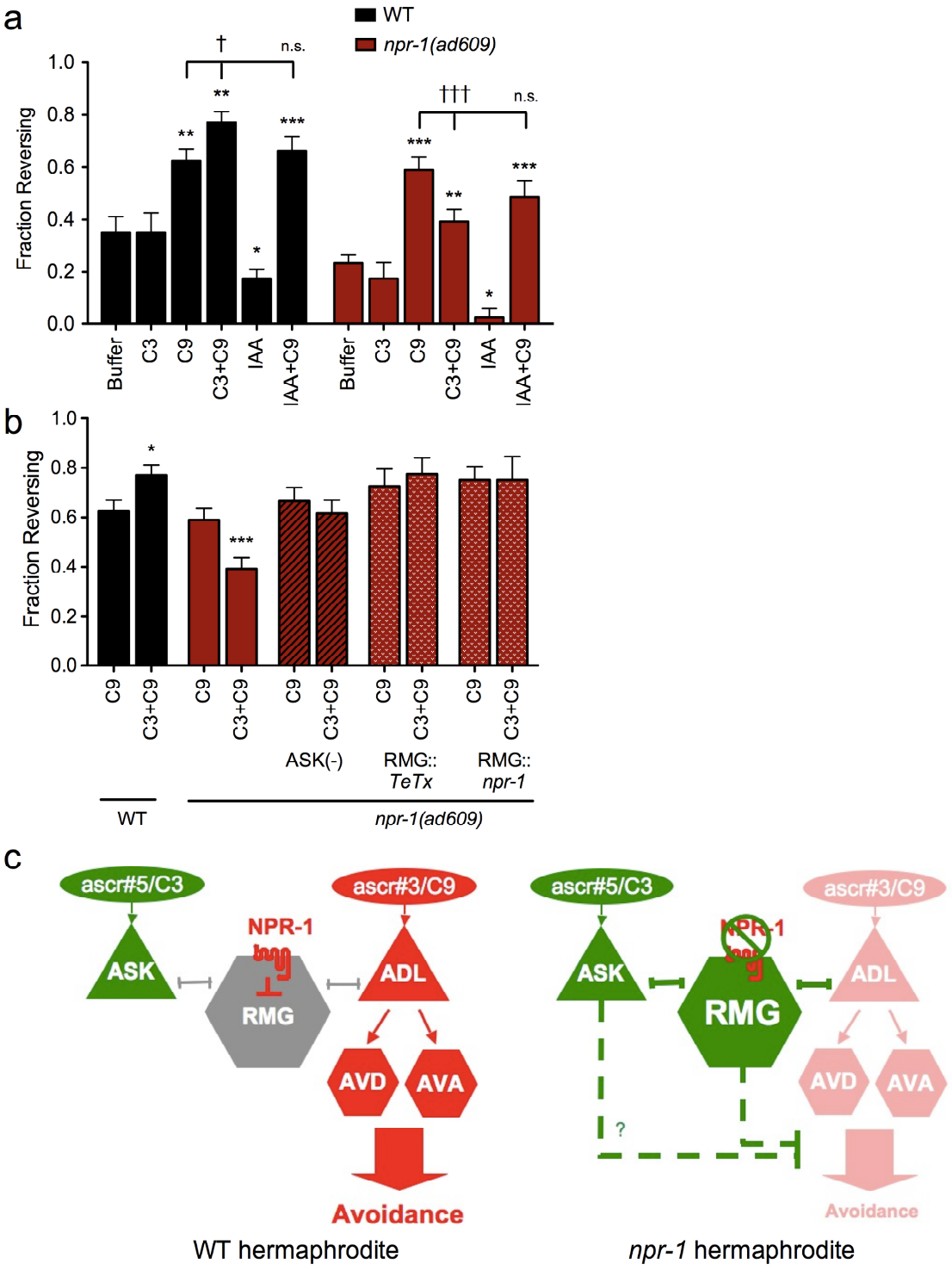
a
WT
npr-1(ad609)
Fraction Reversing
1.0
0.8
0.6
0.4
0.2
0.0
†
n.s.
†††
n.s.
Buffer
C3
C9
C3+C9
IAA
IAA+C9
b
Fraction Reversing
ASK(-)
RMG::
TeTx
RMG::
npr-1
WT
npr-1(ad609)
c
ascr#5/C3
ascr#3/C9
NPR-1
ASK
ADL
RMG
AVD
AVA
Avoidance
?
WT hermaphrodite
npr-1 hermaphrodite

Figure 2-11. Synaptic output from ADL and ASH antagonizes aggregation and bordering behavior

a. Synaptic inhibition of both ADL and ASH promotes aggregation, whereas the activation of both ADL and ASH inhibits aggregation in *npr-1(ad609)* mutants. Asterisks indicate statistical significance at $P<0.01$ by two-tailed unpaired t-test with Welch's correction. Error bars are the SEM. n ≥3 for each genotype.

b. Synaptic inhibition of ADL or ASH does not affect bordering in *npr-1(ad609)* mutants. No significance between values was found by two-tailed unpaired t-test with Welch's correction. Error bars are the SEM. n ≥3 for each genotype.

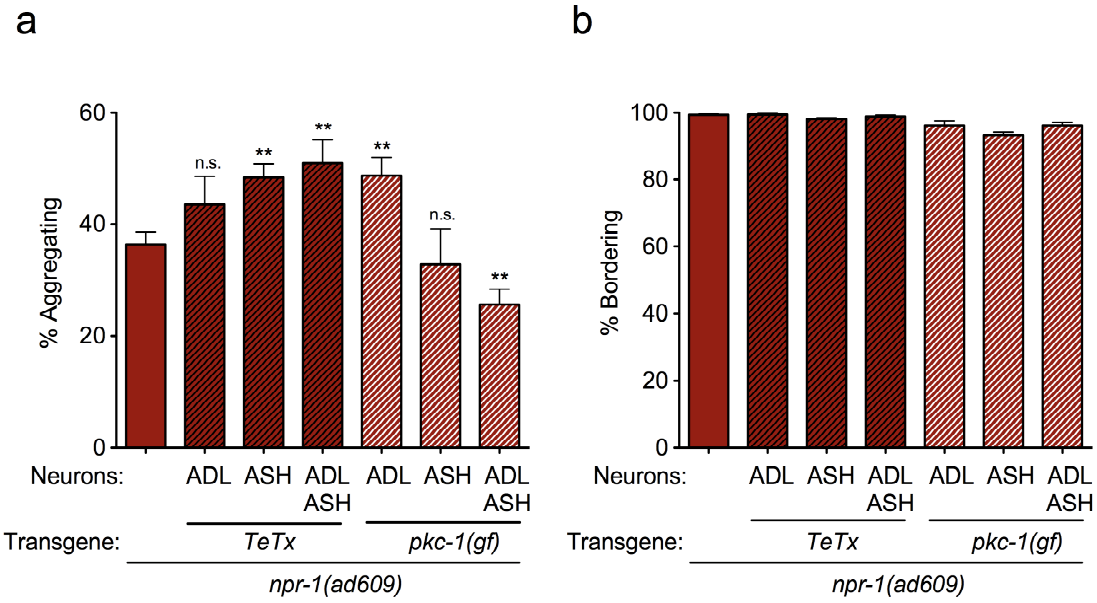
a
b
% Aggregating
% Bordering
60
40
20
0
100
80
60
40
20
0
n.s.
**
**
**
n.s.
**
Neurons:
ADL
ASH
ADL ASH
ADL
ASH
ADL ASH
Transgene:
TeTx
pkc-1(gf)
npr-1(ad609)

Appendix 2-A. Synaptic potentiation of ADL in *flp-21* enhances ascr#3/C9 avoidance

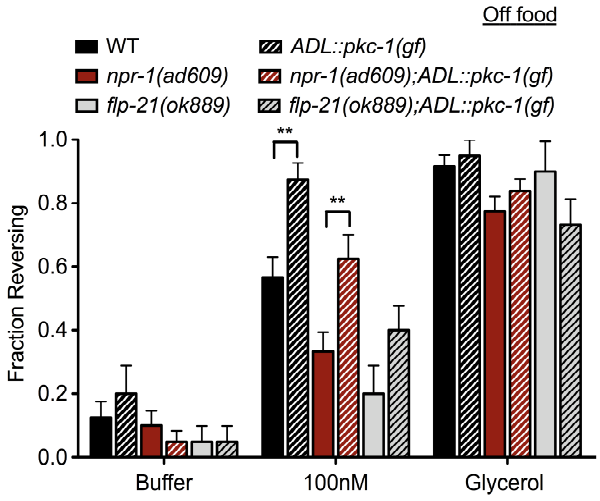

As *flp-21* is expressed in ADL, I hypothesized that FLP-21 released from ADL upon activation by ascr#3/C9 could bind to NPR-1 on RMG and suppress its activity, and therefore contributing to ascr#3/C9 avoidance. However, preliminary results show that synaptic potentiation of ADL in the *flp-21* null mutant background enhances ascr#3/C9 avoidance, suggesting that ascr#3/C9 avoidance is not dependent on FLP-21 release from ADL. Note that this effect did not reach statistical significance and requires more data. * and ** indicate values that are different at $P<0.05$ and 0.01 between values indicated by brackets (chi-square test with Yates' correction for continuity). Error bars indicate SEP. n=20-100 animals each. Assays were performed in the absence of food.

Appendix 2-B. Wild-type males avoid high oxygen and exhibit similar aggregation and bordering as *npr-1* hermaphrodites

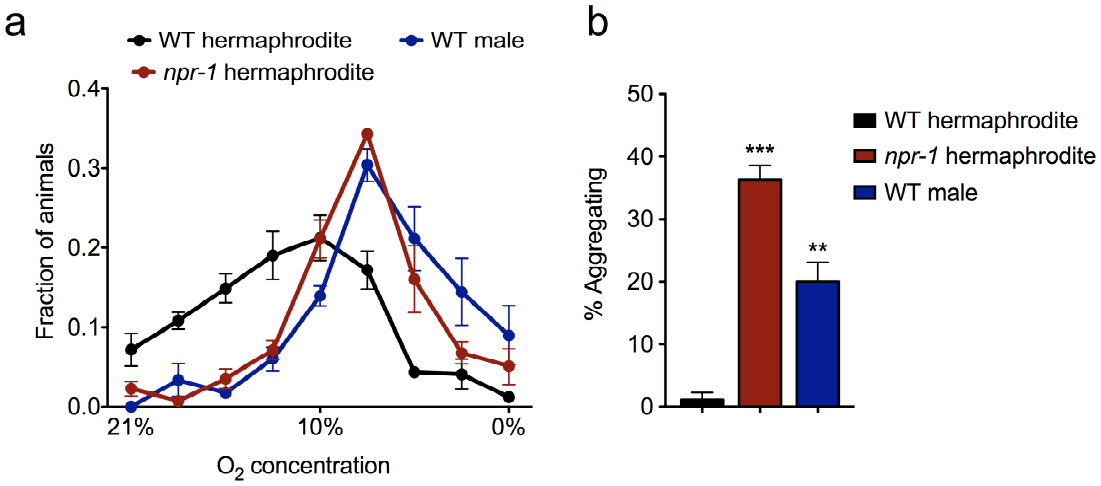

Wild-type males and *npr-1* hermaphrodites are similar in avoidance of high oxygen level and accumulation at 7-14% O_2 **(a),** and aggregation behavior on the bacterial food **(b)**. The avoidance of high oxygen might promote aggregation in both wild-type males and *npr-1* hermaphrodites. ** and *** indicate values that are different at $P<0.01$ and 0.001 from the wild-type hermaphrodite value. Error bars indicate SEP. n ≥3 for each genotype.

Appendix 2-C. Loss of NPR-1 activity enhances aggregation in males or in masculinized hermaphrodites

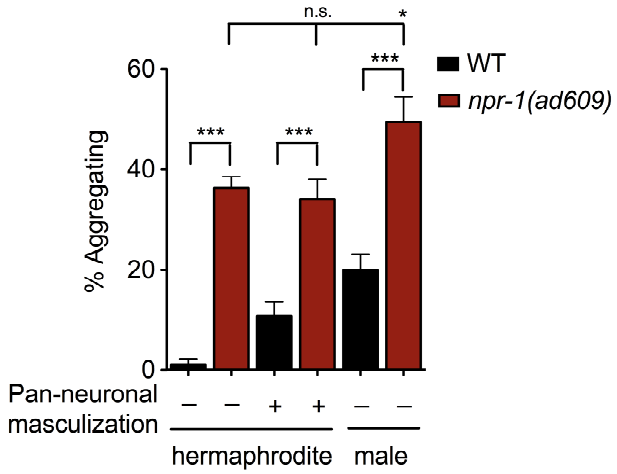

npr-1 males exhibit enhanced aggregation behavior compared to wild-type males or *npr-1* hermaphrodites. Similarly, *npr-1* hermaphrodites with pan-neuronal masculinization show enhanced aggregation compared to wild-type hermaphrodites with pan-neuronal masculinization. These results further support that the male circuit and the *npr-1*/RMG circuit are distinct pathways. Asterisks indicate statistical significance (*P<0.05, **P <0.01 and ***P <0.001 by two-tailed unpaired t-test) between values indicated by brackets. Error bars are SEM. n ≥3 for each genotype.

Appendix 2-D. Masculinized *npr-1* hermaphrodites exhibit reduced ascr#3/C9 avoidance

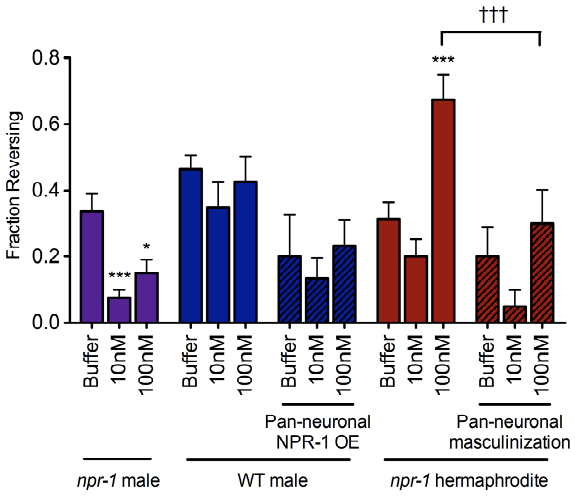

Males with pan-neuronal overexpression of NPR-1 are similar to wild-type males in their ascr#3/C9 avoidance in the presence of food, arguing against the hypothesis that reduced NPR-1 levels in males is responsible for their diminished ascr#3/C9 avoidance. The level of NPR-1 expression seems to affect the basal reversal rate, but not the relative reversal to ascr#3/C9 compared to buffer alone.

Pan-neuronally masculinized *npr-1(ad609)* hermaphrodites exhibit reduced ascr#3/C9 avoidance compared to *npr-1(ad609)* hermaphrodites in the presence of food, supporting the hypothesis that sexual dimorphism in the nervous system regulates avoidance of ascr#3/C9 additively with the *npr-1*-regulated circuit.

For pan-neuronal expression of *npr-1* cDNA and *fem-3* cDNA, H20 and *unc-31* promoters were used, respectively. * and *** indicate responses that are different from the responses to buffer alone for each genotype at $P<0.05$ and 0.001. ††† indicates values that are different at $P<0.001$ between values indicated by brackets (chi-square test with Yates' correction for continuity). Error bars indicate SEP. n ≥10 animals each.

Appendix 2-E. Short-chain ascarosides are not essential for aggregation and bordering behavior

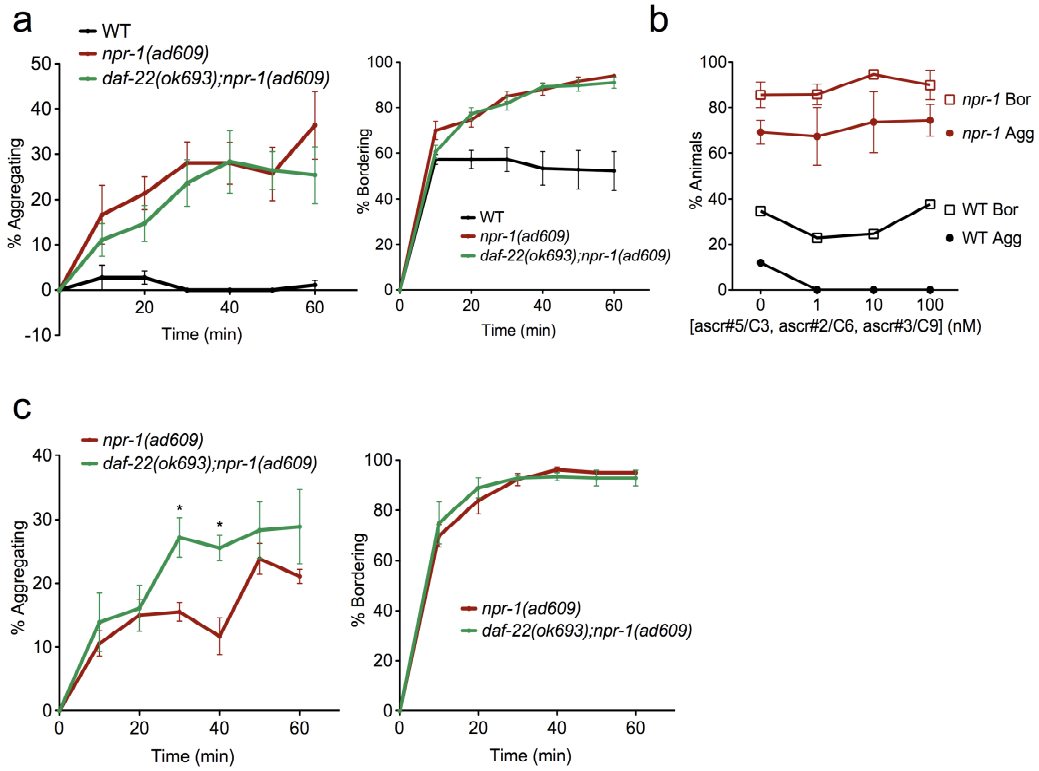

The activity of *daf-22*, the *C. elegans* ortholog of human sterol carrier protein SCPx that catalyzes the final step in peroxisomal fatty acid beta-oxidation, is required for biosynthesis of short-chain fatty acid-derived side chains of ascarosides [128]. To ask whether these ascarosides are required for social behavior in *npr-1* mutants, a null mutation of *daf-22(ok693)* was introduced into *npr-1(ad09)* mutants, and the double mutants were monitored for aggregation and bordering behavior. *daf-22(ok693);npr-1(ad609)* animals were similar to *npr-1(ad609)* animals at room temperature **((a),** no significant difference between *npr-1(ad609)* and *daf-22(ok693);npr-1(ad609)* by 2-way ANOVA), suggesting that short-chain fatty acid ascaroside derivatives are not essential for these behaviors. Consistent with this result, various concentrations of an ascaroside

cocktail of ascr#5/C3, ascr#2/C6 and ascr#3/C9 failed to alter aggregation or bordering behavior in wild-type or in *npr-1* animals (**b)**. It is possible that other subsets of pheromone compounds that bypass DAF-22 pathway, i.e., long-chain fatty acid ascaroside derivatives produced in *daf-22* mutants with weaker dauer-inducing activity [207], are the major pheromone regulators of *npr-1*-dependent aggregation.

When assays are performed at 25°C, preliminary data shows that *daf-22(ok693)* mutation accelerated aggregation in *npr-1(ad609)* background (**(c),** statistical difference at P=0.0011 by 2-way ANOVA; asterisks indicate statistical significance at P<0.05 by two-tailed unpaired t-test compared to *npr-1(ad609)* values for each time point). As ascaroside composition varies in different temperatures [129], pheromone produced at 25°C by DAF-22 pathway may contain more repulsive components. Error bars indicate SEM. n=3 for each genotype.

Chapter 3:

Identification of genes that regulate social behavior

This study was partly performed in collaboration with Manuel Zimmer who contributed his data for oxygen responses to Table 3-1 and Figure 3-2d, and his *in vivo* Ca^{2+} imaging to Figure 3-5d. The *glb-5* study was performed in collaboration with Patrick T. McGrath who identified the allelic difference in *glb-5* between lab strain N2 and CB4856 as described in Figure 3-5b, and generated most strains for Figure 3-5c and 3-5d together with Matthew V. Rockman; this study was published in [146]. Lindsay L. Bellani performed aggregation and bordering assays for some of *npr-1* and innexin double mutants, contributing to the graphs on the left in Figure 3-1a and 3-1b.

Introduction

Neuropeptides and their receptors coordinate complex social behaviors in many animal species. In female mammals, oxytocin released during labor triggers uterine contraction, lactation, and maternal behavior. Oxytocin, vasopressin, and prolactin modulate rodent maternal behaviors including licking and grooming (reviewed in [208]). The release of oxytocin and vasopressin also regulate pair-bonding and social attachment in rodents, and differential activation and expression of their receptors generate variation in social behavior in different species of voles [47, 48]. Other neuropeptides also have roles in social behavior; for example, substance P and its receptor NK1 induce aggressive behaviors such as defensive rage and predatory attack in rodents and cats [209-211].

Social behaviors in *C. elegans* are also regulated by a neuropeptide receptor, *npr-1*, which falls within the neuropeptide Y/neuropeptide F receptor family. Neuropeptide Y (NPY), a conserved 36 amino acid neuromodulator, plays diverse roles in the brains of other species, but these are not generally social. NPY in the hypothalamus regulates feeding in vertebrates; NPYergic activity increases food intake and decreases physical activity [212-216]. In the amygdala, NPY and neuropeptide Y/Y2 receptors mediate regulation of rodent anxiety and depression [217-219]. *Drosophila* neuropeptide F (dNPF), the homolog of human NPY in flies, acts through the G-protein-coupled NPF receptor NPFR1, promoting resilience to diverse stressors and prevention of uncontrolled aggressive behavior [220-222]. Developmental down-regulation of dNPF in older fly larvae induces food aversion and cooperative burrowing [223].

The role of *npr-1* in *C. elegans* social behavior was first discovered through analysis of an aggregating *npr-1* mutant in the non-aggregating, solitary laboratory *C. elegans* strain N2 [136]. Subsequent studies showed that the N2 strain is solitary due to a gain-of-function *npr-1* isoform, NPR-1 215V (valine), whereas most wild strains have a less active NPR-1 215 F (phenylalanine) isoform and show social behaviors [136, 146]. Formally, these results demonstrate that high NPR-1 (215V) activity suppresses social behavior. The most prominent behavior of low NPR-1 (215F) or *npr-1* null mutants is aggregation into small feeding groups, but these strains also differ from N2 in other behaviors, showing faster movement on a bacterial lawn, reduced avoidance of CO_2, enhanced avoidance of O_2, and altered responses to bacterial pathogens [142, 147, 149, 199, 224].

As a way to identify the genes and neural circuits that promote aggregation, mutagenesis has been performed on the social *npr-1* mutant, followed by identification of genes, functional analysis, and determination of the their sites of action. Prior to my work, about 20 aggregation suppressor genes had been identified since the first report implicating *npr-1* in social behavior [136]. The majority of these genes encode enzymes and channels involved in G protein-mediated sensory transduction, cGMP signaling, and Ca^{2+} signaling (Table 3-1). Genes required for neuropeptide biosynthesis and synaptic transmission, chemoreceptor localization to sensory cilia, and transcriptional regulators are also involved in the regulation of *npr-1*-dependent social behaviors (Table 3-1).

The characterization of the site of *npr-1* action led to a circuit model for social behavior called “the hub and spoke circuit”. In this model, the aggregation-promoting neuron RMG – the hub – coordinates sensory inputs from many other neurons – the

spokes – through a network of gap junctions predicted by the *C. elegans* wiring diagram [149]. NPR-1 215V inhibits RMG thereby uncoupling the sensory inputs and preventing aggregation. The hub-and-spoke model predicts that gap junctions between RMG and other neurons are essential for aggregation [149]. To test this hypothesis, I have systematically made and analyzed double mutants between *npr-1* and viable gap junction structural subunits (innexins) of *C. elegans.* I have also characterized other potential *npr-1* suppressors. In this chapter, I report the identification of gap junction genes including *inx-6*, as well as the CB4856-derived allele of the neuronal globin gene *glb-5*, as suppressors of aggregation behavior in *npr-1* mutants, and discuss their functions.

Results

Identification of gap junction genes that regulate social behavior in *npr-1*

In the proposed aggregation circuit regulated by *npr-1*, the electrical (gap junction) synapses between sensory neurons and the hub neuron RMG play a central role [149]. The gap junctions of *C. elegans* and other invertebrates are thought to be composed of a family of proteins called innexins. *C. elegans* has 25 innexin genes, among which viable mutant alleles are available for 21. To identify gap junction genes that regulate aggregation behavior, double mutants were generated between these innexin mutants and *npr-1(ad609)* (Table 3-2). Among 21 innexin genes tested, *inx-6, unc-7* and *unc-9* exhibited strong suppression of aggregation and bordering behavior (Table 3-2, Figure 3-1a and 3-1b). Weak suppression of aggregation and/or bordering was observed in *inx-1, inx-4, inx-11, inx-17* and *inx-22* double mutants with *npr-1* (Table 3-2, Figure 3-1a and 3-1b).

Of the three strong suppressor mutants, *inx-6* was of particular interest because it moved well, unlike *unc-7* or *unc-9,* which are highly uncoordinated and whose motor defect might indirectly disrupt aggregation behavior. Therefore the *inx-6;npr-1* double mutant was characterized further. The *inx-6(rr5)* allele has missense mutation from cytosine to thymine at the seventh exon, changing the proline 353 to leucine (Figure 3-2b) [225]. It is a temperature-sensitive allele: at the restrictive temperature of 25°C, *inx-6(rr5)* mutants are arrested in the L1 larval stage, but they grow normally at the permissive temperature of 15°C [225]. At 20°C, *inx-6(rr5)* can bypass the developmental arrest and grow into adult animals.

CX13742 and CX13748, two independent outcrossed strains of *inx-6(rr5);npr-1(ad609),* differed in their suppression of aggregation and bordering, and in their temperature sensitivity (Figure 3-2a, Table 3-3). CX13742 showed complete suppression of aggregation and bordering regardless of the growth and assay temperatures (Figure 3-2a, Table 3-3). CX13748 exhibited strong temperature dependence with partial suppression of aggregation when grown at 20°C and assayed at 25°C (Figure 3-2a, Table 3-3). The temperature-dependent L1 larval arrest phenotype of *inx-6(rr5)* was present in both of the *inx-6(rr5);npr-1(ad609)* double mutant strains (Table 3-2).

The L1 larval arrest phenotype of CX13742 and CX13748 was completely rescued by a genomic transgene consisting of the *inx-6* coding region under its 3 kb endogenous promoter (Table 3-3). This transgene fully restored aggregation in CX13748, the partially-defective, temperature-dependent strain (Figure 3-2c, Table 3-3). However, the *inx-6* transgene only weakly rescued the defective CX13742 strain in the same conditions (Figure 3-2c, Table 3-3). These results suggest that the *inx-6(rr5)* allele weakly suppresses aggregation, and that the CX13742 strain contains an additional suppressor that yields a stronger phenotype.

In addition to aggregation and bordering behavior, *npr-1* mutants have characteristic behavioral responses to a shift in oxygen (O_2) concentration. *npr-1* shows a sustained slowing response upon downshift from 21 to 10% O_2, whereas wild-type has a transient slowing response (Figure 3-2d, indicated by arrowhead). The strongly suppressed CX13742 is also suppressed for the O_2 responses, resembling wild-type rather than *npr-1(ad609)* (Figure 3-2d). CX13748 does not differ from *npr-1(ad609)* animals in

O_2 shift responses (data not shown). Studies are underway to identify the strong suppressor gene in CX13742.

unc-7 and *unc-9* are widely expressed in body muscles as well as the nervous system of *C. elegans.* They form electrical synapses in the locomotory system as well as regulating some aspects of neuronal development [226-230]. Expression of *unc-7* or *unc-9* cDNAs driven by the pan-neuronal *unc-31* promoter partially restored the aggregation and bordering defect in *unc-7(e5) npr-1(ad609)* and *unc-9(e101) npr-1(ad609)*, respectively (Figure 3-3a and 3-3b). However, expression of the cDNAs in RMG and several "spoke" sensory neurons using the *flp-21* promoter failed to rescue the mutant aggregation and bordering defects (Figure 3-3a and 3-3b). In previous studies, the expression of *unc-7* from a motor neuron promoter rescued the aggregation defect of an *unc-7(e5) npr-1(ad609)* double mutant [231]. Thus, it is likely that the aggregation defect of *unc-7* and *unc-9* mutants is secondary to a locomotory defect, although there could be subtle roles in the RMG hub and spoke circuit.

A forward genetic screen for aggregation-specific suppressors in CB4856

CB4856, a wild strain isolated from Hawaii, has long been used as a tool for mapping mutants isolated in the lab strain N2 using single nucleotide polymorphism (SNP) differences between two strains [232-234]. Due to *npr-1*$_{HW}$, its naturally-occurring allele of *npr-1* encoding the NPR-1 215F isoform with weaker activity, CB4856 exhibits social aggregation behavior in the presence of food, accumulation at the border of a bacterial lawn, and enhanced preference of 7-12% O_2 (Figure 3-4c) [136, 142, 146, 199]. Hyperoxia avoidance, the avoidance of ambient oxygen levels, promotes aggregation and

bordering behavior: an aggregating group of worms has an internal 6-14% O_2 level and the border of a bacterial lawn has about 13% O_2 [142, 200]. Many known suppressors of *npr-1*-dependent aggregation also have a defect in oxygen preference in a gradient assay, showing changes in median preferred oxygen level or an overall reduction in hyperoxia avoidance [199].

In order to isolate genes that regulate aggregation independent of oxygen sensation and signaling, I performed a forward genetic suppressor screen using random chemical mutagenesis in the naturally social CB4856 background and searched for mutants with defective aggregation but intact bordering behavior (Figure 3-4a, See Materials and Methods). In a pilot screen of 800 haploid genome, 12 interesting mutants were isolated. Among them, four were characterized in more stringent aggregation and bordering assays and showed mostly intact bordering but defective aggregation (Table 3-4 and Figure 3-4b). However, in the oxygen gradient assay used for close examination of oxygen preferences, only CX861 showed the exact distribution and hyperoxia avoidance index of CB4856 (Figure 3-4c). CX861 also had mild defects in turning rate and speed to changes in CO_2 and chemotaxis to volatile attractants benzaldehyde (bz) and diacetyl (da), mediated by AWC and AWA sensory neurons, respectively (Table 3-4, see Materials and Methods). Together, these results identified CX861 as an interesting mutant strain with the desired phenotypes separating aggregation from other O_2-dependent behaviors.

The CB4856 variant of *glb-5* suppresses aggregation in *npr-1*

I progressively outcrossed CX861 to an *npr-1(ad609)* social mutant strain in the N2 background to remove CB4856-derived DNA that was not specific for the mutant phenotype. In the outcrossed strains, an interesting observation was made with respect to the CB4856-derived allele of the *glb-5* gene.

First, the SNP mapping results of recombinant CX861 demonstrated that CB4856-derived DNA around the *glb-5* locus correlated with the aggregation suppression phenotype. Outcrossed strains homozygous for the $glb\text{-}5_{HW}$ allele exhibited suppression of aggregation, whereas strains homozygous for the $glb\text{-}5_{N2}$ allele were indistinguishable from the starting *npr-1(ad609)* strain (Table 3-5).

As an independent approach to characterize the effect of *glb-5*, I characterized recombinant inbred advanced intercrossed lines (RIAILs) generated by intercrossing CB4856 and N2 and selfing for ten generations [235]. RIAILs that have $npr\text{-}1_{HW}$, the CB4856 allele of *npr-1*, aggregated, and their degree of aggregation correlated with the *glb-5* allele in the strain (Figure 3-5a). RIAILs with stronger aggregation had the N2-derived allele of *glb-5*, whereas RIAILs with weaker aggregation had the CB4856-derived allele of *glb-5*.

Independent studies in the laboratory showed that the variation in the *glb-5* gene between CB4856 and N2 strains modulates responses to small changes in O_2 and combined CO_2/O_2 levels [146]. In the N2 strain, the genomic sequence of *glb-5* contains a 765-bp duplication/insertion not present in any wild strains or other *Caenorhabditis* species (Figure 3-5b, [146, 236]). The duplication results in an in-frame stop codon that truncates the last 179 amino acids [146].

Therefore, I hypothesize that the genetic variation of *glb-5* gene and the CB4856-derived GLB-5 activity modulates aggregation behavior in $npr\text{-}1_{HW}$ background. I tested strains combining $glb\text{-}5_{HW}$ or $glb\text{-}5_{N2}$ and $npr\text{-}1_{HW}$ or $npr\text{-}1_{N2}$ in an N2 background. These strains were generated by outcrossing RIAILs to wild-type N2 multiple times to remove other CB4856-derived DNA from the rest of the genome. However, aggregation in an $npr\text{-}1_{HW}$ genetic background was significantly modulated by the *glb-5* allele: strains with $glb\text{-}5_{N2}$ aggregated more strongly than strains with $glb\text{-}5_{HW}$ (Figure 3-5c, [146]). $glb\text{-}5_{HW}$ also suppressed the aggregation of an *npr-1(ad609)* loss of function allele (Figure 3-5c, Table 3-5, [146]). In addition, bordering in *npr-1(ad609)* but not in $npr\text{-}1_{HW}$ animals was slightly suppressed by presence of $glb\text{-}5_{HW}$. However, the genotypes of *glb-5* did not influence the solitary behavior of $npr\text{-}1_{N2}$ animals (Figure 3-5c, [146]).

GLB-5 functions in the oxygen-sensing neurons AQR, PQR, and URX neurons to sensitize their oxygen response (Figure 3-5d, [146, 236]). To ask whether its activity in these neurons regulate aggregation, I tested animals expressing a *glb-5* cDNA encoding the CB4856 allele of *glb-5* in $npr\text{-}1_{HW}$ animals. Expression of $glb\text{-}5_{HW}$ under its own promoter or under the *gcy-36* promoter expressed in URX, AQR, and PQR neurons was sufficient for suppression of aggregation (Figure 3-5c, [146]). The genotype of the *glb-5* allele had relatively little effect on bordering behavior, which was largely determined by *npr-1* genotype (Figure 3-5c, [146]). These results indicate that the CB4856-derived wild-type allele of *glb-5* encodes an active form of GLB-5 that suppresses aggregation.

The *ky861* mutation on chromosome V further suppresses aggregation and bordering in *npr-1* in the presence of the CB4856 *glb-5* variant

Although the wild-type allele of $glb\text{-}5_{HW}$ contributes to the suppression of aggregation in CX861-derived recombinants, it is not sufficient to explain the complete suppression of aggregation observed in the original strain, or in a subset of the CX861-derived recombinants (Table 3-5). Both #1-2 and #3-4 recombinants contain $glb\text{-}5_{HW}$ that suppresses aggregation compared to #5-7 recombinants with $glb\text{-}5_{N2}$ (Table 3-5). However, aggregation is completely suppressed to levels comparable to wild-type N2 in #1-2 recombinants but not in #3-4 recombinants. Consistent with this phenotype, #1-2 recombinants contain a longer piece of CB4856-derived genomic DNA between the *glb-5* locus at -1.5cM and 0.1cM on chromosome V (Table 3-5). SNP mapping data suggest that no other genomic region in other chromosomes correlates with the suppression of aggregation phenotype (data not shown). Therefore, the mutation of *ky861* introduced by random mutagenesis lies in this region of 861kb. This *ky861* mutation suppresses aggregation in CB4856 and in the *npr-1(ad609);*$glb\text{-}5_{HW}$ background.

Discussion

Innexin genes regulate the *npr-1* aggregation circuit in a complex way

Examination of double mutants between all available innexin mutant alleles and *npr-1(ad609)* identifies multiple innexin regulators of *npr-1* aggregation, consistent with the complexity in the aggregation circuit (Table 3-2). However, no single mutation fully suppressed aggregation without causing other defects (Figure 3-1a and 3-1b, Table 3-2). Two full suppressors caused motor defects (*unc-7(e5) npr-1(ad609)* and *unc-9(e101) npr-1(ad609))*, and an additional mutation contributed to suppression in *inx-6(rr5);npr-1(ad609)*.

Multiple innexin mutants were found to weakly suppress *npr-1* aggregation behavior (Table 3-2). These results suggest that there might be redundancy between innexin genes that regulate the *npr-1* circuit for aggregation. In general, identification of genes that affect aggregation has been easier for genes that function at the sensory level, than for genes that affect the aggregation circuit (Table 3-1). Moreover, some innexin genes important for aggregation may have pleiotropic effects such as lethality or uncoordinated movement. Investigation of triple or quadruple mutants between weak suppressor innexins and *npr-1(ad609)*, and confirmation of their functions by genetic rescue followed by determining their sites of action in the circuit, will be the next steps.

npr-1 and *glb-5$_{HW}$* have opposite effects on aggregation

The CB4856 (HW)-derived variants of *npr-1* and *glb-5* have opposite effects on aggregation in N2 animals. *npr-1$_{HW}$* and *npr-1(ad609)* encode weaker activity NPR-1 isoforms and promote aggregation. *glb-5$_{HW}$* encodes the active GLB-5 isoform and suppresses aggregation in the *npr-1* background (Figure 3-5c). On the other hand, both *npr-1$_{HW}$* and *glb-5$_{HW}$* have similar effects on O_2 responses, making N2 animals more sensitive to changes in ambient O_2 levels [146]. This discrepancy may be attributed to the level where each gene functions. GLB-5 primarily regulates sensory responses to O_2 in O_2-sensing neurons. NPR-1, however, regulates a more complex circuit that integrates diverse sensory information sensed by multiple sensory neurons as well as O_2. Detailed analysis of neuronal activity across the circuit may distinguish signals important for aggregation, compared to signals related more purely to oxygen sensation.

Table 3-1. Identified *npr-1* suppressor genes

Loss-of-function mutations in these genes suppress aggregation (social behavior)

G protein, cyclic nucleotide and Ca^{2+} signaling		
tax-6	Calcineurin A	Katherine P. Weber (pers. comm.)
egl-8	Phospholipase C beta homolog	Mario de Bono (unpublished)
pitp-1	Phosphatidylinositol transfer protein rdgB	Evan Z. Macosko (unpublished)
osm-9, ocr-2	TRPV channel	[144]
tax-2, tax-4	Cyclic nucleotide-gated cation channel	[152]
gcy-35, gcy-36	Soluble guanylyl cyclase	[142]
daf-11	Transmembrane guanylate cyclase	Katherine P. Weber (pers. comm.)
egl-4	Cyclic GMP-dependent protein kinase	Katherine P. Weber (pers. comm.)
gpb-2	G-protein beta subunit	Katherine P. Weber (pers. comm.)
egl-30	G protein alpha subunit Gq	Andres Bendesky (unpublished)
Neuropeptide biosynthesis		
egl-21	Carboxypeptidase E	Evan Z. Macosko (unpublished)
tph-1	Tryptophan hydroxylase	Heeun Jang (unpublished)
Synaptic transmission		
eat-4	Vesicular glutamate transporter	Katherine P. Weber (pers. comm.)
unc-11	Clathrin-adapted protein AP180	Lindsay L. Bellani (unpublished)
Transcription regulator		
che-1	Zinc finger-containing transcription factor	Katherine P. Weber (pers. comm.)
ncl-1	E3 ubiquitin ligase	Katherine P. Weber (pers. comm.)
Localization of chemoreceptors or guanylyl cyclase		
odr-4	Transmembrane protein	[144]
odr-8	Ubiquitin-like modification system (Tapan Maniar, pers. comm.)	[144]
daf-25	MYND zinc-finger and ankyrin repeat protein	Katherine P. Weber (pers. comm.)
Gap junction molecules		
inx-1	Innexin	This work (unpublished)
inx-4	Innexin	This work (unpublished)
inx-6	Innexin	This work (unpublished)
inx-17	Innexin	This work (unpublished)
inx-22	Innexin	This work (unpublished)
unc-7	Innexin	This work (unpublished)
unc-9	Innexin	This work (unpublished)
Oxygen binding		
glb-5$_{HW}$	Neuronal globin	This work ([146])

Table 3-2. Summary of suppression of *npr-1* behaviors by innexin mutations

Double mutant strain with *npr-1*	Genotype of innexin	Aggregation	Bordering	ascr#3/C9 avoidance	Oxygen response
*DA609	-	+++	+++	+++	+++
CX13067	***inx-1 (tm3524)***	++	++	+++	+++++
CX10040	*inx-2 (ok376)*	+++	+++	++	**Not tested**
CX13808	***inx-4 (ok2373)***	++	+++	+++	++++
CX13742	***inx-6 (rr5)***	+	+	+++	+
CX13748	***inx-6 (rr5)***	++	++	+++	+++
CX10042	*inx-7 (tm2738)*	+++	+++	**Not tested**	**Not tested**
CX10044	*inx-8 (gk42)*	+++	+++	**Not tested**	**Not tested**
CX10028	*inx-9 (ok1502)*	+++	+++	**Not tested**	**Not tested**
CX13103	*inx-10 (tm3393)*	+++	+++	**Not tested**	**Not tested**
CX13382	***inx-11 (ok2783)***	+++	++	**Not tested**	+++
CX13045	*inx-14 (ag17)*	+++	+++	**Not tested**	**Not tested**
CX13318	*inx-15 (tm3394)*	+++	+++	**Not tested**	**Not tested**
CX13534	*inx-16 (tm1589)*	+++	+++	**Not tested**	**Not tested**
CX13277	***inx-17 (tm3829)***	++	++	++	++++
CX13278	*inx-18 (ok2454)*	+++	+++	**Not tested**	**Not tested**
CX12275	*inx-19 (tm1896)*	+++	+++	**Not tested**	**Not tested**
CX13016	*inx-20 (ok681)*	+++	+++	**Not tested**	**Not tested**
CX13535	*inx-21 (tm4591)*	+++	+++	**Not tested**	**Not tested**
CX13470	***inx-22 (tm1661)***	++	+++	**Not tested**	+++
CX10001	*****unc-7 (e5)***	+	+	**Not tested**	+
CX10041	*****unc-9 (e101)***	+	+	**Not tested**	+
CX10173	*eat-5 (ad464)*	+++	+++	**Not tested**	**Not tested**
	inx-5	Mutant allele not available			
	inx-3 (ok481)	Embryonic lethal			
	inx-12 (tm3279)	Embryonic lethal			
	inx-13 (ok235)	Embryonic lethal			

*DA609 is the *npr-1(ad609)* strain used to generate a double mutant with innexins.

**Defects can be due to strong motor defects.

+++, the phenotype of DA609; ++, weak defect; + strong defect;

++++, weak phenotypic enhancement; +++++, strong phenotypic enhancement

Table 3-3. Temperature-dependent defects and rescues in two *inx-6(rr5);npr-1(ad609)* strains

	L1 arrest		Aggregation/Bordering			
	Growth (°C)		Growth (°C)			
	15	25	15		20	
			Assay (°C)			
			15	25	15	25
CX13742	No defect	Strong defect	Strong defect	Strong defect	Strong defect	Strong defect
CX13748	No defect	Strong defect	No defect	No defect	Weak to no defect	Weak defect

inx-6p::*inx-6* transgene rescue

	L1 arrest	Aggregation/Bordering	
	Growth (°C)	Growth (°C)	
	25	20	
		Assay (°C)	
		15	25
CX13742	Full rescue	Partial rescue	Partial rescue
CX13748	Full rescue	Full rescue	Full rescue

Table 3-4. Summary of characterized behaviors in aggregation-defective mutants from an EMS screen in CB4856

Strain name	Mutant allele	Aggregation	Bordering	Hyperoxia avoidance	CO_2 responses	Chemotaxis to bz, da
CX859	*ky859*	Strong defect	Weak defect	Weak defect	Weak defect	No defect
CX860	*ky860*	Strong defect	No defect	Weak defect	Strong defect	No defect
CX861	*ky861*	Weak defect	No defect	No defect	Weak defect	Weak defect
CX870	*ky870*	Weak defect	No defect	Weak defect	No defect	No defect

Table 3-5. *glb-5* and candidate region of *ky861* narrowed by SNP mapping

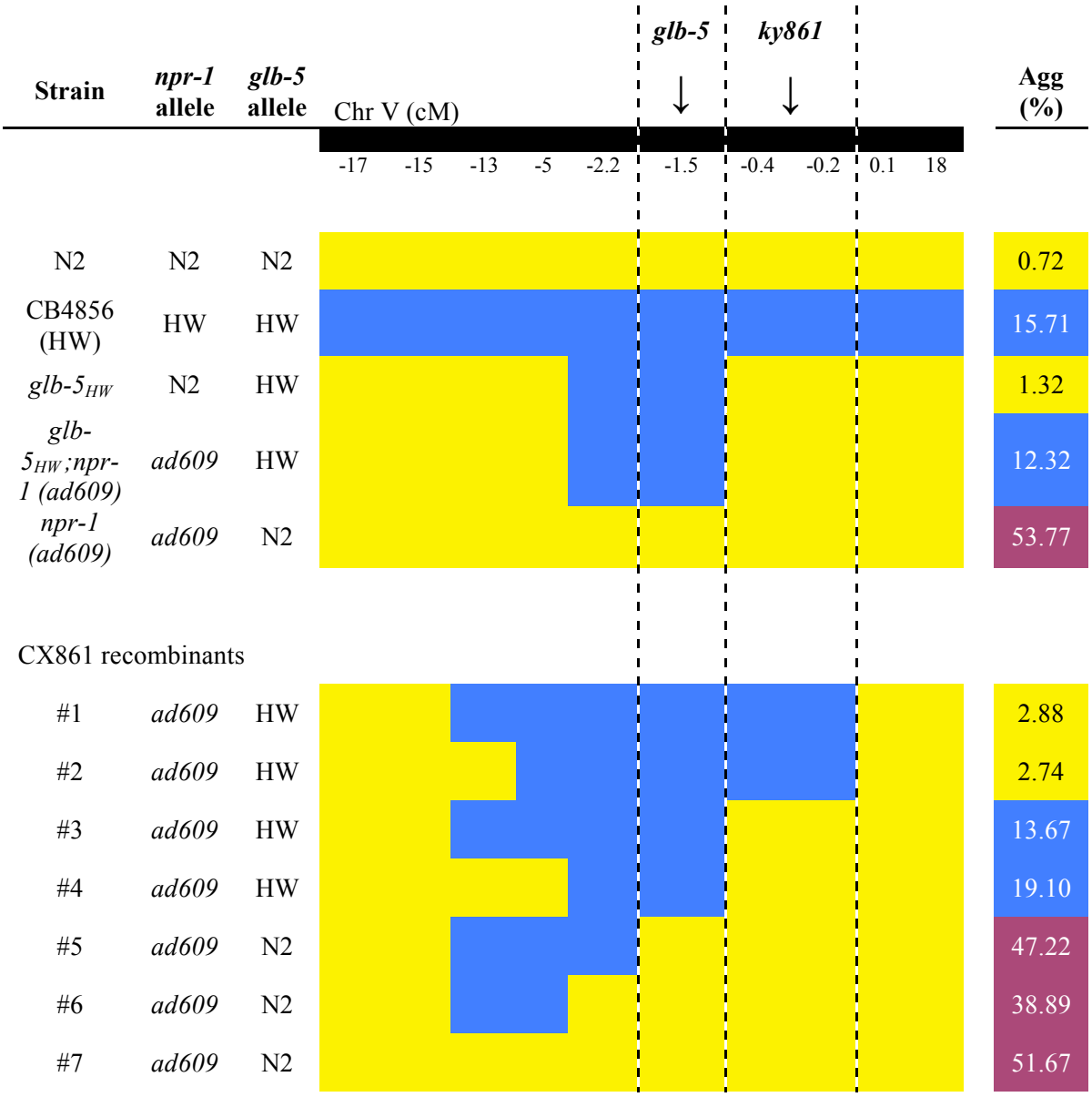

Blue, CB4856-derived DNA; yellow, N2-derived DNA

Figure 3-1. A subset of innexin mutants suppress social behavior of *npr-1(ad609)*

a. Aggregation behavior of all available *C. elegans* innexin mutants in *npr-1(ad609)* background. The percentage of animals that aggregate in feeding groups on bacterial food was scored one hour after 60 adult hermaphrodites were placed on the assay plate. Asterisks indicate statistical significance (***P* <0.01 and ****P* <0.001 by two-tailed unpaired t-test with Welch's correction) compared to the values for *npr-1(ad609)*. Error bars are the standard error of the mean (SEM). n ≥3 for each genotype. Animals were grown at 20°C and assays were performed at room temperature.

b. Bordering behavior of all available *C. elegans* innexin mutants in *npr-1(ad609)* background. The percentage of animals that reside on the thick border of the bacterial food was scored one hour after 60 adult hermaphrodites were placed on the assay plate. Asterisks indicate statistical significance (**P* <0.05, ***P* <0.01 and ****P* <0.001 by two-tailed unpaired t-test with Welch's correction) compared to the values for *npr-1(ad609)*. Error bars are the SEM. n ≥3 for each genotype. Animals were grown at 20°C and assays were performed at room temperature.

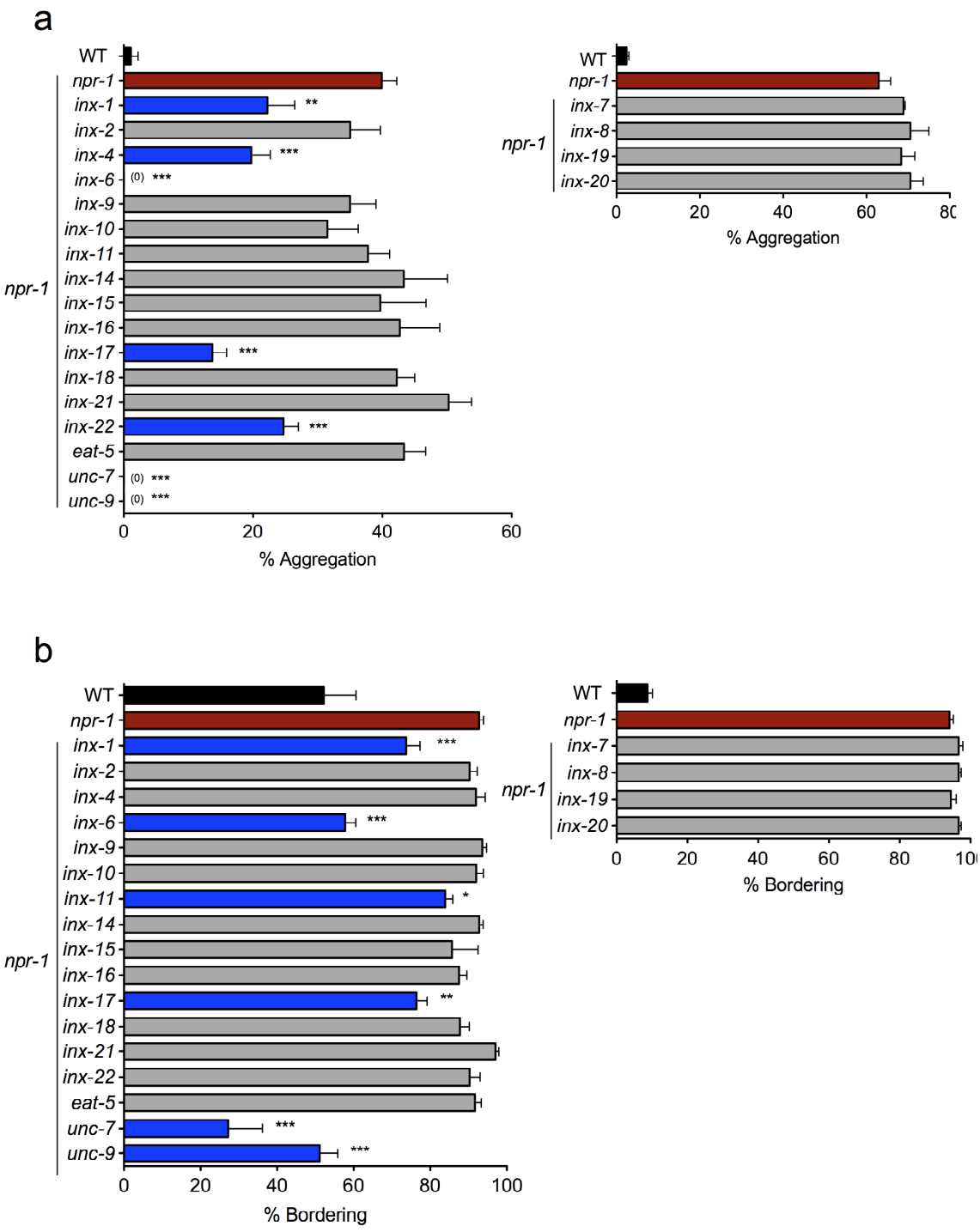
a
WT
npr-1
inx-1
inx-2
inx-4
inx-6
inx-9
inx-10
inx-11
inx-14
inx-15
inx-16
inx-17
inx-18
inx-21
inx-22
eat-5
unc-7
unc-9
npr-1
**
***
(0) ***
***
***
(0) ***
(0) ***
0
20
40
60
% Aggregation
WT
npr-1
inx-7
inx-8
inx-19
inx-20
npr-1
0
20
40
60
% Aggregation
b
WT
npr-1
inx-1
inx-2
inx-4
inx-6
inx-9
inx-10
inx-11
inx-14
inx-15
inx-16
inx-17
inx-18
inx-21
inx-22
eat-5
unc-7
unc-9
npr-1
***
***
*
**
***
***
0
20
40
60
80
100
% Bordering
WT
npr-1
inx-7
inx-8
inx-19
inx-20
npr-1
0
20
40
60
80
% Bordering

Figure 3-2. Social suppression of *inx-6(rr5);npr-1(ad609)* is rescued by expression of its genomic fragment

a. CX13742 and CX13748, two independent outcrossed strains of *inx-6(rr5);npr-1(ad609)*, exhibit differences in the degree and temperature sensitivity of aggregation (left) and bordering (right). Asterisks indicate statistical significance (**P <0.01 and ***P <0.001 by two-tailed unpaired t-test) between values indicated by brackets. n.s. – not significant. Error bars are the SEM. n ≥3 for each genotype.

b. Structure of *inx-6* gene. The *rr5* allele has a cytosine (C) to thymine (T) transition at the seventh exon, causing a missense mutation from proline (P) 353 to leucine (L).

c. The *inx-6(rr5);npr-1(ad609)* strains, CX13742 and CX13748 are partially or full rescued respectively in their (left) aggregation and (right) bordering behaviors by expression of genomic fragment of *inx-6* driven by the endogenous 3kb promoter. Plasmids were injected at 5 ng/μL or 20 ng/μL. Animals were grown at 20°C and assays were performed at 25°C, where CX13748 shows a defect. *, ** and *** indicate responses that are different from the responses to the value of *npr-1(ad609)* at P<0.05, 0.01 and 0.001, respectively. †, †† and ††† indicate values that are different at P<0.05, 0.01 and 0.001 between values indicated by brackets (two-tailed unpaired t-test with Bonferroni's correction). n.s. – not significant. Error bars are the SEM. n ≥3 for each genotype.

d. CX13742 speed in response to an O_2 shift from 21%-10%-21% resembles wild-type responses, but is distinct from *npr-1(ad609)* responses. The arrowhead indicates sustained speed changes observed in *npr-1(ad609).* Animals were well fed and moved to the behavioral arena without food for the assay. Speed is the averaged value of n ≥100 animals for each genotype.

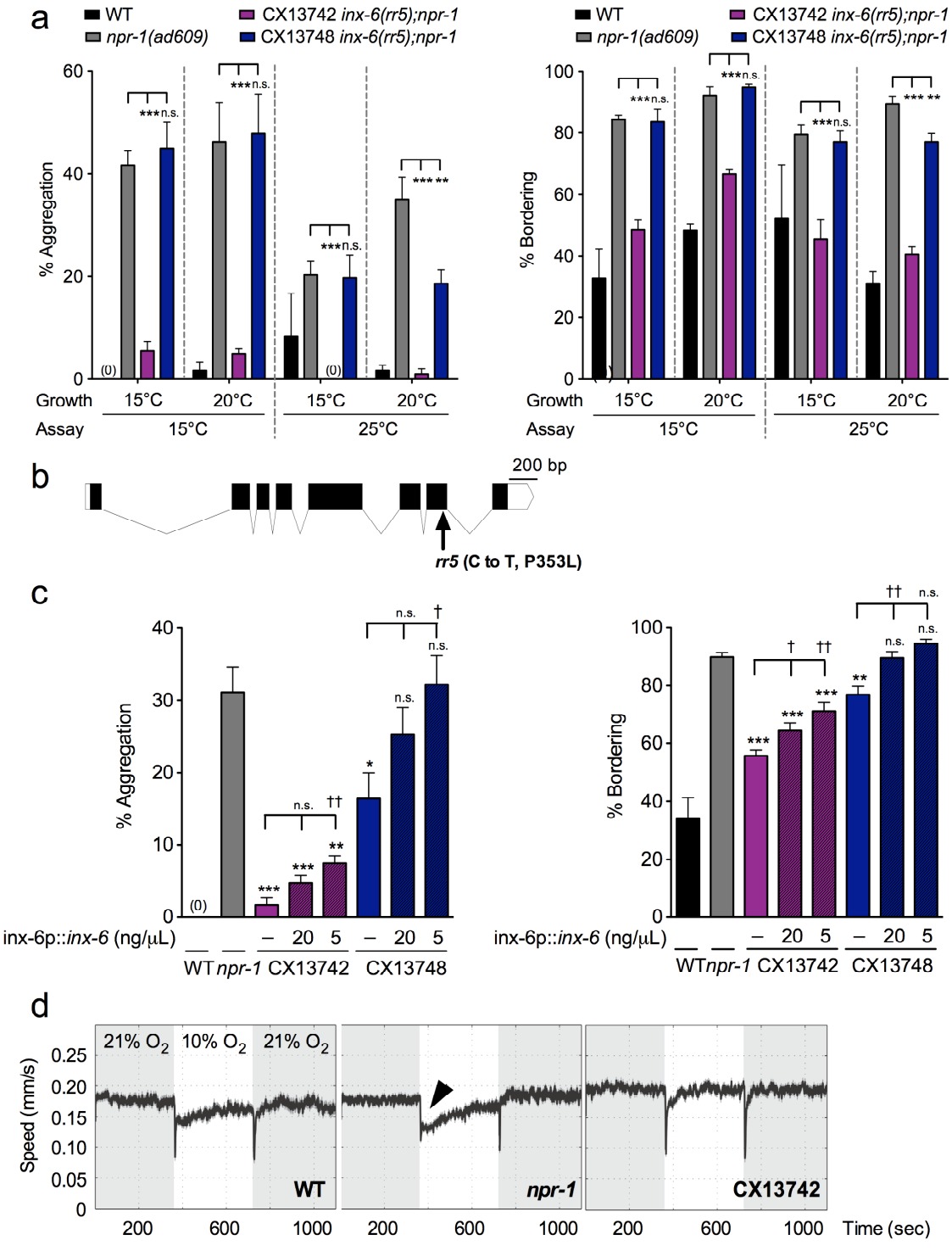
a
WT
npr-1(ad609)
CX13742 inx-6(rr5);npr-1
CX13748 inx-6(rr5);npr-1
% Aggregation
% Bordering
Growth
Assay
15°C
20°C
25°C
b
200 bp
rr5 (C to T, P353L)
c
inx-6p::inx-6 (ng/μL)
WT
npr-1
CX13742
CX13748
d
21% O2
10% O2
21% O2
Speed (mm/s)
WT
npr-1
CX13742
Time (sec)

Figure 3-3. **Pan-neuronal expression but not RMG expression of *unc-7* or *unc-9* cDNA partially rescues social behavior**

a. Pan-neuronal expression but not RMG expression of *unc-7* cDNA partially restores aggregation (left) and bordering (right) behavior to *unc-7(e5) npr-1(ad609)*. The *unc-31* promoter was used for pan-neuronal expression. The *flp-21* promoter was used for expression in RMG and other neurons including ASK, ASH, ASI, ASG and ADF. *** indicates responses that are different from the responses of *npr-1(ad609)* at $P<0.001$. ††† indicate values that are different at $P<0.001$ between values indicated by brackets (two-tailed unpaired t-test with Bonferroni's correction). n.s. – not significant. Error bars indicate SEM. n ≥3 for each genotype.

b. Pan-neuronal expression but not RMG expression of *unc-9* cDNA partially restores aggregation (left) and bordering (right) behavior to *unc-9(e101) npr-1(ad609)*. The *unc-31* promoter was used for pan-neuronal expression. The *flp-21* promoter was used for expression in RMG and other neurons including ASK, ASH, ASI, ASG, ADF and more. ** and *** indicate responses that are different from the responses of *npr-1(ad609)* at $P<0.01$ and 0.001, respectively. ††† indicates values that are different at $P<0.001$ between values indicated by brackets (two-tailed unpaired t-test with Bonferroni's correction). n.s. – not significant. Error bars indicate SEM. n ≥3 for each genotype.

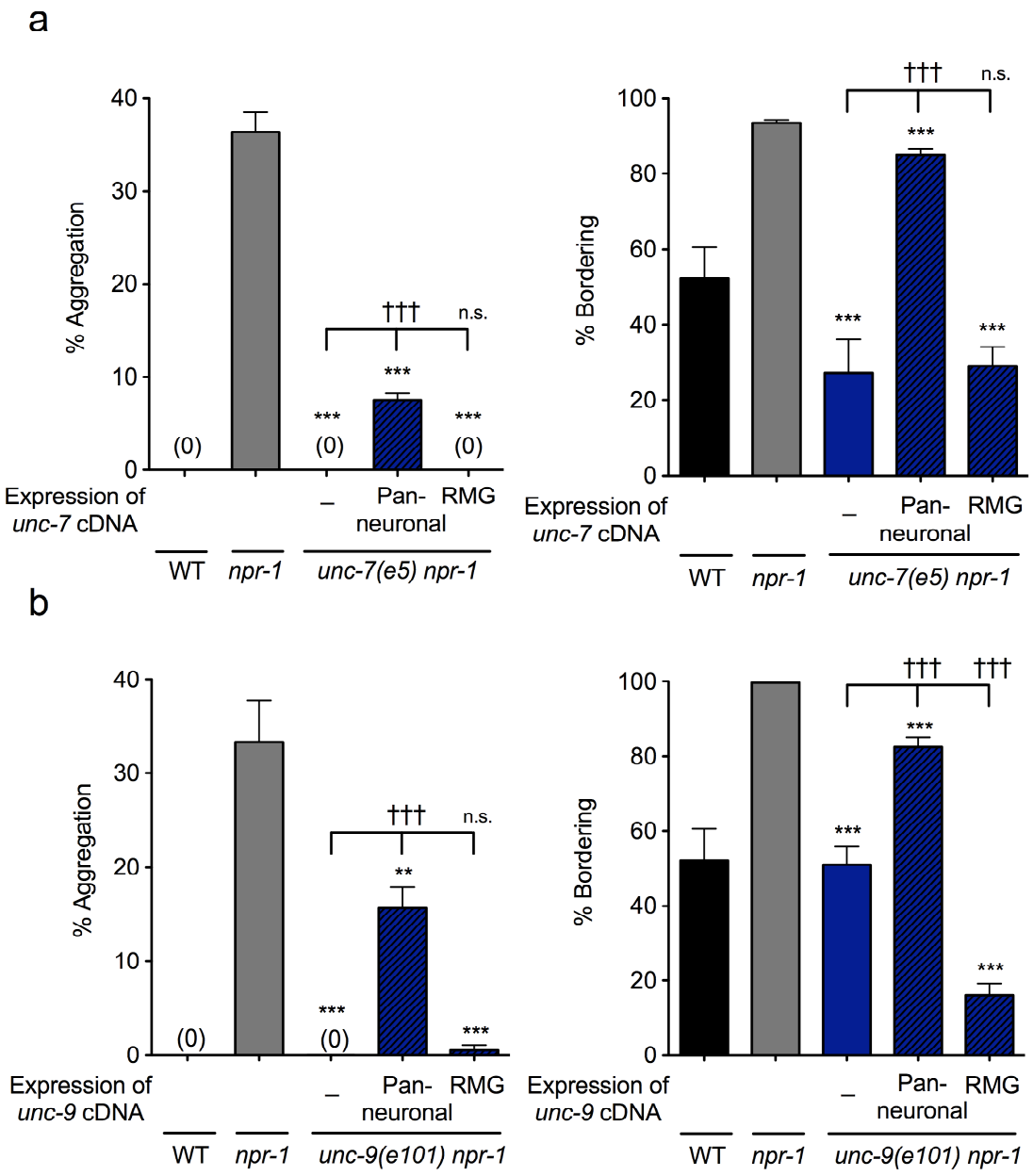
a
% Aggregation
40
30
20
10
0
(0)
(0)
(0)
***
***
***
†††
n.s.
Expression of unc-7 cDNA
–
Pan-neuronal
RMG
WT
npr-1
unc-7(e5) npr-1
% Bordering
100
80
60
40
20
0
***
***
***
†††
n.s.
Expression of unc-7 cDNA
–
Pan-neuronal
RMG
WT
npr-1
unc-7(e5) npr-1
b
% Aggregation
40
30
20
10
0
(0)
(0)
***
**
***
†††
n.s.
Expression of unc-9 cDNA
–
Pan-neuronal
RMG
WT
npr-1
unc-9(e101) npr-1
% Bordering
100
80
60
40
20
0
***
***
***
†††
†††
Expression of unc-9 cDNA
–
Pan-neuronal
RMG
WT
npr-1
unc-9(e101) npr-1

Figure 3-4. Forward genetic screen for aggregation-specific suppressors in CB4856

a. Scheme of the forward genetic screen in CB4856 using random mutagenesis. CB4856 animals in the L4 stage were mutagenized with ethyl methanesulfonate (EMS) and 6 F2 were individually cloned from each F1 into a 6-well plate with each well having NGM and a small bacterial lawn. The growth plates of their F3 progeny were examined visually and mutants with defective aggregation but intact bordering phenotype were picked for further analysis.

b. (Top) Fraction of animals alone and not touching other animals and (bottom) fraction of animals on the border in N2, CB4856 and isolated mutants. * and ** indicate responses that are different from the responses of CB4856 at $P<0.05$ and 0.01, respectively (two-tailed unpaired t-test). n.s. – not significant. Error bars indicate SEM. n ≥2 for each genotype.

c. (Left) Among four isolated mutants, CX861 showed intact CB4856 hyperoxia avoidance behavior in the O_2 gradient of 0 to 21%. Hyperoxia avoidance index is defined as [(fraction of animals in 7%–14% O_2) − (fraction of animals in 14%–21% O_2)] / (fraction of animals in 7%–21% O_2). *** indicates responses that are different from the value of CB4856 at $P<0.001$ (two-tailed unpaired t-test with Bonferroni's correction). n.s. – not significant. (Right) CX861 animals are distributed in the O_2 gradient of 0 to 21% in a similar pattern to CB4856. Error bars indicate SEM. n ≥3 for each genotype. (See Materials and Methods).

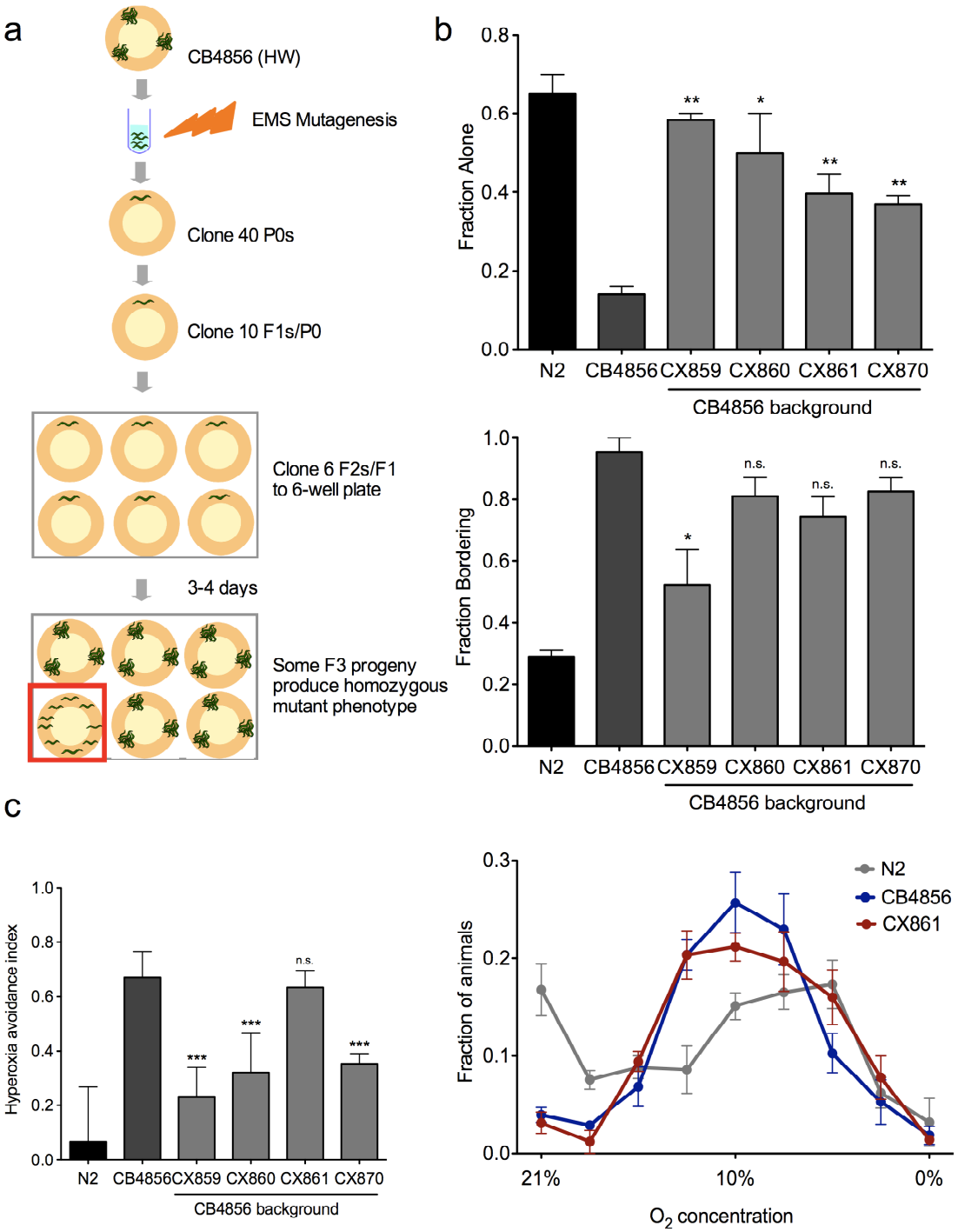
a
CB4856 (HW)
EMS Mutagenesis
Clone 40 P0s
Clone 10 F1s/P0
Clone 6 F2s/F1
to 6-well plate
3-4 days
Some F3 progeny
produce homozygous
mutant phenotype
b
Fraction Alone
0.0
0.2
0.4
0.6
0.8
**
*
**
**
N2
CB4856
CX859
CX860
CX861
CX870
CB4856 background
Fraction Bordering
0.0
0.2
0.4
0.6
0.8
1.0
*
n.s.
n.s.
n.s.
N2
CB4856
CX859
CX860
CX861
CX870
CB4856 background
c
Hyperoxia avoidance index
0.0
0.2
0.4
0.6
0.8
1.0
***
***
n.s.
***
N2
CB4856
CX859
CX860
CX861
CX870
CB4856 background
Fraction of animals
0.0
0.1
0.2
0.3
N2
CB4856
CX861
21%
10%
0%
O2 concentration

Figure 3-5. The CB4856 variant of *glb-5* suppresses aggregation in *npr-1* backgrounds

a. Aggregation behavior of CB4856, N2 and Recombinant Inbred Lines (RIL) between CB4856 (HW) and N2 that have the CB4856 allele of *npr-1*. The allelic origin of *glb-5* gene for each strain is indicated. n ≥3 for each genotype.

b. Sequence polymorphisms in *glb-5* between CB4856 (HW) and N2. In N2, a 765 bp duplication covering the sixth exon truncates the predicted GLB-5 protein. cc, coiled-coil domain; ct, alternate C-terminal domain caused by the duplicated exon. (Adapted from [146])

c. (Left) Aggregation behavior is suppressed by $glb\text{-}5_{HW}$ genotype or transgene in the $npr\text{-}1_{HW}$ or *npr-1(ad609)* background, but not in $npr\text{-}1_{N2}$ background. (Right) Bordering is not affected by the genotype of *glb-5* allele. For transgenic expressions of $glb\text{-}5_{HW}$, *glb-5* endogenous promoter and *gcy-36* promoter were used. The transgenes were in bicistronic transcripts followed by SL2::GFP. *, ** and *** indicate values that are different at $P<0.05$, 0.01 and 0.001 between values indicated by brackets (two-tailed unpaired t-test). n.s. – not significant. Error bars indicate SEM. n ≥3 for each genotype.

d. (Left) Calcium responses of URX neurons in strains with four combinations of *npr-1* and *glb-5* alleles, as indicated. Fluorescence increases in the *G-CaMP* indicator is caused by Ca^{2+} increases, likely associated with depolarization. Light shading indicates time at 21% O_2; dark shading indicates SEM; n= 20–23 animals for each genotype. (Right) Average calcium increase at t=15–25s. ** indicates responses different at $P<0.01$ between values indicated by brackets (two-tailed unpaired t-test). (Adapted from [146])

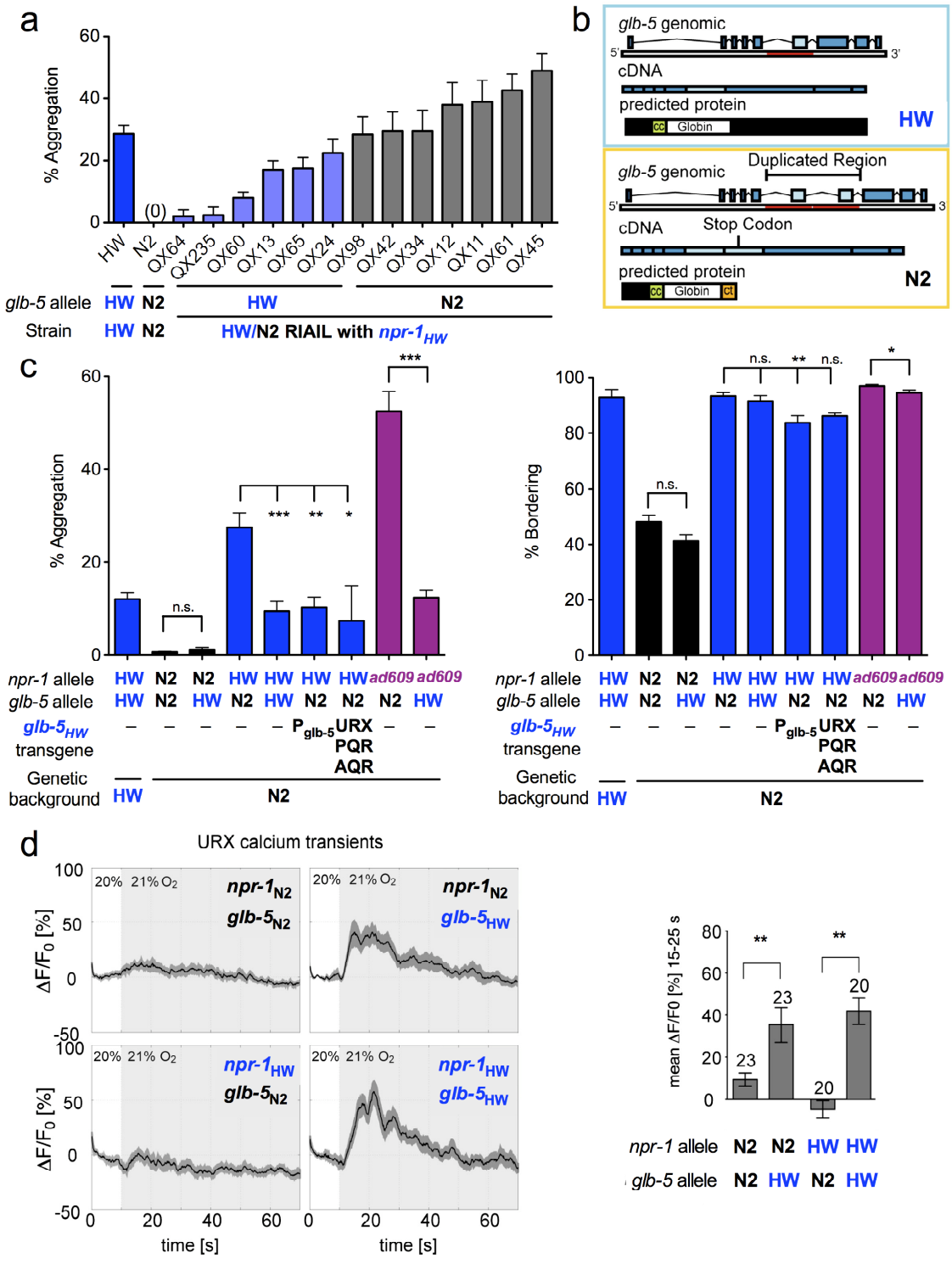
a
% Aggregation
HW
N2
QX64
QX235
QX60
QX13
QX65
QX24
QX98
QX42
QX34
QX12
QX11
QX61
QX45
glb-5 allele
Strain
HW/N2 RIAIL with npr-1HW
b
glb-5 genomic
cDNA
predicted protein
Globin
Duplicated Region
Stop Codon
c
% Aggregation
% Bordering
npr-1 allele
glb-5 allele
glb-5HW transgene
Genetic background
ad609
d
URX calcium transients
ΔF/F0 [%]
time [s]
mean ΔF/F0 [%] 15-25 s

Appendix 3-A. Temperature alone does not affect aggregation behavior

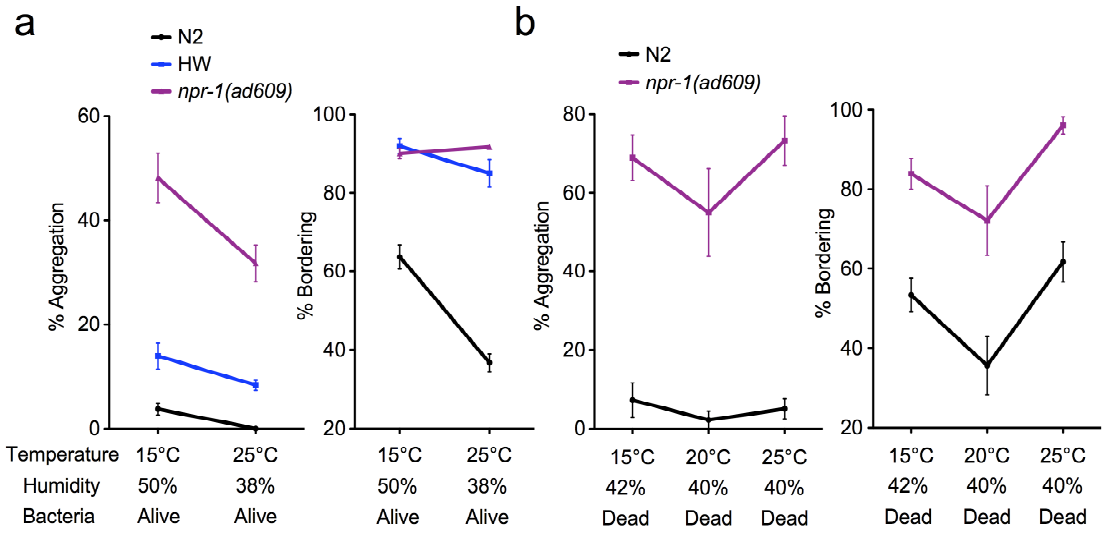

Decrease in temperature enhances aggregation behavior in numerous species, including flies [237, 238]. To ask whether aggregation is regulated by temperature, one of the environmental cues in *C. elegans*, I initially tested the wild-type N2, the social wild-strain CB4856 (HW) and *npr-1(ad609)* social mutant in the N2 background. Aggregation and bordering were slightly enhanced at 15°C compared to 25°C **(a)**. At subsequent experiments in which humidity was controlled at the similar level and the bacterial lawn was killed on the day of the assay by 20 min exposure to UV light, however, neither the wild-type N2 nor the social mutant *npr-1(ad609)* showed significant temperature-dependence in their social behavior **(b)**. This suggests that temperature alone does not modulate aggregation/bordering behavior. Increased humidity and differences in the secreted chemicals from the live bacteria (*E. coli* OP50) may contribute to enhanced aggregation at lower temperature. Animals and assay plates were incubated for 2 hrs prior to the assay. $n \geq 2$ for each genotype.

Chapter 4:

Conclusions and future directions

Pheromone avoidance is modulated by *npr-1,* sex, and interactions between pheromone components

In Chapter 2, I demonstrate that the nociceptive ADL neurons sense the pheromone compound ascr#3/C9 and drive avoidance behavior through their chemical synapses. This circuit is antagonized by the gap junction circuit involving the "social hub" RMG interneuron, whose activity is regulated by the neuropeptide receptor NPR-1. In *npr-1* mutants, ascr#5/C3 sensed by ASK further antagonizes ADL-mediated avoidance of ascr#3/C9 via the RMG gap junction circuit. Although the gap junctions are present in electron micrographs [141], but they have not yet been observed to mediate intercellular signaling in direct functional studies, nor are their molecular components known. The molecular identity of innexin genes that form RMG gap junctions can be elucidated by further studies based upon Chapter 3. Once the genes are identified, cell-specific manipulation of gap junctions using the cre/lox system followed by behavioral and functional analysis should refine our understanding of the social circuit. First, the innexin mutants have the potential to provide direct molecular evidences that gap junctions are important. Second, these genetic tools may be combined with calcium imaging, which has successfully detected signals associated with gap junctions in another hub-and-spoke circuit [198], to ask how npr-1 modifies the circuit.

ascr#3/C9 is a strong male attractant [132]. In wild-type males, ADL is less responsive to ascr#3/C9 and less able to drive avoidance compared to hermaphrodites. Due to even weaker ADL responses and presumably due to strong ASK responses to ascr#3/C9, *npr-1* mutant males exhibit a behavioral shift to attraction to ascr#3/C9. It will be interesting to test whether the behavioral alteration to ascr#3/C9 by *npr-1* signaling

results in different mating efficiencies in wild-type and *npr-1* males. In addition, since synaptic potentiation of ADL enhances avoidance of ascr#3/C9 in both wild-type and *npr-1* males, it can be tested whether it also inhibits mating behavior in males.

Dissection of behavioral responses to pheromones

The drop test, the behavioral avoidance assay predominantly used in Chapter 2, measures the fraction of animals that make long reversals in response to a repellent. It is a simple and straightforward readout for quantifying avoidance behavior, and can efficiently address the circuit that drives AVD/AVA backward command interneurons for immediate reversal behavior. However, the drop test is insufficient to address additional behavioral motifs that worms use to respond to various stimuli, including head swings, acceleration, and turning [239-241].

A more comprehensive analysis of the behavioral components of pheromone responses can be carried out in a better-controlled microfluidic environment developed in the laboratory [242]. As ascarosides are highly water-soluble, they can be applied at various concentrations with precise spatial and temporal control, in single or multiple stream(s) of constant buffer flow. For example, the stripe assay and the gradient assay apply spatial stimuli in steep and shallow gradients, respectively, whereas the pulse assay generates temporal pulses of stimulus [242]. The device arena is video-recorded and the movements of individual worms are subsequently tracked and analyzed to generate a rich dataset over time and space. Attraction to ascaroside blends can be more directly addressed by quantifying the fraction of animals accumulating in the pheromone, and

changes in their speed or turning rate. Studies are currently underway to utilize microfluidic device for pheromone responses.

ASH and ADL nociceptive neurons act redundantly to regulate aggregation

Results in Chapter 2 and previous results [144] indicate that ASH and ADL act redundantly to regulate aggregation behavior in *npr-1* animals. To analyze ADL function more specifically, synaptic manipulations of ADL can be performed in the a genetic background in which ASH has been inactivated by genetic ablation; this will require the development of intersectional strategies, as no ASH-specific promoters exist. . Conversely, ASH function can be analyzed in an ADL-ablated line, perhaps using cell-specific expression of the *egl-1* cDNA that drives cell death [243, 244]. As an intermediate tool, I have used the TRPV channel mutants *ocr-2* or *osm-9* with ADL-or ASH-specific rescue as functional mutant/rescue pairs for ASH and ADL, respectively. Optogenetic approaches may be a useful alternative approach to address ASH and ADL functions separately ([245] and Navin Pokala, unpublished). For example, ADL or ASH can be specifically activated by expression of the light-gated cation channel channelrhodopsin-2 and exposure to light.

Pheromone composition in N2, social mutants and wild isolates

The pheromones ascr#3/C9 and ascr#5/C3 examined in Chapter 2 are major components of naturally-produced *C. elegans* pheromones with relatively high activity in dauer formation and male attraction (Table 2-1 in Chapter 2). The identification of these *C. elegans* pheromone components was based on their abundance in liquid culture

extracts of wild-type N2 or several pheromone synthesis mutants [127-129, 131, 132, 207]. The history of the pheromone field, however, suggests that molecules of very low abundance may have relatively high potency and tightly regulated activity, often in a specific temporal window. A library of ascaroside-based *C. elegans* pheromones reaching a thousand kinds has been described recently (Frank Schroeder, pers. comm.), expanding the possibility for orchestrated usage of diverse ascaroside compounds. Moreover, specific pheromones that promote aggregation with high potency have been identified in other studies (Jagan Srinivasan and Paul W. Sternberg, pers. comm.). Study on the functions of additional ascarosides are clearly warranted, and should be accompanied by identification of the cognate pheromone receptors, and expression and functional analysis. The recent discovery that genes in the *srg* family as well as genes in the *srbc* family can act as pheromone receptors provides a set of potential receptor genes [133, 134]. Heterologous expression of these receptor genes in the ASH neurons, which do not normally respond to pheromones in calcium imaging expeirments, is a tool that can be used to match receptors with ascaroside ligands [134].

The pheromone production profile of *npr-1* social mutants or of wild isolates such as CB4856 has not been directly analyzed. Animals with low *npr*-1 activity have behavioral alterations in response to multiple stimulus such as oxygen [142, 199], CO_2 [147], heat [204], and ethanol [246], as well as differences in pathogen susceptibility [224]. Due to these sensory changes, such strains will expose themselves to microenvironments distinct from those preferred by the laboratory N2 strain. The release and production of pheromone composition are highly dependent on developmental and environmental conditions in *C. elegans* [157]. It will be interesting to analyze the

pheromone profile in *npr-1* strains, and identify components that are causal to or caused by behavioral differences.

Altered neuropeptide signaling may also affect pheromone profiles in *npr-1* and CB4856 independent of its role in altering behavior. For example, pheromone production is regulated by neuropeptide regulation in moth species [247]. The role of intrinsic *npr-1* signaling in pheromone profiles may be assessed by examining strains that vary in *npr-1* genotype, but cannot "select" their own environment due to growth in liquid culture or due to the presence of mutations causing paralysis.

In flies, the composition of cuticular hydrocarbons (CHs) of *D. melanogaster* varies by inhabiting latitudes [248]. *D. serrata* raised on different diets evolve differences in male CH profiles and in female mating preferences [249]. Wild *C. elegans* strains might also produce different pheromones, a question of interest independent of the role of *npr-1*.

Regulation of the *npr-1* aggregation circuit by innexin genes

Identification of multiple innexin mutants that act as weak suppressors of *npr-1* social behavior in Chapter 3 suggests that there may be redundancy among innexins that act in the hub-and-spoke circuit. As gap junctions are assembled by two hemichannels each consisting of six innexin subunits [250], the innexin genes may have complex genetic interactions with one another. This possibility can be examined by making triple or quadruple mutants between *npr-1* and two or three weak innexin suppressors. Moreover, several innexin genes are lethal when mutated, and *unc-7* and *unc-9* exhibit severely uncoordinated body movement, which may indirectly affect social behavior

(Table 3-2 in Chapter 3). To test the roles of these genes further, dsRNA/RNAi experiments targeting the relevant innexins specifically in RMG will be useful. The sense sequence and the antisense sequence of the gene of interest can be injected under two different promoters whose expression patterns overlap only in RMG to induce RMG-specific RNA interference.

The innexin screen also yielded an interesting mutant allele in the *inx-6(rr5)* genetic background that fully suppresses aggregation, presumably present in CX13742 *inx-6(rr5);npr-1(ad609)* but not in CX13748 *inx-6(rr5);npr-1(ad609)*. Further outcrossing and of CX13742 can be used to map the additional mutation, and ask whether it is unlinked or closely linked to *inx-6*. As rescue of innexin mutants seems highly dose-sensitive in general (Heeun Jang, unpublished, Steven W. Flavell, unpublished, and Taishi Emmei, pers. comm.), it will be interesting to see whether injection of the genomic construct of *inx-6* into CX13742 at lower concentration enhances rescue. Eventually, whole genome sequencing of the strong suppressor strain CX13742 will help to identify the additional mutation that enhances the weak suppressor phenotype of *inx-6(rr5)*.

Functions and potential interactions of *ky861* and *glb-5*

In Chapter 3, a forward genetic screen in the naturally social strain CB4856 identified two aggregation-specific suppressors, *glb-5*$_{HW}$ and the *ky861* mutation. *ky861* lies within an 817 kb candidate region, but its molecular identity is unknown. It can be identified by the next-generation whole-genome sequencing, followed by alignment of short reads to a reference genome, detection of mismatched bases within the candidate region, confirmation by Sanger sequencing, and rescue with cosmids or fosmids [251].

However, this can be challenging, as the CB4856 reference sequence is not yet available. The N2 reference genome may not be useful for the alignment, as CB4856 has a significantly different genomic landscape from N2, including large deletions, insertions and indels, as well as single nucleotide polymorphisms (SNPs) [233, 252].

glb-5 regulates aggregation in the oxygen-sensing neurons. It will be interesting to see how *glb-5* interacts with other sensory cues that are relevant for aggregation. As *glb-5* is also expressed in BAG neurons [146], which sense low O_2 as well as CO_2 [201, 253], it will be interesting to see if responses to changes or in gradients of CO_2 are modulated by *glb-5*. Food is also an important regulator of aggregation behavior. *glb-5*$_{N2}$ and *glb-5*$_{HW}$ strains can be tested for altered responses to food in aggregation and other assays.

Identification of additional cues for aggregation

The identified regulators of aggregation include food, oxygen, CO_2, population density, and other stressors as well as ascaroside pheromones. Yet the full complement of cues regulating aggregation remains unknown. One candidate worth investigating is surface stimuli, especially conveyed via the cuticle. The cuticle is the exoskeleton structure in worms and is important not only for maintenance of morphology and motility but also for interactions with the external environment, especially interspecific interactions via its surface coat [254]. In the parasitic nematode *Toxocara canis*, a carbohydrate-rich glycocalyx in the surface coat mediates interaction with the host [255]. In *C. elegans*, many genes can change cuticle surface properties, often altering its interaction with pathogenic bacteria [256, 257]. For example, 8 *srf* genes affect expression of surface antigens, including the *srf-2*, *srf-3*, *srf-5*, and *srf-6* mutants, which

specifically have altered lectin-binding phenotypes [258-261]. 17 *bus* genes regulate resistance to pathogen *Microbacterium nematophilum*, including *bus-2*, *bus-4*, *bus-8*, *bus-12*, and *bus-17* genes important for glycoconjugate biosynthesis [256, 262]. *bus-2* mutants lack core-1 type *O*-glycans that are presumably secreted to the carbohydrate-rich surface coat of the cuticle [263]. 3 identified *bah* mutants, *bah-1*, *bah-2*, and *bah-3*, are resistant to biofilm production on the head by the pathogens *Yersinia pestis* and *Y. pseudotuberculosis* [256].

These surface coat molecules may function as an intraspecific cue that modulates social recognition or association. In flies, specific cuticular hydrocarbons sensed by gustatory neurons influence several features of courtship behavior [97, 264, 265]. Among the social behaviors of *C. elegans*, both aggregation and mating involve intense surface contact. It will be interesting to investigate aggregation behavior in known surface coat mutants, either in single or in double mutant background with *npr-1*. Additionally, a mutation in the *che-1* gene, a transcription factor that specifically directs development of ASE, the main gustatory neurons in *C. elegans* [266], suppresses aggregation in *npr-1* (Table 3-1 in Chapter 3). It will be interesting to ask whether ASE-specific expression of *che-1* rescues aggregation and whether ablation of ASE affects aggregation, in parallel to the studies on surface coat genes.

Ecological meaning of aggregation behavior in the wild

Many *Caenorhabditis* species inhabit rotting fruits, plant stems and compost piles in the wild [267]. In *C. elegans,* the *npr-1* (215V) allele that leads to solitary behavior is thought to have developed as a laboratory adaptation, whereas the *npr-1* (215F) allele that promotes social behavior is present in most and probably all wild isolates [136, 146]. Behavioral alterations attributed to *npr-1* (215F) such as increased foraging, enhanced burrowing, and attraction to lower oxygen levels may be advantageous for survival in the wild [199, 236, 268, 269]. Indeed, a competition assay demonstrates that patchy sources of food enhance the relative fitness of the N2 strain with an *npr-1(null)* mutation with respect to the standard N2 strain with *npr-1* (215V) [268].

The prominence of aggregation and related behaviors in many wild nematode species suggests that aggregation is evolutionarily favored and often occurs in the natural environment. What ecological roles might aggregation behavior play in the wild? Aggregation may have costs, such as increased competition for food, increased transmission of disease and pathogens, and increased conspicuousness to predators [270, 271]. Possible counteracting benefits include reduced chances of being eaten of individuals in the interior of the group [270, 271] and an enhanced ability to locate food sources and mating partners. These potential benefits of aggregation may be tested in the laboratory by mimicking the natural environment. Various stressors including predators, i.e. the flatworm *Dugesia gonocephala* [272], pathogens, i.e. *Pseudomonas aeruginosa* [273, 274], and less food can be added to and manipulated in the artificial habitat, and the relative survival of *C. elegans* strains can be quantified.

Conclusion

My thesis work shows that behavioral responses to pheromone in the nematode *C. elegans* can be modulated by the neuropeptide receptor signaling, sexual dimorphism in the circuit, and an interaction with another pheromone compound within the circuit. The neural circuit consists of primary sensory neurons and a few interneurons that actively interact with each other by chemical synapses and gap junctions.

Understanding the neural circuit from pheromone perception to behavioral responses will help answer one of the crucial questions in social neuroscience research. At a practical level, it can help us treat more effectively species such as parasitic nematodes that are harmful for agriculture or human health [275, 276]. Ultimately, it could deepen our understanding of the principles by which we interact with each other and organize our own society.

Materials and Methods

Strains

Strains were cultured under standard conditions [277] and fed *E. coli* OP 50. Mutant strains were obtained from the *Caenorhabditis* Genetics Center or from the National Bioresource Project in Japan. Strains used in this study include: N2, CB4856, DA609 *npr-1(ad609)* X, CX4535 *ocr-2(ak47)* IV, CX4537 *osm-9(ky10)* IV, CX3073 *odr-8(ky173)* IV, PY6539 *srbc-64(tm1946)* I*; srbc-66(tm2943)* V, NL335 *gpa-3(pk35)* V, NL797 *gpa-15(pk477)* I, NL792 *gpc-1(pk298)* X, CX9191 *egl-3(n150ts)* V, MT1241 *egl-21(n611)* IV, NY192 *flp-21(pk1601)* V, CX14117 *flp-21(ok889)* V, CX9136 *flp-18(tm2179)* X*;flp-21(ok889)* V, CX13067 *inx-1(tm3524) npr-1(ad609)* X, CX13469 *inx-2(ok376) npr-1(ad609)* X, CX13808 *inx-4(ok2373)* V*;npr-1(ad609)* X, CX13742 *inx-6(rr5)* IV*;npr-1(ad609)* X, CX13748 *inx-6(rr5)* IV*;npr-1(ad609)* X, CX10042 *inx-7(tm2738)* IV*;npr-1(ad609)* X, CX10044 *inx-8(gk42)* IV*;npr-1(ad609)* X, CX10028 *inx-9(ok1502)* IV*;npr-1(ad609)* X, CX13103 *inx-10(tm3393)* V*;npr-1(ad609)* X, CX13382 *inx-11(ok2783)* V*;npr-1(ad609)* X, CX13045 *inx-14(ag17)* I*;npr-1(ad609)* X, CX13318 *inx-15(tm3394)* I*;npr-1(ad609)* X, CX13534 *inx-16(tm1589)* I*;npr-1(ad609)* X, CX13277 *inx-17(tm3839)* I*;npr-1(ad609)* X, CX13278 *inx-18(ok2454)* IV*;npr-1(ad609)* X, CX12275 *inx-19(tm1896)* I*;npr-1(ad609)* X, CX13016 *inx-20(ok681)* I*;npr-1(ad609)* X, CX13535 *inx-21(tm4591)* I*;npr-1(ad609)* X, CX13470 *inx-22(tm1661)* I*;npr-1(ad609)* X, CX10001 *unc-7(e5) npr-1(ad609)* X, CX10041 *unc-9(e101) npr-1(ad609)* X, CX10173 *eat-5(ad464)* I*;npr-1(ad609)* X, CX12813 *daf-22(ok693)* II*;npr-1(ad609)* X, CX8151 *tph-1(mg280)* II*;npr-1(ad609)* X, CX6234 *ocr-2(ak47)* IV*;kyEx685 [odr-*

10p::ocr-2], CX6235 *ocr-2(ak47)* IV*;kyEx685 [odr-10p::ocr-2]*, CX6237 *ocr-2(ak47)* IV*;kyEx686 [srh-142p::ocr-2]*, CX6238 *ocr-2(ak47)* IV*;kyEx686 [srh-142p::ocr-2]*, CX6239 *ocr-2(ak47)* IV*;kyEx687 [sra-6p::ocr-2]*, CX6240 *ocr-2(ak47)* IV*;kyEx687 [sra-6p::ocr-2]*, CX6241 *ocr-2(ak47)* IV*;kyEx687 [sra-6p::ocr-2]*, CX6378 *ocr-2(ak47)* IV*;kyEx689 [srh-220::ocr-2]*, CX6382 *ocr-2(ak47)* IV*;kyEx693 [srh-220::ocr-2]*, CX6383 *ocr-2(ak47)* IV*;kyEx694 [srh-220::ocr-2]*, CX12328 *kyEx3438 [sre-1p::TeTx]*, CX12329 *kyEx3438 [sre-1p::TeTx]*, CX12330 *kyEx3440 [sre-1p::TeTx]*, CX8862 *kyEx1661 [sra-6p::TeTx]*, CX8863 *kyEx1662 [sra-6p::TeTx]*, CX12457 *kyEx3466 [sre-1p::pkc-1(gf)]*, CX12483 *kyEx3476 [sre-1p::pkc-1(gf)]*, CX12494 *kyEx3487 [sre-1p::pkc-1(gf)]*, CX12727 *kyEx3564 [sre-1p::pkc-1(gf) + sre-1p::TeTx]*, CX12378 *npr-1(ad609);kyEx3439 [sre-1p::TeTx]*, CX13283 *npr-1(ad609)* X*;kyEx3439 [sre-1p::TeTx]*, CX13284 *npr-1(ad609)* X*;kyEx3440 [sre-1p::TeTx]*, CX12484 *npr-1(ad609)* X*;kyEx3477 [sre-1p::pkc-1(gf)]*, CX12485 *npr-1(ad609)* X*;kyEx3478 [sre-1p::pkc-1(gf)]*, CX12643 *npr-1(ad609)* X*;kyEx3539 [sre-1p::pkc-1(gf) + sre-1p::TeTx]*, CX12644 *npr-1(ad609)* X*;kyEx3540 [sre-1p::pkc-1(gf) + sre-1p::TeTx]*, CX12648 *npr-1(ad609)* X*;kyEx3543 [sra-6p::pkc-1(gf)]*, CX12649 *npr-1(ad609)* X*;kyEx3544 [sra-6p::pkc-1(gf)]*, CX12650 *npr-1(ad609)* X*;kyEx3545 [sra-6p::pkc-1(gf)]*, CX12645 *npr-1(ad609)* X*;kyEx3541 [sre-1p::pkc-1(gf) + sra-6p::pkc-1(gf)]*, CX12646 *npr-1(ad609)* X*;kyEx3542 [sre-1p::pkc-1(gf), sra-6p::pkc-1(gf)]*, CX12455 *npr-1(ad609)* X*;kyEx1661 [sra-6p::TeTx]*, CX12331 *npr-1(ad609)* X*;qrIs2 [sra-9p::mCaspase1]*, CX12728 *kyEx3577 [sre-1p::fem-3]*, CX12729 *kyEx3578 [sre-1p::fem-3]*, CX12730 *kyEx3579 [sre-1p::fem-3]*, CX12819 *kyEx3606 [sre-1p::fem-3]*, CX12820 *kyEx3607 [sre-1p::fem-3]*, PY6572 *Ex[sre-1p::fem-3]*, PY6576 *Ex[srh-234p::fem-3]*, CX12491 *kyEx3484 [unc-*

31p::fem-3], CX12492 *kyEx3485 [unc-31p::fem-3]*, CX12493 *kyEx3486 [unc-31p::fem-3]*, CX12689 *kyEx1960 [H20::npr-1]*, CX13186 *npr-1(ad609)* X*;kyEx2295 [ncs-1p::Cre]*, CX13145 *npr-1(ad609)* X*;kyEx2352 [flp-21p::loxP lacZ STOP loxP::npr-1]*, CX13507 *npr-1(ad609)* X*;kyEx2353 [flp-21p::loxP lacZ STOP loxP::npr-1]*, CX13505 *npr-1(ad609)* X*;kyEx2354 [flp-21p::loxP lacZ STOP loxP::TeTx]*, CX13506 *npr-1(ad609)* X*;kyEx2355 [flp-21p::loxP lacZ STOP loxP::TeTx]*, CX13743 *inx-6(rr5)* IV;*npr-1(ad609)* X*;kyEx4204 [inx-6p::inx-6 20ng/µL]*, CX13744 *inx-6(rr5)* IV;*npr-1(ad609)* X*;kyEx4205 [inx-6p::inx-6 20ng/µL]*, CX13745 *inx-6(rr5)* IV*;npr-1(ad609)* X*;kyEx4206 [inx-6p::inx-6 20ng/µL]*, CX13746 *inx-6(rr5)* IV*;npr-1(ad609)* X*;kyEx4207 [inx-6p::inx-6 5ng/µL]*, CX13747 *inx-6(rr5)* IV*;npr-1(ad609)* X*;kyEx4208 [inx-6p::inx-6 5ng/µL]*, CX13749 *inx-6(rr5)* IV*;npr-1(ad609)* X*;kyEx4209 [inx-6p::inx-6 5ng/µL]*, CX13750 *inx-6(rr5)* IV*;npr-1(ad609)* X*;kyEx4210 [inx-6p::inx-6 20ng/µL]*, CX13751 *inx-6(rr5)* IV;*npr-1(ad609)* X*;kyEx4211 [inx-6p::inx-6 20ng/µL]*, CX13752 *inx-6(rr5)* IV;*npr-1(ad609)* X*;kyEx4212 [inx-6p::inx-6 20ng/µL]*, CX13753 *inx-6(rr5)* IV;*npr-1(ad609)* X*;kyEx4213 [inx-6p::inx-6 5ng/µL]*, CX13754 *inx-6(rr5)* IV;*npr-1(ad609)* X*;kyEx4214 [inx-6p::inx-6 5ng/µL]*, CX13789 *inx-6(rr5)* IV;*npr-1(ad609)* X*;kyEx4232 [inx-6p::inx-6 5ng/µL]*, CX12988 *unc-9(e101) npr-1(ad609)* X*;kyEx3709 [flp-21p::unc-9]*, CX12989 *unc-9(e101) npr-1(ad609)* X*;kyEx3710 [flp-21p::unc-9]*, CX12990 *unc-9(e101) npr-1(ad609)* X*;kyEx3711 [flp-21p::unc-9]*, CX12991 *unc-9(e101) npr-1(ad609)* X*;kyEx3712 [flp-21p::unc-9]*, CX12992 *unc-9(e101) npr-1(ad609)* X*;kyEx3713 [unc-31p::unc-9]*, CX12993 *unc-9(e101) npr-1(ad609)* X*;kyEx3714 [unc-31p::unc-9]*, CX12994 *unc-9(e101) npr-1(ad609)* X*;kyEx3715 [unc-31p::unc-9]*, CX859 *ky859*, CX860 *ky860*, CX861 *ky861*, CX870 *ky870*, QX1155 *npr-1*$_{HW}$ X, CX10774 *glb-*

5$_{HW}$ V, CX10776 *glb-5$_{HW}$* V;*npr-1$_{HW}$* X, CX10872 *npr-1$_{HW}$* X;*kyEx2802 [glb-5p::glb-5$_{HW}$]*, CX10861 *glb-5$_{HW}$* V;*npr-1(ad609)*, CX10873 *npr-1$_{HW}$* X;*kyEx2802 [glb-5p::glb-5$_{HW}$]*, CX10840 *npr-1$_{HW}$* X;*kyEx2791 [gcy-36p::glb-5$_{HW}$]*, CX7376 *kyIs511* V *[gcy-36p::GCaMP1.0]*, CX11035 *glb-5$_{HW}$* V;*npr-1$_{HW}$* X;*kyIs511* V *[gcy-36p::GCaMP1.0]*, CX11037 *glb-5$_{HW}$* V;*kyIs511* V *[gcy-36p::GCaMP1.0]*, PY6567 *oyEx1 [sre-1p::GCaMP3.0]*, PY6574 *ocr-2(ak47)* IV; *oyEx1 [sre-1p::GCaMP3.0]*, PY6568 *npr-1(ad609)* X; *oyEx1 [sre-1p::GCaMP3.0]*, PY6575 *oyEx[osm-10p::GCaMP3.0]*, CX10981 *kyEx2866 [sra-9p::GCaMP2.2b]*, CX10982 *npr-1(ad609)* X;*kyEx2866 [sra-9p::GCaMP2.2b]*, Germline transformations were carried out as described [278]. CX13742 is the parent strain of CX13743-CX13747 and CX13749. CX13748 is the parent strain of CX13750-CX13754 and CX13789.

Molecular Biology

Constructs driving *ocr-2* genomic fragment were under cell-specific promoters were generated using *srh-220p* for ADL, *sra-6p* for ASH, *odr-10p* for AWA and *srh-142p* for ADF as described in [144]. Tetanus toxin light chain (*TeTx*) was amplified from the Drosophila tetanus toxin light chain expression vector pTNT (courtesy S. Sweeney, Univ. of York, [279]) using the oligonucleotides 5'-gcgatcggatcgctagcatgccgatcaccatcaaca-3' and 5'-cgcgatccgatggtaccctagcggtacggttgtaca-3'and cloned into the pSM-mCherry vector using the NheI and KpnI sites to generate an mCherry fusion protein [149]. The *pkc-1* cDNA was amplified by RT-PCR from the *C. elegans* mixed stage RNAs using the oligonuecleodies 5'-ctgttcacaggcaccgtgcgcgttc-3' and 5'-gtaggtaaaatgcggattgataaatg-3' and cloned into a bicistronic pSM vector containing

SL2::*gfp* as the downstream gene via the NheI and KpnI sites. The gain-of-function A160E mutation was introduced by QuikChange (Stratagene) [149]. The *fem-3* cDNA including 5'UTR and 3'UTR was also amplified using the oligonucleotides 5'-acgctgtccgaacagttgtaggagtg-3' and 5'-cgatattatctatacctttattttaaattaaac-3', and was cloned into a bicistronic pSM vector containing SL2::*gfp* as the downstream gene via the NheI and KpnI sites. The *unc-9* cDNA having the end sequences of 5'-atgggttctatgttactttactactttg-3' and 5'-gaattcctagacgtcgtgcatctttc-3' (a gift of Loren L. Looger) was cloned into a bicistronic pSM vector containing SL2::*gfp* as the downstream gene via the NheI and AgeI sites. The *unc-7* cDNA was amplified by RT-PCR from the *C. elegans* mixed stage RNAs using the oligonucleotides 5'-atgctcggctcctccagcaatcctgaaccg-3' and 5'-gacagtcttgaacaggtttcagatata-3', and was cloned into a bicistronic pSM vector containing SL2::*gfp* as the downstream gene via the NheI and KpnI sites. The genomic fragment of *inx-6* including 5'UTR and the entire coding region was amplified from N2 wild-type genomic DNA extract using the oligonucleotides 5'- agcatctagaaacatcgagtggcaactccagc-3' and 5'-tcaagtatgcttaatcgatttgacaaatggggt-3', and was cloned into a bicistronic pSM vector containing SL2::*gfp* as the downstream gene via the XmaI and KpnI sites. The *glb-5*$_{HW}$ cDNA was amplified from CB4856 (HW) wild-type genomic DNA extract using the oligonucleotides 5'- agcatctagaaacatcgagtggcaactccagc-3' and 5'-tcaagtatgcttaatcgatttgacaaatggggt-3', and was cloned into a bicistronic pSM vector containing SL2::*gfp* as the downstream gene via the XmaI and KpnI sites.

To generate ASK genetic cell ablation line integrated array of *sra-6p::mCaspase* (*qrIs2*) was used (a gift of Ryuzo Shingai).

1kb of sequences upstream of *sre-1* was used to drive ADL-specific expression of *pkc-1(gf), TeTx*, *G-CaMP3.0* and *fem-3* cDNAs. The *srh-234* promoter was additionally used to drive *fem-3* expression in ADL. For pan-neuronal expression of *fem-3*, *unc-7* and *unc-9*, upstream regulatory sequences of *unc-31*, *rab-3,* or H20 promoter was used. To generate calcium imaging lines in URX and ASH neurons, the *gcy-36* promoter and the *osm-10* promoter were used to drive expression of *G-CaMP1.0* and *G-CaMP2.2b*, respectively. For URX, AQR and PQR specific expression of $glb\text{-}5_{HW}$, a 1kb *gcy-36* promoter was used. All promoters were amplified from N2 wild-type genomic DNA extracts except for $glb\text{-}5_{HW}$, which was amplified from CB4856 (HW) wild-type genomic DNA extracts. Each plasmid was injected with *unc-122p::dsRed*, *unc-122p::gfp*, *elt-2p::gfp* or *elt-2p::mcherry* as the coinjection marker. The sequences of the promoter ends are shown below, with the concentration at which resulting plasmids were injected for generation of transgenic lines:

unc-31p (15 ng/µL for *unc-7* and *unc-9* rescues, 50 ng/µL otherwise)

5’-gtgcatttttggcattttccctgtattcttttgaaat-3’, 5’-aacaaggagacttgaaattgaattgaaacgagcg-3’

sre-1p (20-30 ng/µL)

5’-cggggctatctgcaaacaatgcaatgcgcg-3’, 5’-ttcatgttggaatgaaaataaaatcaaaag-3’

flp-21p (15 ng/µL for *unc-7* and *unc-9* rescues, 40 ng/µL otherwise)

5’-tgaggtcacgcaacttgatgatcat-3’, 5’-ctccaaaatccaaaaagtcattttc-3’

ncs-1p (20 ng/µL)

5’-ccaatctgcaataagctttactgtt-3’, 5’-agagagaatcaagttgcaaatcaa-3’

inx-6p (5 or 20 ng/µL)

5’-tagtcacatggtcttgaaggcaggcaggc-3’, 5’-cgctggagttgccactcgatgtttcta-3’

gcy-36p (0.5 ng/μL)

5’-ttggccggccatgatgttggtagatggggtttgg-3’, 5’-ttggcgcgcctgttgggtagcccttgtttgaattt-3’

Pheromone drop test

20-30 young adult worms grown at 20˚C were transferred to an unseeded NGM plate followed by transfer to assay plates. Animals exhibited a higher reversal rate to buffer alone in the presence of food. Thus, for quantification of attraction (suppression of reversals), assays were performed in the presence of food, whereas most measurements of avoidance were performed in the absence of food. For drop tests in the presence of food, the nematode growth media (NGM) plates were uniformly seeded with OP50 bacteria the day before the assay and grown overnight at 37˚C, followed by incubation at room temperature for at least one hour prior to the assay. For tests in the absence of food, care was taken that no food was transferred to the unseeded assay plate. After 30-60 minutes on the assay plate, a drop of M13 buffer (30 mM Tris, 100 mM NaCl, 10 mM KCl) with dissolved pheromone or other chemicals was delivered to individual worms moving forward using glass capillaries. Responses were scored as reversals if animals initiated backward movements longer than half their body length within 4 seconds. All assays were performed at room temperature on at least two different days. All genotypes were also assayed for the ability to reverse in response to 2M glycerol dissolved in water.

Aggregation/Bordering assay

Aggregation and bordering behaviors were measured simultaneously. The assay plates were prepared by seeding 50 μL of *E. coli* OP50 on NGM plate from a liquid

culture at 0.5~0.7 O.D. and grown at room temperature for four days. The resulting circular lawn of OP50 was ~1 cm in diameter. On the day of the assay, 60 young adult animals that were grown at 20°C were picked onto the plate off food. The lid was kept closed and after one hour, the aggregation and bordering fraction was scored. Each strain was analyzed at least three times.

For aggregation and bordering assays in the presence of pheromone, ascr#5/C3, ascr#2/C6 and ascr#3/C9 at equi-molar final concentration of 0, 1, 10 or 100 nM each was added from the ethanol stock of 10 mM of each ascaroside compound to the NGM media. The assay plates were hardened overnight used for seeding *E. coli* OP50 and subsequent assays as above. For temperature shift assays, animals grown at either 15°C or 20°C for their entire life were transferred to the assay plates that were seeded and grown at room temperature for four days and incubated at 15°C or 25°C one hour prior to the assay. Fraction of animals aggregating and bordering were scored after one-hour incubation at the assay temperature.

Calcium imaging

Calcium imaging experiments were performed as previously described [133, 149] using custom-fabricated microfluidics devices (Microfluidics Facility, Brandeis Materials Research Science and Engineering Center). To image males, microfluidics imaging chambers with modified dimensions were used (channel height=25 μm; channel width for body=60 μm , channel width for nose=22 μm). Imaging was performed on an Olympus BX52WI microscope with a 40X objective and a CCD camera (Hamamatsu). Images were processed and analyzed using OpenLab 4.0 software (Improvision), ImageJ (NIH),

and custom-written MATLAB (The Mathworks) scripts. The ascr#3/C9 avoidance responses of *G-CaMP3.0*-expressing transgenic worms were examined prior to use in imaging experiments, and found to be similar to those of wild-type animals. For quantification of fluorescence changes, the cell body area of the ADL neurons was selected as the region of interest and a similar sized area near the cell body was selected as the background. To ensure that fluorescence measurements were performed within the linear dynamic range, only images exhibiting less than 1,000 average fluorescence intensity units in the region of interest and background were used for further analysis. Average fluorescence intensities in the first 5 seconds of imaging were used for normalization. Animals were pre-exposed to near-UV light for 1 min prior to initiation of imaging; pre-exposure did not affect Ca^{2+} responses in the ADL neurons. For ASH imaging, animals were pre-exposed to near-UV light for 3 min before imaging. The ASH neurons in these animals responded robustly to 10 mM $CuSO_4$, confirming that expression of *G-CaMP2.2b* in ASH did not hinder the its sensory transduction [161]. Wild-type and all experimental conditions were examined together on multiple days.

For URX imaging, transgenic animals expressing the integrated *gcy-36::G-CaMP1.0* in URX neurons were exposed to O_2 upshifts and downshifts while trapped in a custom-fabricated PDMS device [146, 253]. The two-layer device allowed rapid diffusion of gas mixtures from a flow chamber into a calibrated channel containing the trapped animal. Fluorescence intensities were measured with a Nikon CoolSnap camera attached to a Zeiss Axioplan microscope while switching between different gas mixtures in the flow chamber, and analyzed with a script written in MetaMorph programming

language. $\Delta F/F_0$ was calculated as the percent change in fluorescence relative to the mean basal fluorescence (F_0) from 1–4 s of each recording.

Forward genetic screen for social suppressors

For random chemical mutagenesis, about 100 animals of the CB4856 (HW) strain in their L4 larval stage were incubated in 2 mL M9 buffer with 50 mM EMS for four hours with shaking. Animals were washed three times with M9 and placed onto a seeded plate overnight. 40 P0 animals were individually placed on plates the next morning and grown for 4 days at room temperature. 10 F1 progeny were cloned from each P0, reaching 800 haploid genome for the screen. 6 F2 progeny from each F1 were cloned onto each well of six-well tissue culture plates (Corning) that had been poured with NGM and seeded with 50 μL *E. coli* HB101. After 3-4 days, the visual aggregation and bordering phenotypes were observed from each F2 clonal well. Most of the mutants with defective aggregation but intact bordering phenotype were found in only one or two wells among the F2 clones from the same F1 animals, suggesting a recessive mutation of interest. Interesting F3 progeny were isolated for further study.

Oxygen gradient assay

Oxygen gradient assays were performed essentially as previously described [142, 199]. Animals were placed on nematode growth medium (NGM) agar in custom-made microfluidic devices fabricated from polydimethylsiloxane (PDMS) with a gas-phase linear gradient from 0%–21% oxygen, and animals' accumulation in nine bins across the gradient was monitored. Gradients were generated by delivering gases under laminar

flow to source and drain chambers immediately outside the behavioral arena, using a syringe pump; diffusion of the gases established the gradient in the small assay chamber. Gases were obtained from Airgas, Matheson, and TW Smith. Animals were prepared for assays as described except that animals were picked instead of washed from their culture plate onto NGM assay plates before the devices were placed onto the assay plate. Thin bacterial lawns of *E. coli* HB101 were made by seeding NGM plates for overnight growth at 37 °C and returning plates to room temperature for at least one hour prior to assay. Results from two devices were binned for one assay (~50–80 animals per assay). Data represent distributions 25 min from start of the assay. The hyperoxia avoidance index is defined as [(fraction of animals in 7%–14% O_2) − (fraction of animals in 14%–21% O_2)] / (fraction of animals in 7%–21% O_2).

Chemotaxis assay

Chemotaxis assays were performed as described [280, 281]. Assay plates were prepared with 2% Difco-agar, 5 mM KPO_4 (pH 6.0), 1 mM $CaCl_2$ and 1 mM $MgSO_4$ poured into the 10 cm tissue culture dishes. Two small x marks were made 180° opposite from each other on the bottom near the edges of the plate. 1 μL of 1 M NaN_3 was placed on the agar above each x mark. Worms were washed off from a growing plate with S-basal (5 mM KPO_4 (pH 6.0), 1 mM $CaCl_2$ and 1 mM $MgSO_4$) and quickly washed 2 additional times in the eppendorf tubes. Worms were pipetted in a small volume onto the petri dish, equidistant from the two x marks, and excess liquid is removed with KimWipes (Kimberley-Clark). 1 μL of 1:200 diluted benzaldehyde or 1:1000 diluted diacetyl was placed at one of the x marks, and 1 μL of ethanol (diluent for benzaldehyde

or diacetyl) was placed on the other x mark. The lid was closed and after 60 minutes, the number of worms anaesthetized at each of the two x marks was counted. The chemotaxis index was calculated as [(number of worms at the attractant) – (number of worms at control)]/(total number of worms participated).

Oxygen flow assay

Oxygen flow assays were performed essentially as described [253]. A custom-fabricated plexiglass frame with a flow area of 30 mm × 30 mm × 0.3 mm was sealed on one side with a glass slide. An inlet to the flow chamber was connected to a multi-valve positioner (MVP) (Hamilton RS-232). Pressurized oxygen gases (21% O_2 +/− 2% and 10% O_2 +/− 2%, balanced with nitrogen; GTS-Welco) were passed from the tanks through gas washing cylinder bottles (PYREX) containing distilled water and flow meters (Cole Parmer EW-32121-16) before entering the MVP. Flow rates were set to 50 mL/min. The MVP was controlled by MatLab software (The MathWorks) and configured so that both gas mixtures flowed constantly but only one at a time led into the flow chamber. For each experiment, a 9 cm piece of Whatman filter paper with a 28 mm × 28 mm square arena cut out of the center was soaked in 20 mM $CuCl_2$ and placed onto a 10 cm NGM plate. The aversive $CuCl_2$ solution prevented animals from leaving the central arena. 120 to 150 animals were transferred to the assay arena for each assay. The Plexiglass device was placed onto the assay arena and animals were accustomed to the 21% oxygen gas flow for 5 min. Recordings were made at 3 fps on a digital camera (Pixelink PL-A741, set to binning 2) connected to a Carl Zeiss Stemi 2000-C stereomicroscope equipped with a 0.3x objective and the 28 mm × 28 mm arena was

captured in a 494 × 494 pixel area. Movies were analyzed by MatLab-based tracking software as described [282, 283]. Animals are detected as areas of defined gray value, and their centroid coordinates are determined for each frame. Centroid positions of adjacent frames are connected to build trajectories, which are used to calculate instantaneous speed and angular velocity. The instantaneous speed was calculated in bins of 5 seconds, only for animals that were moving forward. To exclude behavioral responses to the $CuCl_2$ solution from the analysis, tracks from animals within 2.46 mm (~ 2 worm lengths) of the filter paper were discarded. Speed change was calculated for each animal that was tracked continuously from 10 seconds before to 20 seconds after the O_2 switch; the difference between the mean speed of the first 10 seconds and last 10 seconds of this period was calculated.

Carbon dioxide assay

Assays were performed essentially as previously described [146]. O_2 and CO_2-evoked turning responses were monitored on an NGM plate seeded with OP50 bacteria (grown overnight), with 20–30 adult animals confined to a 28mm × 28mm region using Whatman filter paper dipped in 20mM $CuCl_2$. A custom-designed Plexiglass device containing an inlet, an outlet and a 30 mm × 30 mm × .3 mm behavioral arena created laminar air flow over the animals. Gas tanks were ordered at primary mixture grade from Matheson TriGas. A standard tank at 21.2%O_2/78.8%N_2 was mixed 99:1 with either 100% N_2 or 100% CO_2 to create a tank at 21%O_2/79%N_2 or 21%O_2/1%CO_2/78%N_2. Gas mixtures were bubbled through water at a flow rate of 50 cm_3/min, and a Hamilton MVP was used to switch between two gas tanks every three minutes for 60 minutes. Animals

were recorded at 3 frames/second using a Zeiss microscope and Pixelink PL-A741 Monochrome Camera, and automatically tracked using Matlab software [282, 283]. For each assay, the first 6-minute cycle between gas mixtures was discarded, leaving 9 identical 6 minute intervals of 21%O_2/79%N_2 to 21%O_2/1%CO_2/78%N_2 that were averaged together. Each recording was binned into 20-second-windows. To create data for changes in turning rate, average turning rates for 80 seconds prior to a shift in gas concentration were subtracted from the average turning rate 20–60 seconds after each shift. Experiments were performed three times on three different days for each strain.

References

1. Wilson, E., *Sociobiology: the new synthesis* 1975: Cambridge: Harvard.
2. Clutton-Brock, T.H., *Mammalian mating systems.* Proc R Soc Lond B Biol Sci, 1989. **236**(1285): p. 339-72.
3. Cacioppo, J.T. and J. Decety, *Social neuroscience: challenges and opportunities in the study of complex behavior.* Ann N Y Acad Sci, 2011. **1224**(1): p. 162-73.
4. Damasio, H., et al., *The return of Phineas Gage: clues about the brain from the skull of a famous patient.* Science, 1994. **264**(5162): p. 1102-5.
5. Kanwisher, N., J. McDermott, and M.M. Chun, *The fusiform face area: a module in human extrastriate cortex specialized for face perception.* J Neurosci, 1997. **17**(11): p. 4302-11.
6. Allison, T., A. Puce, and G. McCarthy, *Social perception from visual cues: role of the STS region.* Trends Cogn Sci, 2000. **4**(7): p. 267-278.
7. Frith, C.D. and U. Frith, *Interacting minds--a biological basis.* Science, 1999. **286**(5445): p. 1692-5.
8. Frith, C.D. and U. Frith, *The neural basis of mentalizing.* Neuron, 2006. **50**(4): p. 531-4.
9. Northoff, G. and F. Bermpohl, *Cortical midline structures and the self.* Trends Cogn Sci, 2004. **8**(3): p. 102-7.
10. Frith, U. and C.D. Frith, *Development and neurophysiology of mentalizing.* Philos Trans R Soc Lond B Biol Sci, 2003. **358**(1431): p. 459-73.
11. Adolphs, R., S. Baron-Cohen, and D. Tranel, *Impaired recognition of social emotions following amygdala damage.* J Cogn Neurosci, 2002. **14**(8): p. 1264-74.

12. Amaral, D.G., et al., *The amygdala: is it an essential component of the neural network for social cognition?* Neuropsychologia, 2003. **41**(4): p. 517-22.

13. Mukamel, R., et al., *Single-Neuron Responses in Humans during Execution and Observation of Actions.* Curr Biol, 2010. **20**(8): p. 750-6.

14. Buccino, G., et al., *Action observation activates premotor and parietal areas in a somatotopic manner: an fMRI study.* Eur J Neurosci, 2001. **13**(2): p. 400-4.

15. Hari, R., et al., *Activation of human primary motor cortex during action observation: a neuromagnetic study.* Proc Natl Acad Sci U S A, 1998. **95**(25): p. 15061-5.

16. Rizzolatti, G., et al., *Localization of grasp representations in humans by PET: 1. Observation versus execution.* Exp Brain Res, 1996. **111**(2): p. 246-52.

17. Bonini, L. and P.F. Ferrari, *Evolution of mirror systems: a simple mechanism for complex cognitive functions.* Ann N Y Acad Sci, 2011. **1225**: p. 166-75.

18. Gazzola, V., L. Aziz-Zadeh, and C. Keysers, *Empathy and the somatotopic auditory mirror system in humans.* Curr Biol, 2006. **16**(18): p. 1824-9.

19. Aziz-Zadeh, L., et al., *Left hemisphere motor facilitation in response to manual action sounds.* Eur J Neurosci, 2004. **19**(9): p. 2609-12.

20. Hauk, O., Y. Shtyrov, and F. Pulvermuller, *The sound of actions as reflected by mismatch negativity: rapid activation of cortical sensory-motor networks by sounds associated with finger and tongue movements.* Eur J Neurosci, 2006. **23**(3): p. 811-21.

21. Iacoboni, M., et al., *Grasping the intentions of others with one's own mirror neuron system.* PLoS Biol, 2005. **3**(3): p. e79.

22. Gangitano, M., F.M. Mottaghy, and A. Pascual-Leone, *Modulation of premotor mirror neuron activity during observation of unpredictable grasping movements.* Eur J Neurosci, 2004. **20**(8): p. 2193-202.

23. Paton, J.J., et al., *The primate amygdala represents the positive and negative value of visual stimuli during learning.* Nature, 2006. **439**(7078): p. 865-70.

24. Semsar, K. and J. Godwin, *Social influences on the arginine vasotocin system are independent of gonads in a sex-changing fish.* J Neurosci, 2003. **23**(10): p. 4386-93.

25. Dewan, A.K., K.P. Maruska, and T.C. Tricas, *Arginine vasotocin neuronal phenotypes among congeneric territorial and shoaling reef butterflyfishes: species, sex and reproductive season comparisons.* J Neuroendocrinol, 2008. **20**(12): p. 1382-94.

26. Dewan, A.K. and T.C. Tricas, *Arginine vasotocin neuronal phenotypes and their relationship to aggressive behavior in the territorial monogamous multiband butterflyfish, Chaetodon multicinctus.* Brain Res, 2011. **1401**: p. 74-84.

27. Greenwood, A.K., et al., *Expression of arginine vasotocin in distinct preoptic regions is associated with dominant and subordinate behaviour in an African cichlid fish.* Proc Biol Sci, 2008. **275**(1649): p. 2393-402.

28. Larson, E.T., D.M. O'Malley, and R.H. Melloni, Jr., *Aggression and vasotocin are associated with dominant-subordinate relationships in zebrafish.* Behav Brain Res, 2006. **167**(1): p. 94-102.

29. Maruska, K.P., *Sex and temporal variations of the vasotocin neuronal system in the damselfish brain.* Gen Comp Endocrinol, 2009. **160**(2): p. 194-204.

30. Livingstone, M.S., R.M. Harris-Warrick, and E.A. Kravitz, *Serotonin and octopamine produce opposite postures in lobsters.* Science, 1980. **208**(4439): p. 76-9.

31. Dickson, B.J., *Wired for sex: the neurobiology of Drosophila mating decisions.* Science, 2008. **322**(5903): p. 904-9.

32. Ryner, L.C., et al., *Control of male sexual behavior and sexual orientation in Drosophila by the fruitless gene.* Cell, 1996. **87**(6): p. 1079-89.

33. Ito, H., et al., *Sexual orientation in Drosophila is altered by the satori mutation in the sex-determination gene fruitless that encodes a zinc finger protein with a BTB domain.* Proc Natl Acad Sci U S A, 1996. **93**(18): p. 9687-92.

34. Billeter, J.C., et al., *Specialized cells tag sexual and species identity in Drosophila melanogaster.* Nature, 2009. **461**(7266): p. 987-91.

35. Demir, E. and B.J. Dickson, *fruitless splicing specifies male courtship behavior in Drosophila.* Cell, 2005. **121**(5): p. 785-94.

36. Manoli, D.S., et al., *Male-specific fruitless specifies the neural substrates of Drosophila courtship behaviour.* Nature, 2005. **436**(7049): p. 395-400.

37. Sakuma, Y., *Neural substrates for sexual preference and motivation in the female and male rat.* Ann N Y Acad Sci, 2008. **1129**: p. 55-60.

38. Zhou, X., *Roles of androgen receptor in male and female reproduction: lessons from global and cell-specific androgen receptor knockout (ARKO) mice.* J Androl, 2010. **31**(3): p. 235-43.

39. Lin, D., et al., *Functional identification of an aggression locus in the mouse hypothalamus.* Nature, 2011. **470**(7333): p. 221-6.

40. Moltz, H., et al., *Hormonal induction of maternal behavior in the ovariectomized nulliparous rat.* Physiol Behav, 1970. **5**(12): p. 1373-7.

41. Bridges, R.S., et al., *Endocrine communication between conceptus and mother: placental lactogen stimulation of maternal behavior.* Neuroendocrinology, 1996. **64**(1): p. 57-64.

42. Fleming, A.S., D.H. O'Day, and G.W. Kraemer, *Neurobiology of mother-infant interactions: experience and central nervous system plasticity across development and generations.* Neurosci Biobehav Rev, 1999. **23**(5): p. 673-85.

43. Giordano, A.L., H.I. Siegel, and J.S. Rosenblatt, *Nuclear estrogen receptor binding in the preoptic area and hypothalamus of pregnancy-terminated rats: correlation with the onset of maternal behavior.* Neuroendocrinology, 1989. **50**(3): p. 248-58.

44. Cameron, N.M., et al., *Epigenetic programming of phenotypic variations in reproductive strategies in the rat through maternal care.* J Neuroendocrinol, 2008. **20**(6): p. 795-801.

45. Francis, D.D., F.C. Champagne, and M.J. Meaney, *Variations in maternal behaviour are associated with differences in oxytocin receptor levels in the rat.* J Neuroendocrinol, 2000. **12**(12): p. 1145-8.

46. Champagne, F.A., et al., *Variations in nucleus accumbens dopamine associated with individual differences in maternal behavior in the rat.* J Neurosci, 2004. **24**(17): p. 4113-23.

47. Lim, M.M., et al., *Enhanced partner preference in a promiscuous species by manipulating the expression of a single gene.* Nature, 2004. **429**(6993): p. 754-7.

48. Pitkow, L.J., et al., *Facilitation of affiliation and pair-bond formation by vasopressin receptor gene transfer into the ventral forebrain of a monogamous vole.* J Neurosci, 2001. **21**(18): p. 7392-6.

49. Lim, M.M., E.A. Hammock, and L.J. Young, *The role of vasopressin in the genetic and neural regulation of monogamy.* J Neuroendocrinol, 2004. **16**(4): p. 325-32.

50. Ramocki, M.B. and H.Y. Zoghbi, *Failure of neuronal homeostasis results in common neuropsychiatric phenotypes.* Nature, 2008. **455**(7215): p. 912-8.

51. Karlson, P. and M. Luscher, *Pheromones': a new term for a class of biologically active substances.* Nature, 1959. **183**(4653): p. 55-6.

52. Touhara, K. and L.B. Vosshall, *Sensing odorants and pheromones with chemosensory receptors.* Annu Rev Physiol, 2009. **71**: p. 307-32.

53. Williams, P., *Quorum sensing, communication and cross-kingdom signalling in the bacterial world.* Microbiology, 2007. **153**(Pt 12): p. 3923-38.

54. Williams, P., et al., *Look who's talking: communication and quorum sensing in the bacterial world.* Philos Trans R Soc Lond B Biol Sci, 2007. **362**(1483): p. 1119-34.

55. Davies, D.G., et al., *The involvement of cell-to-cell signals in the development of a bacterial biofilm.* Science, 1998. **280**(5361): p. 295-8.

56. Rybtke, M.T., et al., *The implication of Pseudomonas aeruginosa biofilms in infections.* Inflamm Allergy Drug Targets, 2011. **10**(2): p. 141-57.

57. Derzelle, S., et al., *Identification, characterization, and regulation of a cluster of genes involved in carbapenem biosynthesis in Photorhabdus luminescens.* Appl Environ Microbiol, 2002. **68**(8): p. 3780-9.

58. Henke, J.M. and B.L. Bassler, *Three parallel quorum-sensing systems regulate gene expression in Vibrio harveyi.* J Bacteriol, 2004. **186**(20): p. 6902-14.

59. Lenz, D.H., et al., *The small RNA chaperone Hfq and multiple small RNAs control quorum sensing in Vibrio harveyi and Vibrio cholerae.* Cell, 2004. **118**(1): p. 69-82.

60. Henke, J.M. and B.L. Bassler, *Quorum sensing regulates type III secretion in Vibrio harveyi and Vibrio parahaemolyticus.* J Bacteriol, 2004. **186**(12): p. 3794-805.

61. Miller, M.B. and B.L. Bassler, *Quorum sensing in bacteria.* Annu Rev Microbiol, 2001. **55**: p. 165-99.

62. Miller, M.B., et al., *Parallel quorum sensing systems converge to regulate virulence in Vibrio cholerae.* Cell, 2002. **110**(3): p. 303-14.

63. Perego, M. and J.A. Hoch, *Cell-cell communication regulates the effects of protein aspartate phosphatases on the phosphorelay controlling development in Bacillus subtilis.* Proc Natl Acad Sci U S A, 1996. **93**(4): p. 1549-53.

64. Vuong, C., et al., *Impact of the agr quorum-sensing system on adherence to polystyrene in Staphylococcus aureus.* J Infect Dis, 2000. **182**(6): p. 1688-93.

65. Beenken, K.E., J.S. Blevins, and M.S. Smeltzer, *Mutation of sarA in Staphylococcus aureus limits biofilm formation.* Infect Immun, 2003. **71**(7): p. 4206-11.

66. Waters, C.M. and B.L. Bassler, *Quorum sensing: cell-to-cell communication in bacteria.* Annu Rev Cell Dev Biol, 2005. **21**: p. 319-46.

67. Xavier, K.B. and B.L. Bassler, *Interference with AI-2-mediated bacterial cell-cell communication.* Nature, 2005. **437**(7059): p. 750-3.

68. Telford, G., et al., *The Pseudomonas aeruginosa quorum-sensing signal molecule N-(3-oxododecanoyl)-L-homoserine lactone has immunomodulatory activity.* Infect Immun, 1998. **66**(1): p. 36-42.

69. Smith, R.S., et al., *The Pseudomonas aeruginosa quorum-sensing molecule N-(3-oxododecanoyl)homoserine lactone contributes to virulence and induces inflammation in vivo.* J Bacteriol, 2002. **184**(4): p. 1132-9.

70. Yuan, Z.C., et al., *The plant signal salicylic acid shuts down expression of the vir regulon and activates quormone-quenching genes in Agrobacterium.* Proc Natl Acad Sci U S A, 2007. **104**(28): p. 11790-5.

71. Bauer, W.D. and U. Mathesius, *Plant responses to bacterial quorum sensing signals.* Curr Opin Plant Biol, 2004. **7**(4): p. 429-33.

72. Dudler, R. and L. Eberl, *Interactions between bacteria and eukaryotes via small molecules.* Curr Opin Biotechnol, 2006. **17**(3): p. 268-73.

73. Schaap, P., *Evolutionary crossroads in developmental biology: Dictyostelium discoideum.* Development, 2011. **138**(3): p. 387-96.

74. Clarke, M. and R.H. Gomer, *PSF and CMF, autocrine factors that regulate gene expression during growth and early development of Dictyostelium.* Experientia, 1995. **51**(12): p. 1124-34.

75. Deery, W.J. and R.H. Gomer, *A putative receptor mediating cell-density sensing in Dictyostelium.* J Biol Chem, 1999. **274**(48): p. 34476-82.

76. Gregor, T., et al., *The onset of collective behavior in social amoebae.* Science, 2010. **328**(5981): p. 1021-5.

77. Matsukuma, S. and A.J. Durston, *Chemotactic cell sorting in Dictyostelium discoideum.* J Embryol Exp Morphol, 1979. **50**: p. 243-51.

78. Traynor, D., R.H. Kessin, and J.G. Williams, *Chemotactic sorting to cAMP in the multicellular stages of Dictyostelium development.* Proc Natl Acad Sci U S A, 1992. **89**(17): p. 8303-7.

79. Weening, K.E., et al., *Contrasting activities of the aggregative and late PDSA promoters in Dictyostelium development.* Dev Biol, 2003. **255**(2): p. 373-82.

80. Bonner, J.T. and D.S. Lamont, *Behavior of cellular slime molds in the soil.* Mycologia, 2005. **97**(1): p. 178-84.

81. Benton, R., *Sensitivity and specificity in Drosophila pheromone perception.* Trends Neurosci, 2007. **30**(10): p. 512-9.

82. Sakurai, T., et al., *Identification and functional characterization of a sex pheromone receptor in the silkmoth Bombyx mori.* Proc Natl Acad Sci U S A, 2004. **101**(47): p. 16653-8.

83. Nakagawa, T., et al., *Insect sex-pheromone signals mediated by specific combinations of olfactory receptors.* Science, 2005. **307**(5715): p. 1638-42.

84. Wang, L. and D.J. Anderson, *Identification of an aggression-promoting pheromone and its receptor neurons in Drosophila.* Nature, 2010. **463**(7278): p. 227-31.

85. Ejima, A., et al., *Generalization of courtship learning in Drosophila is mediated by cis-vaccenyl acetate.* Curr Biol, 2007. **17**(7): p. 599-605.

86. Kurtovic, A., A. Widmer, and B.J. Dickson, *A single class of olfactory neurons mediates behavioural responses to a Drosophila sex pheromone.* Nature, 2007. **446**(7135): p. 542-6.

87. Bartelt, R.J., A.M. Schaner, and L.L. Jackson, *Cis-Vaccenyl acetate as an aggregation pheromone in Drosophila melanogaster.* Journal of Chemical Ecology, 1985. **11**(12): p. 1747-1756.

88. Xu, P., et al., *Drosophila OBP LUSH is required for activity of pheromone-sensitive neurons.* Neuron, 2005. **45**(2): p. 193-200.

89. van der Goes van Naters, W. and J.R. Carlson, *Receptors and neurons for fly odors in Drosophila.* Curr Biol, 2007. **17**(7): p. 606-12.

90. Ha, T.S. and D.P. Smith, *A pheromone receptor mediates 11-cis-vaccenyl acetate-induced responses in Drosophila.* J Neurosci, 2006. **26**(34): p. 8727-33.

91. Liu, W., et al., *Social regulation of aggression by pheromonal activation of Or65a olfactory neurons in Drosophila.* Nat Neurosci, 2011. **14**(7): p. 896-902.

92. Benton, R., K.S. Vannice, and L.B. Vosshall, *An essential role for a CD36-related receptor in pheromone detection in Drosophila.* Nature, 2007. **450**(7167): p. 289-93.

93. Jin, X., T.S. Ha, and D.P. Smith, *SNMP is a signaling component required for pheromone sensitivity in Drosophila.* Proc Natl Acad Sci U S A, 2008. **105**(31): p. 10996-1001.

94. Laughlin, J.D., et al., *Activation of pheromone-sensitive neurons is mediated by conformational activation of pheromone-binding protein.* Cell, 2008. **133**(7): p. 1255-65.

95. Fishilevich, E. and L.B. Vosshall, *Genetic and functional subdivision of the Drosophila antennal lobe.* Curr Biol, 2005. **15**(17): p. 1548-53.

96. Couto, A., M. Alenius, and B.J. Dickson, *Molecular, anatomical, and functional organization of the Drosophila olfactory system.* Curr Biol, 2005. **15**(17): p. 1535-47.

97. Bray, S. and H. Amrein, *A putative Drosophila pheromone receptor expressed in male-specific taste neurons is required for efficient courtship.* Neuron, 2003. **39**(6): p. 1019-29.

98. Montell, C., *A taste of the Drosophila gustatory receptors.* Curr Opin Neurobiol, 2009. **19**(4): p. 345-53.

99. Miyamoto, T. and H. Amrein, *Suppression of male courtship by a Drosophila pheromone receptor.* Nat Neurosci, 2008. **11**(8): p. 874-6.

100. Moon, S.J., et al., *A Drosophila gustatory receptor essential for aversive taste and inhibiting male-to-male courtship.* Curr Biol, 2009. **19**(19): p. 1623-7.

101. Sato, K., et al., *Insect olfactory receptors are heteromeric ligand-gated ion channels.* Nature, 2008. **452**(7190): p. 1002-6.

102. Kaupp, U.B., *Olfactory signalling in vertebrates and insects: differences and commonalities.* Nat Rev Neurosci, 2010. **11**(3): p. 188-200.

103. Wekesa, K.S. and R.R. Anholt, *Pheromone regulated production of inositol-(1, 4, 5)-trisphosphate in the mammalian vomeronasal organ.* Endocrinology, 1997. **138**(8): p. 3497-504.

104. Thompson, R.N., A. Napier, and K.S. Wekesa, *Chemosensory cues from the lacrimal and preputial glands stimulate production of IP3 in the vomeronasal organ and aggression in male mice.* Physiol Behav, 2007. **90**(5): p. 797-802.

105. Leinders-Zufall, T., et al., *Contribution of the receptor guanylyl cyclase GC-D to chemosensory function in the olfactory epithelium.* Proc Natl Acad Sci U S A, 2007. **104**(36): p. 14507-12.

106. Spehr, M., et al., *Essential role of the main olfactory system in social recognition of major histocompatibility complex peptide ligands.* J Neurosci, 2006. **26**(7): p. 1961-70.

107. Rodriguez, I., et al., *A putative pheromone receptor gene expressed in human olfactory mucosa.* Nat Genet, 2000. **26**(1): p. 18-9.

108. Liberles, S.D. and L.B. Buck, *A second class of chemosensory receptors in the olfactory epithelium.* Nature, 2006. **442**(7103): p. 645-50.

109. Lin, W., et al., *Olfactory neurons expressing transient receptor potential channel M5 (TRPM5) are involved in sensing semiochemicals.* Proc Natl Acad Sci U S A, 2007. **104**(7): p. 2471-6.

110. Dulac, C. and A.T. Torello, *Molecular detection of pheromone signals in mammals: from genes to behaviour.* Nat Rev Neurosci, 2003. **4**(7): p. 551-62.

111. Zufall, F. and T. Leinders-Zufall, *Mammalian pheromone sensing.* Curr Opin Neurobiol, 2007. **17**(4): p. 483-9.

112. Juilfs, D.M., et al., *A subset of olfactory neurons that selectively express cGMP-stimulated phosphodiesterase (PDE2) and guanylyl cyclase-D define a unique olfactory signal transduction pathway.* Proc Natl Acad Sci U S A, 1997. **94**(7): p. 3388-95.

113. Lin, D.Y., et al., *Encoding social signals in the mouse main olfactory bulb.* Nature, 2005. **434**(7032): p. 470-7.

114. Dulac, C. and R. Axel, *A novel family of genes encoding putative pheromone receptors in mammals.* Cell, 1995. **83**(2): p. 195-206.

115. Matsunami, H. and L.B. Buck, *A multigene family encoding a diverse array of putative pheromone receptors in mammals.* Cell, 1997. **90**(4): p. 775-84.

116. Ryba, N.J. and R. Tirindelli, *A new multigene family of putative pheromone receptors.* Neuron, 1997. **19**(2): p. 371-9.

117. Riviere, S., et al., *Formyl peptide receptor-like proteins are a novel family of vomeronasal chemosensors.* Nature, 2009. **459**(7246): p. 574-7.

118. Liberles, S.D., et al., *Formyl peptide receptors are candidate chemosensory receptors in the vomeronasal organ.* Proc Natl Acad Sci U S A, 2009. **106**(24): p. 9842-7.

119. Boschat, C., et al., *Pheromone detection mediated by a V1r vomeronasal receptor.* Nat Neurosci, 2002. **5**(12): p. 1261-2.

120. Del Punta, K., et al., *Deficient pheromone responses in mice lacking a cluster of vomeronasal receptor genes.* Nature, 2002. **419**(6902): p. 70-4.

121. Kimoto, H., et al., *Sex-specific peptides from exocrine glands stimulate mouse vomeronasal sensory neurons.* Nature, 2005. **437**(7060): p. 898-901.

122. Cavaggioni, A. and C. Mucignat-Caretta, *Major urinary proteins, alpha(2U)-globulins and aphrodisin.* Biochim Biophys Acta, 2000. **1482**(1-2): p. 218-28.

123. Flower, D.R., *The lipocalin protein family: structure and function.* Biochem J, 1996. **318 (Pt 1)**: p. 1-14.

124. Chamero, P., et al., *Identification of protein pheromones that promote aggressive behaviour.* Nature, 2007. **450**(7171): p. 899-902.

125. Leinders-Zufall, T., et al., *MHC class I peptides as chemosensory signals in the vomeronasal organ.* Science, 2004. **306**(5698): p. 1033-7.

126. Nodari, F., et al., *Sulfated steroids as natural ligands of mouse pheromone-sensing neurons.* J Neurosci, 2008. **28**(25): p. 6407-18.

127. Butcher, R.A., et al., *Small-molecule pheromones that control dauer development in Caenorhabditis elegans.* Nat Chem Biol, 2007. **3**(7): p. 420-2.

128. Butcher, R.A., J.R. Ragains, and J. Clardy, *An indole-containing dauer pheromone component with unusual dauer inhibitory activity at higher concentrations.* Org Lett, 2009. **11**(14): p. 3100-3.

129. Butcher, R.A., et al., *A potent dauer pheromone component in Caenorhabditis elegans that acts synergistically with other components.* Proc Natl Acad Sci U S A, 2008. **105**(38): p. 14288-92.

130. Jeong, P.Y., et al., *Chemical structure and biological activity of the Caenorhabditis elegans dauer-inducing pheromone.* Nature, 2005. **433**(7025): p. 541-5.

131. Pungaliya, C., et al., *A shortcut to identifying small molecule signals that regulate behavior and development in Caenorhabditis elegans.* Proc Natl Acad Sci U S A, 2009. **106**(19): p. 7708-13.

132. Srinivasan, J., et al., *A blend of small molecules regulates both mating and development in Caenorhabditis elegans.* Nature, 2008. **454**(7208): p. 1115-8.

133. Kim, K., et al., *Two chemoreceptors mediate developmental effects of dauer pheromone in C. elegans.* Science, 2009. **326**(5955): p. 994-8.

134. McGrath, P.T., et al., *Parallel evolution of domesticated Caenorhabditis species targets pheromone receptor genes.* Nature, 2011. **477**(7364): p. 321-5.

135. Zoghbi, H.Y. and S.T. Warren, *Neurogenetics: advancing the "next-generation" of brain research.* Neuron, 2010. **68**(2): p. 165-73.

136. de Bono, M. and C.I. Bargmann, *Natural variation in a neuropeptide Y receptor homolog modifies social behavior and food response in C. elegans.* Cell, 1998. **94**(5): p. 679-89.

137. Liu, K.S. and P.W. Sternberg, *Sensory regulation of male mating behavior in Caenorhabditis elegans.* Neuron, 1995. **14**(1): p. 79-89.

138. Barr, M.M. and L.R. Garcia, *Male mating behavior*, in *WormBook*, T.C.e.R. Community, Editor, WormBook.

139. Golden, J.W. and D.L. Riddle, *A pheromone influences larval development in the nematode Caenorhabditis elegans.* Science, 1982. **218**(4572): p. 578-80.

140. Hu, P.J., *Dauer*, in *WormBook*, T.C.e.R. Community, Editor, WormBook.

141. White, J.G., et al., *The structure of the nervous system of the nematode Caenorhabditis elegans.* Philosophical Transactions of the Royal Society of London. B, Biological Sciences, 1986. **314**(1165): p. 1.

142. Gray, J.M., et al., *Oxygen sensation and social feeding mediated by a C. elegans guanylate cyclase homologue.* Nature, 2004. **430**(6997): p. 317-22.

143. Cheung, B.H., et al., *Experience-dependent modulation of C. elegans behavior by ambient oxygen.* Curr Biol, 2005. **15**(10): p. 905-17.

144. de Bono, M., et al., *Social feeding in Caenorhabditis elegans is induced by neurons that detect aversive stimuli.* Nature, 2002. **419**(6910): p. 899-903.

145. Rogers, C., et al., *Inhibition of Caenorhabditis elegans social feeding by FMRFamide-related peptide activation of NPR-1.* Nat Neurosci, 2003. **6**(11): p. 1178-85.

146. McGrath, P.T., et al., *Quantitative mapping of a digenic behavioral trait implicates globin variation in C. elegans sensory behaviors.* Neuron, 2009. **61**(5): p. 692-9.

147. Bretscher, A.J., K.E. Busch, and M. de Bono, *A carbon dioxide avoidance behavior is integrated with responses to ambient oxygen and food in Caenorhabditis elegans.* Proc Natl Acad Sci U S A, 2008. **105**(23): p. 8044-9.

148. Hallem, E.A. and P.W. Sternberg, *Acute carbon dioxide avoidance in Caenorhabditis elegans.* Proc Natl Acad Sci U S A, 2008. **105**(23): p. 8038-43.

149. Macosko, E.Z., et al., *A hub-and-spoke circuit drives pheromone attraction and social behaviour in C. elegans.* Nature, 2009. **458**(7242): p. 1171-5.

150. Thomas, J.H., D.A. Birnby, and J.J. Vowels, *Evidence for parallel processing of sensory information controlling dauer formation in Caenorhabditis elegans.* Genetics, 1993. **134**(4): p. 1105-17.

151. Cheung, B.H., et al., *Soluble guanylate cyclases act in neurons exposed to the body fluid to promote C. elegans aggregation behavior.* Curr Biol, 2004. **14**(12): p. 1105-11.

152. Coates, J.C. and M. de Bono, *Antagonistic pathways in neurons exposed to body fluid regulate social feeding in Caenorhabditis elegans.* Nature, 2002. **419**(6910): p. 925-9.

153. Byer, J.A., *Pheromone component patterns of moth evolution revealed by computer analysis of the Pherolist.* J Anim Ecol, 2006. **75**(2): p. 399-407.

154. Bone, L.W. and H.H. Shorey, *Disruption of sex pheromone communication in a nematode.* Science, 1977. **197**(4304): p. 694-5.

155. Chasnov, J.R., et al., *The species, sex, and stage specificity of a Caenorhabditis sex pheromone.* Proc Natl Acad Sci U S A, 2007. **104**(16): p. 6730-5.

156. Golden, J.W. and D.L. Riddle, *The Caenorhabditis elegans dauer larva: developmental effects of pheromone, food, and temperature.* Dev Biol, 1984. **102**(2): p. 368-78.

157. Kaplan, F., et al., *Ascaroside expression in Caenorhabditis elegans is strongly dependent on diet and developmental stage.* PLoS One, 2011. **6**(3): p. e17804.

158. Hilliard, M.A., C.I. Bargmann, and P. Bazzicalupo, *C. elegans responds to chemical repellents by integrating sensory inputs from the head and the tail.* Curr Biol, 2002. **12**(9): p. 730-4.

159. Bargmann, C.I., J.H. Thomas, and H.R. Horvitz, *Chemosensory cell function in the behavior and development of Caenorhabditis elegans.* Cold Spring Harb Symp Quant Biol, 1990. **55**: p. 529-38.

160. Kaplan, J.M. and H.R. Horvitz, *A dual mechanosensory and chemosensory neuron in Caenorhabditis elegans.* Proc Natl Acad Sci U S A, 1993. **90**(6): p. 2227-31.

161. Sambongi, Y., et al., *Sensing of cadmium and copper ions by externally exposed ADL, ASE, and ASH neurons elicits avoidance response in Caenorhabditis elegans.* Neuroreport, 1999. **10**(4): p. 753-7.

162. Colbert, H.A., T.L. Smith, and C.I. Bargmann, *OSM-9, a novel protein with structural similarity to channels, is required for olfaction, mechanosensation, and olfactory adaptation in Caenorhabditis elegans.* J Neurosci, 1997. **17**(21): p. 8259-69.

163. Chao, M.Y., et al., *Feeding status and serotonin rapidly and reversibly modulate a Caenorhabditis elegans chemosensory circuit.* Proc Natl Acad Sci U S A, 2004. **101**(43): p. 15512-7.

164. Hilliard, M.A., et al., *Worms taste bitter: ASH neurons, QUI-1, GPA-3 and ODR-3 mediate quinine avoidance in Caenorhabditis elegans.* EMBO J, 2004. **23**(5): p. 1101-11.

165. Tobin, D., et al., *Combinatorial expression of TRPV channel proteins defines their sensory functions and subcellular localization in C. elegans neurons.* Neuron, 2002. **35**(2): p. 307-18.

166. Dwyer, N.D., et al., *Odorant receptor localization to olfactory cilia is mediated by ODR-4, a novel membrane-associated protein.* Cell, 1998. **93**(3): p. 455-66.

167. Jansen, G., et al., *The complete family of genes encoding G proteins of Caenorhabditis elegans.* Nat Genet, 1999. **21**(4): p. 414-9.

168. Jansen, G., D. Weinkove, and R.H. Plasterk, *The G-protein gamma subunit gpc-1 of the nematode C.elegans is involved in taste adaptation.* EMBO J, 2002. **21**(5): p. 986-94.

169. Nakai, J., M. Ohkura, and K. Imoto, *A high signal-to-noise Ca(2+) probe composed of a single green fluorescent protein.* Nat Biotechnol, 2001. **19**(2): p. 137-41.

170. Chronis, N., M. Zimmer, and C.I. Bargmann, *Microfluidics for in vivo imaging of neuronal and behavioral activity in Caenorhabditis elegans.* Nat Methods, 2007. **4**(9): p. 727-31.

171. Madison, J.M., S. Nurrish, and J.M. Kaplan, *UNC-13 interaction with syntaxin is required for synaptic transmission.* Curr Biol, 2005. **15**(24): p. 2236-42.

172. Chalfie, M., et al., *The neural circuit for touch sensitivity in Caenorhabditis elegans.* J Neurosci, 1985. **5**(4): p. 956-64.

173. Schiavo, G., et al., *Tetanus and botulinum-B neurotoxins block neurotransmitter release by proteolytic cleavage of synaptobrevin.* Nature, 1992. **359**(6398): p. 832-5.

174. Sieburth, D., et al., *Systematic analysis of genes required for synapse structure and function.* Nature, 2005. **436**(7050): p. 510-7.

175. Sieburth, D., J.M. Madison, and J.M. Kaplan, *PKC-1 regulates secretion of neuropeptides.* Nat Neurosci, 2007. **10**(1): p. 49-57.

176. Fricker, L.D., *Neuropeptide-processing enzymes: applications for drug discovery.* AAPS J, 2005. **7**(2): p. E449-55.

177. Husson, S.J., et al., *Impaired processing of FLP and NLP peptides in carboxypeptidase E (EGL-21)-deficient Caenorhabditis elegans as analyzed by mass spectrometry.* J Neurochem, 2007. **102**(1): p. 246-60.

178. Veenstra, J.A., *Mono- and dibasic proteolytic cleavage sites in insect neuroendocrine peptide precursors.* Arch Insect Biochem Physiol, 2000. **43**(2): p. 49-63.

179. Wolff, J.R. and D. Zarkower, *Somatic sexual differentiation in Caenorhabditis elegans.* Curr Top Dev Biol, 2008. **83**: p. 1-39.

180. Hodgkin, J., *A genetic analysis of the sex-determining gene, tra-1, in the nematode Caenorhabditis elegans.* Genes Dev, 1987. **1**(7): p. 731-45.

181. Hodgkin, J.A. and S. Brenner, *Mutations causing transformation of sexual phenotype in the nematode Caenorhabditis elegans.* Genetics, 1977. **86**(2 Pt. 1): p. 275-87.

182. Lee, K. and D.S. Portman, *Neural sex modifies the function of a C. elegans sensory circuit.* Curr Biol, 2007. **17**(21): p. 1858-63.

183. Mehra, A., et al., *Negative regulation of male development in Caenorhabditis elegans by a protein-protein interaction between TRA-2A and FEM-3.* Genes Dev, 1999. **13**(11): p. 1453-63.

184. Starostina, N.G., et al., *A CUL-2 ubiquitin ligase containing three FEM proteins degrades TRA-1 to regulate C. elegans sex determination.* Dev Cell, 2007. **13**(1): p. 127-39.

185. Luo, L., et al., *Olfactory behavior of swimming C. elegans analyzed by measuring motile responses to temporal variations of odorants.* J Neurophysiol, 2008. **99**(5): p. 2617-25.

186. Miller, A.C., et al., *Step-response analysis of chemotaxis in Caenorhabditis elegans.* J Neurosci, 2005. **25**(13): p. 3369-78.

187. Kaissling, K.E., *Peripheral mechanisms of pheromone reception in moths.* Chem Senses, 1996. **21**(2): p. 257-68.

188. Rogers, E., et al., *The aurora kinase AIR-2 functions in the release of chromosome cohesion in Caenorhabditis elegans meiosis.* J Cell Biol, 2002. **157**(2): p. 219-29.

189. Marder, E. and D. Bucher, *Central pattern generators and the control of rhythmic movements.* Curr Biol, 2001. **11**(23): p. R986-96.

190. Dickinson, P.S., *Neuromodulation of central pattern generators in invertebrates and vertebrates.* Curr Opin Neurobiol, 2006. **16**(6): p. 604-14.

191. Yew, J.Y., et al., *A new male sex pheromone and novel cuticular cues for chemical communication in Drosophila.* Curr Biol, 2009. **19**(15): p. 1245-54.

192. Ruta, V., et al., *A dimorphic pheromone circuit in Drosophila from sensory input to descending output.* Nature, 2010. **468**(7324): p. 686-90.

193. Kimchi, T., J. Xu, and C. Dulac, *A functional circuit underlying male sexual behaviour in the female mouse brain.* Nature, 2007. **448**(7157): p. 1009-14.

194. Leypold, B.G., et al., *Altered sexual and social behaviors in trp2 mutant mice.* Proc Natl Acad Sci U S A, 2002. **99**(9): p. 6376-81.

195. Stowers, L., et al., *Loss of sex discrimination and male-male aggression in mice deficient for TRP2.* Science, 2002. **295**(5559): p. 1493-500.

196. Sorensen, P.W., T.A. Christensen, and N.E. Stacey, *Discrimination of pheromonal cues in fish: emerging parallels with insects.* Curr Opin Neurobiol, 1998. **8**(4): p. 458-67.

197. Meredith, M.A. and B.E. Stein, *Interactions among converging sensory inputs in the superior colliculus.* Science, 1983. **221**(4608): p. 389-91.

198. Chatzigeorgiou, M. and W.R. Schafer, *Lateral facilitation between primary mechanosensory neurons controls nose touch perception in C. elegans.* Neuron, 2011. **70**(2): p. 299-309.

199. Chang, A.J., et al., *A distributed chemosensory circuit for oxygen preference in C. elegans.* PLoS Biol, 2006. **4**(9): p. e274.

200. Rogers, C., et al., *Behavioral motifs and neural pathways coordinating O2 responses and aggregation in C. elegans.* Curr Biol, 2006. **16**(7): p. 649-59.

201. Bretscher, A.J., et al., *Temperature, oxygen, and salt-sensing neurons in C. elegans are carbon dioxide sensors that control avoidance behavior.* Neuron, 2011. **69**(6): p. 1099-113.

202. Kimura, K.D., et al., *The C. elegans thermosensory neuron AFD responds to warming.* Curr Biol, 2004. **14**(14): p. 1291-5.

203. Ramot, D., B.L. MacInnis, and M.B. Goodman, *Bidirectional temperature-sensing by a single thermosensory neuron in C. elegans.* Nat Neurosci, 2008. **11**(8): p. 908-15.

204. Glauser, D.A., et al., *Heat avoidance is regulated by transient receptor potential (TRP) channels and a neuropeptide signaling pathway in Caenorhabditis elegans.* Genetics, 2011. **188**(1): p. 91-103.

205. Troemel, E.R., et al., *Divergent seven transmembrane receptors are candidate chemosensory receptors in C. elegans.* Cell, 1995. **83**(2): p. 207-18.

206. Landolt, P.J. and T.W. Phillips, *Host plant influences on sex pheromone behavior of phytophagous insects.* Annu Rev Entomol, 1997. **42**: p. 371-91.

207. Butcher, R.A., et al., *Biosynthesis of the Caenorhabditis elegans dauer pheromone.* Proc Natl Acad Sci U S A, 2009. **106**(6): p. 1875-9.

208. Bosch, O.J., *Maternal nurturing is dependent on her innate anxiety: the behavioral roles of brain oxytocin and vasopressin.* Horm Behav, 2011. **59**(2): p. 202-12.

209. De Felipe, C., et al., *Altered nociception, analgesia and aggression in mice lacking the receptor for substance P.* Nature, 1998. **392**(6674): p. 394-7.

210. Halasz, J., et al., *Substance P neurotransmission and violent aggression: the role of tachykinin NK(1) receptors in the hypothalamic attack area.* Eur J Pharmacol, 2009. **611**(1-3): p. 35-43.

211. Katsouni, E., et al., *The involvement of substance P in the induction of aggressive behavior.* Peptides, 2009. **30**(8): p. 1586-91.

212. Elmquist, J.K., C.F. Elias, and C.B. Saper, *From lesions to leptin: hypothalamic control of food intake and body weight.* Neuron, 1999. **22**(2): p. 221-32.

213. Nakazato, M., et al., *A role for ghrelin in the central regulation of feeding.* Nature, 2001. **409**(6817): p. 194-8.

214. Schwartz, M.W. and D. Porte, Jr., *Diabetes, obesity, and the brain.* Science, 2005. **307**(5708): p. 375-9.

215. Spiegelman, B.M. and J.S. Flier, *Obesity and the regulation of energy balance.* Cell, 2001. **104**(4): p. 531-43.

216. Yang, L., et al., *Role of dorsomedial hypothalamic neuropeptide Y in modulating food intake and energy balance.* J Neurosci, 2009. **29**(1): p. 179-90.

217. Morales-Medina, J.C., Y. Dumont, and R. Quirion, *A possible role of neuropeptide Y in depression and stress.* Brain Res, 2010. **1314**: p. 194-205.

218. Tasan, R.O., et al., *The central and basolateral amygdala are critical sites of neuropeptide Y/Y2 receptor-mediated regulation of anxiety and depression.* J Neurosci, 2010. **30**(18): p. 6282-90.

219. Mickey, B.J., et al., *Emotion processing, major depression, and functional genetic variation of neuropeptide Y.* Arch Gen Psychiatry, 2011. **68**(2): p. 158-66.

220. Wu, Q., et al., *Regulation of hunger-driven behaviors by neural ribosomal S6 kinase in Drosophila.* Proc Natl Acad Sci U S A, 2005. **102**(37): p. 13289-94.

221. Wu, Q., Z. Zhao, and P. Shen, *Regulation of aversion to noxious food by Drosophila neuropeptide Y- and insulin-like systems.* Nat Neurosci, 2005. **8**(10): p. 1350-5.

222. Xu, J., M. Li, and P. Shen, *A G-protein-coupled neuropeptide Y-like receptor suppresses behavioral and sensory response to multiple stressful stimuli in Drosophila.* J Neurosci, 2010. **30**(7): p. 2504-12.

223. Wu, Q., et al., *Developmental control of foraging and social behavior by the Drosophila neuropeptide Y-like system.* Neuron, 2003. **39**(1): p. 147-61.

224. Reddy, K.C., et al., *A polymorphism in npr-1 is a behavioral determinant of pathogen susceptibility in C. elegans.* Science, 2009. **323**(5912): p. 382-4.

225. Li, S., J.A. Dent, and R. Roy, *Regulation of intermuscular electrical coupling by the Caenorhabditis elegans innexin inx-6.* Mol Biol Cell, 2003. **14**(7): p. 2630-44.

226. Starich, T., et al., *Innexins in C. elegans.* Cell Commun Adhes, 2001. **8**(4-6): p. 311-4.

227. Starich, T.A., R.K. Herman, and J.E. Shaw, *Molecular and genetic analysis of unc-7, a Caenorhabditis elegans gene required for coordinated locomotion.* Genetics, 1993. **133**(3): p. 527-41.

228. Altun, Z.F., et al., *High resolution map of Caenorhabditis elegans gap junction proteins.* Dev Dyn, 2009. **238**(8): p. 1936-50.

229. Starich, T.A., et al., *Interactions between innexins UNC-7 and UNC-9 mediate electrical synapse specificity in the Caenorhabditis elegans locomotory nervous system.* Neural Dev, 2009. **4**: p. 16.

230. Chen, B., et al., *UNC-1 regulates gap junctions important to locomotion in C. elegans.* Curr Biol, 2007. **17**(15): p. 1334-9.

231. Macosko, E.Z., *The neural circuitry of social behavior in C. elegans*, 2009, The Rockefeller University: New York.

232. Swan, K.A., et al., *High-throughput gene mapping in Caenorhabditis elegans.* Genome Res, 2002. **12**(7): p. 1100-5.

233. Wicks, S.R., et al., *Rapid gene mapping in Caenorhabditis elegans using a high density polymorphism map.* Nat Genet, 2001. **28**(2): p. 160-4.

234. Davis, M.W. and M. Hammarlund, *Single-nucleotide polymorphism mapping.* Methods Mol Biol, 2006. **351**: p. 75-92.

235. Rockman, M.V. and L. Kruglyak, *Recombinational landscape and population genomics of Caenorhabditis elegans.* PLoS Genet, 2009. **5**(3): p. e1000419.

236. Persson, A., et al., *Natural variation in a neural globin tunes oxygen sensing in wild Caenorhabditis elegans.* Nature, 2009. **458**(7241): p. 1030-3.

237. Navarro, J. and E. del Solar, *Pattern of spatial distribution in Drosophila melanogaster.* Behav Genet, 1975. **5**(1): p. 9-16.

238. Gilbert, C., et al., *One for all and all for one: the energetic benefits of huddling in endotherms.* Biol Rev Camb Philos Soc, 2010. **85**(3): p. 545-69.

239. Pierce-Shimomura, J.T., T.M. Morse, and S.R. Lockery, *The fundamental role of pirouettes in Caenorhabditis elegans chemotaxis.* J Neurosci, 1999. **19**(21): p. 9557-69.

240. Iino, Y. and K. Yoshida, *Parallel use of two behavioral mechanisms for chemotaxis in Caenorhabditis elegans.* J Neurosci, 2009. **29**(17): p. 5370-80.

241. Chiba, C.M. and C.H. Rankin, *A developmental analysis of spontaneous and reflexive reversals in the nematode Caenorhabditis elegans.* J Neurobiol, 1990. **21**(4): p. 543-54.

242. Albrecht, D.R. and C.I. Bargmann, *High-content behavioral analysis of Caenorhabditis elegans in precise spatiotemporal chemical environments.* Nat Methods, 2011. **8**(7): p. 599-605.

243. Liu, Q.A. and M.O. Hengartner, *The molecular mechanism of programmed cell death in C. elegans.* Ann N Y Acad Sci, 1999. **887**: p. 92-104.

244. Conradt, B. and H.R. Horvitz, *The C. elegans protein EGL-1 is required for programmed cell death and interacts with the Bcl-2-like protein CED-9.* Cell, 1998. **93**(4): p. 519-29.

245. Nagel, G., et al., *Light activation of channelrhodopsin-2 in excitable cells of Caenorhabditis elegans triggers rapid behavioral responses.* Curr Biol, 2005. **15**(24): p. 2279-84.

246. Davies, A.G., et al., *Natural variation in the npr-1 gene modifies ethanol responses of wild strains of C. elegans.* Neuron, 2004. **42**(5): p. 731-43.

247. Altstein, M., *Role of neuropeptides in sex pheromone production in moths.* Peptides, 2004. **25**(9): p. 1491-501.

248. Rouault, J.D., et al., *Relations between cuticular hydrocarbon (HC) polymorphism, resistance against desiccation and breeding temperature; a model for HC evolution in D. melanogaster and D. simulans.* Genetica, 2004. **120**(1-3): p. 195-212.

249. Rundle, H.D., et al., *Divergent selection and the evolution of signal traits and mating preferences.* PLoS Biol, 2005. **3**(11): p. e368.

250. Phelan, P., *Innexins: members of an evolutionarily conserved family of gap-junction proteins.* Biochim Biophys Acta, 2005. **1711**(2): p. 225-45.

251. Sarin, S., et al., *Caenorhabditis elegans mutant allele identification by whole-genome sequencing.* Nat Methods, 2008. **5**(10): p. 865-7.

252. Maydan, J.S., et al., *Copy number variation in the genomes of twelve natural isolates of Caenorhabditis elegans.* BMC Genomics, 2010. **11**: p. 62.

253. Zimmer, M., et al., *Neurons detect increases and decreases in oxygen levels using distinct guanylate cyclases.* Neuron, 2009. **61**(6): p. 865-79.

254. Maizels, R.M., M.L. Blaxter, and M.E. Selkirk, *Forms and functions of nematode surfaces.* Exp Parasitol, 1993. **77**(3): p. 380-4.

255. Blaxter, M.L., et al., *Nematode surface coats: actively evading immunity.* Parasitol Today, 1992. **8**(7): p. 243-7.

256. Darby, C., et al., *Caenorhabditis elegans mutants resistant to attachment of Yersinia biofilms.* Genetics, 2007. **176**(1): p. 221-30.

257. Gravato-Nobre, M.J., et al., *Multiple genes affect sensitivity of Caenorhabditis elegans to the bacterial pathogen Microbacterium nematophilum.* Genetics, 2005. **171**(3): p. 1033-45.

258. Hoflich, J., et al., *Loss of srf-3-encoded nucleotide sugar transporter activity in Caenorhabditis elegans alters surface antigenicity and prevents bacterial adherence.* J Biol Chem, 2004. **279**(29): p. 30440-8.

259. Link, C.D., et al., *Characterization of Caenorhabditis elegans lectin-binding mutants.* Genetics, 1992. **131**(4): p. 867-81.

260. Politz, S.M., et al., *Genes that can be mutated to unmask hidden antigenic determinants in the cuticle of the nematode Caenorhabditis elegans.* Proc Natl Acad Sci U S A, 1990. **87**(8): p. 2901-5.

261. Hemmer, R.M., et al., *Altered expression of an L1-specific, O-linked cuticle surface glycoprotein in mutants of the nematode Caenorhabditis elegans.* J Cell Biol, 1991. **115**(5): p. 1237-47.

262. Partridge, F.A., et al., *The C. elegans glycosyltransferase BUS-8 has two distinct and essential roles in epidermal morphogenesis.* Dev Biol, 2008. **317**(2): p. 549-59.

263. Palaima, E., et al., *The Caenorhabditis elegans bus-2 mutant reveals a new class of O-glycans affecting bacterial resistance.* J Biol Chem, 2010. **285**(23): p. 17662-72.

264. Greenspan, R.J. and J.F. Ferveur, *Courtship in Drosophila.* Annu Rev Genet, 2000. **34**: p. 205-232.

265. Scott, D., *Sexual mimicry regulates the attractiveness of mated Drosophila melanogaster females.* Proc Natl Acad Sci U S A, 1986. **83**(21): p. 8429-33.

266. Uchida, O., et al., *The C. elegans che-1 gene encodes a zinc finger transcription factor required for specification of the ASE chemosensory neurons.* Development, 2003. **130**(7): p. 1215-24.

267. Felix, M.A. and C. Braendle, *The natural history of Caenorhabditis elegans.* Curr Biol, 2010. **20**(22): p. R965-9.

268. Gloria-Soria, A. and R.B. Azevedo, *npr-1 Regulates foraging and dispersal strategies in Caenorhabditis elegans.* Curr Biol, 2008. **18**(21): p. 1694-9.

269. Bendesky, A., et al., *Catecholamine receptor polymorphisms affect decision-making in C. elegans.* Nature, 2011. **472**(7343): p. 313-8.

270. Hamilton, W., *The genetical evolution of social behaviour. I.* Journal of theoretical biology, 1964. **7**(1): p. 1-16.

271. Hamilton, W., *The genetical evolution of social behaviour. II*1.* Journal of theoretical biology, 1964. **7**(1): p. 17-52.

272. Barron, G.L., *The nematode-destroying fungi* 1977: Canadian Biological Publications Ltd.

273. Tan, M.W., et al., *Pseudomonas aeruginosa killing of Caenorhabditis elegans used to identify P. aeruginosa virulence factors.* Proc Natl Acad Sci U S A, 1999. **96**(5): p. 2408-13.

274. Tan, M.W., S. Mahajan-Miklos, and F.M. Ausubel, *Killing of Caenorhabditis elegans by Pseudomonas aeruginosa used to model mammalian bacterial pathogenesis.* Proc Natl Acad Sci U S A, 1999. **96**(2): p. 715-20.

275. Holden-Dye, L. and R.J. Walker, *Neurobiology of plant parasitic nematodes.* Invert Neurosci, 2011. **11**(1): p. 9-19.

276. Tan, M.W. and M. Shapira, *Genetic and molecular analysis of nematode-microbe interactions.* Cell Microbiol, 2011. **13**(4): p. 497-507.

277. Brenner, S., *The genetics of Caenorhabditis elegans.* Genetics, 1974. **77**(1): p. 71-94.

278. Mello, C.C., et al., *Efficient gene transfer in C.elegans: extrachromosomal maintenance and integration of transforming sequences.* EMBO J, 1991. **10**(12): p. 3959-70.

279. Sweeney, S.T., et al., *Targeted expression of tetanus toxin light chain in Drosophila specifically eliminates synaptic transmission and causes behavioral defects.* Neuron, 1995. **14**(2): p. 341-51.

280. Bargmann, C.I., E. Hartwieg, and H.R. Horvitz, *Odorant-selective genes and neurons mediate olfaction in C. elegans.* Cell, 1993. **74**(3): p. 515-527.

281. Ward, S., *Chemotaxis by the nematode Caenorhabditis elegans: identification of attractants and analysis of the response by use of mutants.* Proc Natl Acad Sci U S A, 1973. **70**(3): p. 817-21.

282. Chalasani, S.H., et al., *Dissecting a circuit for olfactory behaviour in Caenorhabditis elegans.* Nature, 2007. **450**(7166): p. 63-70.

283. Ramot, D., et al., *The Parallel Worm Tracker: a platform for measuring average speed and drug-induced paralysis in nematodes.* PLoS One, 2008. **3**(5): p. e2208.